uOttawa

L'Université canadienne
Canada's university

FACULTÉ DES ÉTUDES SUPÉRIEURES ET POSTOCTORALES

u Ottawa

L'Université canadienne
Canada's university

FACULTY OF GRADUATE AND POSDOCTORAL STUDIES

David R. Blais
AUTEUR DE LA THÈSE / AUTHOR OF THESIS

Ph.D. (Biochemistry)
GRADE / DEGREE

Department of Biochemistry, Microbiology and Immunology
FACULTÉ, ÉCOLE, DÉPARTEMENT / FACULTY, SCHOOL, DEPARTMENT

Fate and function of soluble CD14 at ocular and gastrointestinal surfaces and in transgenic tobacco seeds

TITRE DE LA THÈSE / TITLE OF THESIS

Illimar Altosaar
DIRECTEUR (DIRECTRICE) DE LA THÈSE / THESIS SUPERVISOR

CO-DIRECTEUR (CO-DIRECTRICE) DE LA THÈSE / THESIS CO-SUPERVISOR

EXAMINATEURS (EXAMINATRICES) DE LA THÈSE / THESIS EXAMINERS

William Cameron

Jeffrey Farber

Pascual Ferrara

May Griffith

Gary W. Slater
LE DOYEN DE LA FACULTÉ DES ÉTUDES SUPÉRIEURES ET POSTDOCTORALES /
DEAN OF THE FACULTY OF GRADUATE AND POSTDOCORAL STUDIES

Fate and function of soluble CD14 at ocular and gastrointestinal surfaces and in transgenic tobacco seeds

David R. Blais

Thesis submitted to the School of Graduate Studies in partial fulfillment of the requirements for the degree of Doctor of Philosophy

Department of Biochemistry, Microbiology and Immunology
Faculty of Medicine
University of Ottawa

Your file Votre référence
ISBN: 0-494-10950-5
Our file Notre référence
ISBN: 0-494-10950-5

Abstract

Mucosal surfaces are constantly challenged with a variety of microorganisms. The pathogen invasion of mucosal surfaces is initially countered by the innate immune system via recognition of microbe-specific motifs. Of these microbial motifs, lipopolysaccharide (LPS) is known to be one of the most powerful bacterial virulence factors. This thesis is an attempt to understand the roles of the LPS receptor complex at mucosal surfaces and the ways by which it discriminates between commensal and pathogenic Gram-negative bacteria. The LPS receptor components studied were the LPS binding protein (LBP), cluster of differentiation 14 (CD14), toll-like receptor 4 (TLR4) and myeloid differentiation protein 2 (MD-2). In the first section of this thesis, biological analyses of the LPS receptor complex at the tear-corneal interface suggested that the LPS receptor components are strategically and spatially expressed to fine-tune and even restrain their LPS response to invasive pathogenic Gram-negative bacteria. To study its function in the developing gastrointestinal mucosal surface, soluble CD14 in breast milk was tracked in human neonates. The lack of detection of CD14 in stools of breast-fed neonates and the *in vitro* proteolysis assays suggested that CD14 is likely to survive its gastrointestinal passage in the low bacteria density lumen of the upper digestive system, but is likely to be absent from the LPS-rich environment of the distal gastrointestinal tract. This controlled and limited spatial distribution could be a strategy to prevent an overzealous immune response against the commensal flora of the distal bowel. The results obtained from these two studies concluded that the function and fate of CD14 at mucosal surfaces was dynamic enough to merit further investigations on a much larger scale. For this to happen, recombinant expression systems needed to be first explored. The successful production of human CD14 in transgenic tobacco proved to be a promising source of a stable and active CD14 to further elucidate the mechanisms of the mucosal LPS response system.

Acknowledgments

I would like to express my gratitude to my supervisor, Dr. Illimar Altosaar, for his unwavering patience, guidance and expertise throughout my research years. He gave me the freedom to pursue my ideas and interests, which allowed me to become an independent scientist. These are the attributes that I am truly grateful for. I would also like to acknowledge the members of my thesis advisory committee for their counsel and assistance.

I express my deepest gratitude to all the volunteers who provided tears and milk samples as well as their time and effort. Their generosity has not only inspired me in many ways, but also made these projects possible. I am very grateful to all my collaborators, who shared my interests and provided invaluable support in this work. Special thanks go to all my fellow colleagues and students who were a great source of inspiration and advice.

I would like to express my gratitude for the financial support provided by NSERC, the University of Ottawa and the Department of Biochemistry, Immunology and Microbiology, without which this research would have been much more difficult to accomplish.

Last but not least, I would also like to thank my family and friends for their constant support and encouragement they have provided me through my entire life and during my graduate studies.

Fate and function of soluble CD14 at ocular and gastrointestinal surfaces and in transgenic tobacco seeds

Table of contents

List of tables

Chapter 1

Chapter 2

Chapter 3

List of figures

Chapter 1

Chapter 2

Chapter 3

Chapter 4

Abbreviations

aa	Amino acid
Abe	Abequose
ANOVA	Analysis of variance
bp	Nucleotide base-pair
BF	Breast-fed
CD14	Cluster of differentiation 14
cDNA	Complementary deoxyribonucleic acid
CFTR	Cystic fibrosis transmembrane conductance regulator
CHO	Chinese hamster ovary cells
CXCR4	Chemokine receptor-4
DAPI	4',6'-diamidino-2-phenylindole nuclear fluorescent dye
DMEM	Dulbecco's minimum essential medium
ELISA	Enzyme-linked immunosorbent assay
ENA	Epithelial neutrophil activator
ER	Endoplasmic reticulum
FBS	Fetal bovine serum
FF	Formula-fed
FITC	Fluorescein isothiocyanate fluorochrome
FLS2	Flagellin-sensing receptor 2
Gal	Galactose
GlcN	Glucosamine
Glu	Glucose
GM-CSF	Granulocyte-macrophage colony-stimulating factor
GPI	Glycosylphosphatidylinositol
Gt-1	Glutelin-1
Gt-1/SS	Glutelin-1 signal sequence
hCD14	Human cluster of differentiation 14
HCEC	Human corneal epithelial cell line
HDL	High density lipoprotein
Hep	Heptose
hLBP	Human lipopolysaccharide-binding protein
hMD-2	Human myeloid differentiation protein 2
HSP	Heat-shock protein
hTLR4	Human toll-like receptor 4
IFN	Interferon
IκB	Inhibitor kappa B
IKK	Inhibitor kappa B kinase
IL	Interleukin
IRAK	Interleukin-1 receptor-associated kinase
IRF3	Interferon regulatory factor 3
JNK	c-Jun N-terminal kinase
Kdo	2-keto-3-desoxyoctogonate
KSFM	Keratinocyte serum-free medium
LAM	Lipoarabinomannan
LB	Left border
LBP	LPS-binding protein
LPS	Lipopolysaccharide or endotoxin

LRR	Leucine-rich repeat
LTA	Lipoteichoic acid
Mal	Myeloid differentiation factor 88 adapter like
Man	Mannose
mCD14	Membrane-bound form of CD14
MD-2	Myeloid differentiation protein 2
MEKK3	Mitogen-activated protein kinase/extracellular-signal-regulated kinase kinase kinase-3
mRNA	Messenger ribonucleic acid
MyD88	Myeloid differentiation factor 88
NAG	N-acetylglucosamine
NEMO	Nuclear factor kappa B essential modulator
NF-κB	Nuclear factor kappa B
NOS-ter	Nopaline synthase gene polyadenylation signal
Npt II	Neomycin phosphotransferase II gene
NT	Non-transgenic tobacco plant
P	Phosphate
PAMP	Pathogen-associated molecular pattern
PBS	Phosphate buffer saline
PCR	Polymerase chain reaction
PMN	Polymorphonuclear leukocyte
PRR	Pattern recognition receptor
RB	Right border
Rha	Rhamnose
rhCD14	Recombinant human CD14
RIP	Receptor interacting protein
RRX	Rhodamine red™-X fluorochrome
RT	Reverse transcriptase
RT-PCR	Reverse transcriptase-polymerase chain reaction
sCD14	Soluble form of CD14
SDS-Page	Sodium dodecyl sulfate-polyacrylamide gel
SHEM	Supplemental hormonal epithelial medium
sIgA	Secretory immunoglobulin A
TAB	Transforming growth factor-β-activated kinase-1 binding protein
TAK	Transforming growth factor-β-activated kinase
TBK1	TRAF-associated NF-κB activator binding kinase-1
TBS	Tris buffer saline
TIR	Toll/IL-1 receptor homology domain
TLR	Toll-like receptor
TNF	Tumor necrosis factor
TRAF	Tumor necrosis factor receptor-associated factor
TRAM	TRIF-related adapter molecule
TRIF	TIR-containing adapter molecule
WT1.8	Transgene containing the wild type hCD14 coding sequence and 1.8 kb glutelin promoter
WT5.1	Transgene containing the wild type hCD14 coding sequence and 5.1 kb glutelin promoter

Chapter 1

General introduction

Innate immunity

Plants and animals are constantly exposed to a multitude of microorganisms that colonize their surfaces. In general, a symbiotic relationship develops between the host and the microbe, which provides benefits and advantages to each organism. However, pathogenic microorganisms often extend their colonizing capacities beyond mucosal surfaces. These pathogenic invasions are initially countered by innate defence mechanisms that preexist in the host and act within minutes after the initial infection. The innate immune response is based on an early recognition of microbe-specific motifs, known as pathogen-associated molecular patterns (PAMPs). Most PAMPs are highly conserved surface-derived molecules, such as lipopolysaccharide (LPS or endotoxin), peptidoglycan and lipopeptide. In the host, PAMP recognition is accomplished by a series of pattern recognition receptors (PRRs), such as the Toll-like receptors (TLRs), found at the surface of innate immune cells. The binding of PAMPs to PRRs promotes inflammatory responses at the site of infection through the secretion of pro-inflammatory mediators and the recruitment of phagocytic cells, such as neutrophils and macrophages.

Lipopolysaccharide

LPS, a major component of the outer membrane of Gram-negative bacteria, is known to be one of the most powerful PAMPs in terms of pro-inflammatory properties (Figure 1) (1). In fact, the immune detection of LPS is so sensitive and robust that a bloodstream infection can

Figure 1. Schematic structure of LPS from *Salmonella*. LPS is composed of three structural regions: the lipid A domain that anchors the molecule to the outer membrane, a core oligosaccharide and a terminal O-antigen polysaccharide formed by up to 50 repeating units. The lipid A moiety is the primary immunostimulatory region of LPS. Legend: Abe, abequose; Gal, galactose; GlcN, glucosamine; Glu, glucose; Kdo, 2-keto-3-desoxyoctogonate; Hep, heptose; Man, mannose; NAG, N-acetylglucosamine; P, phosphate; Rha, rhamnose. Figure modified from (2, 3).

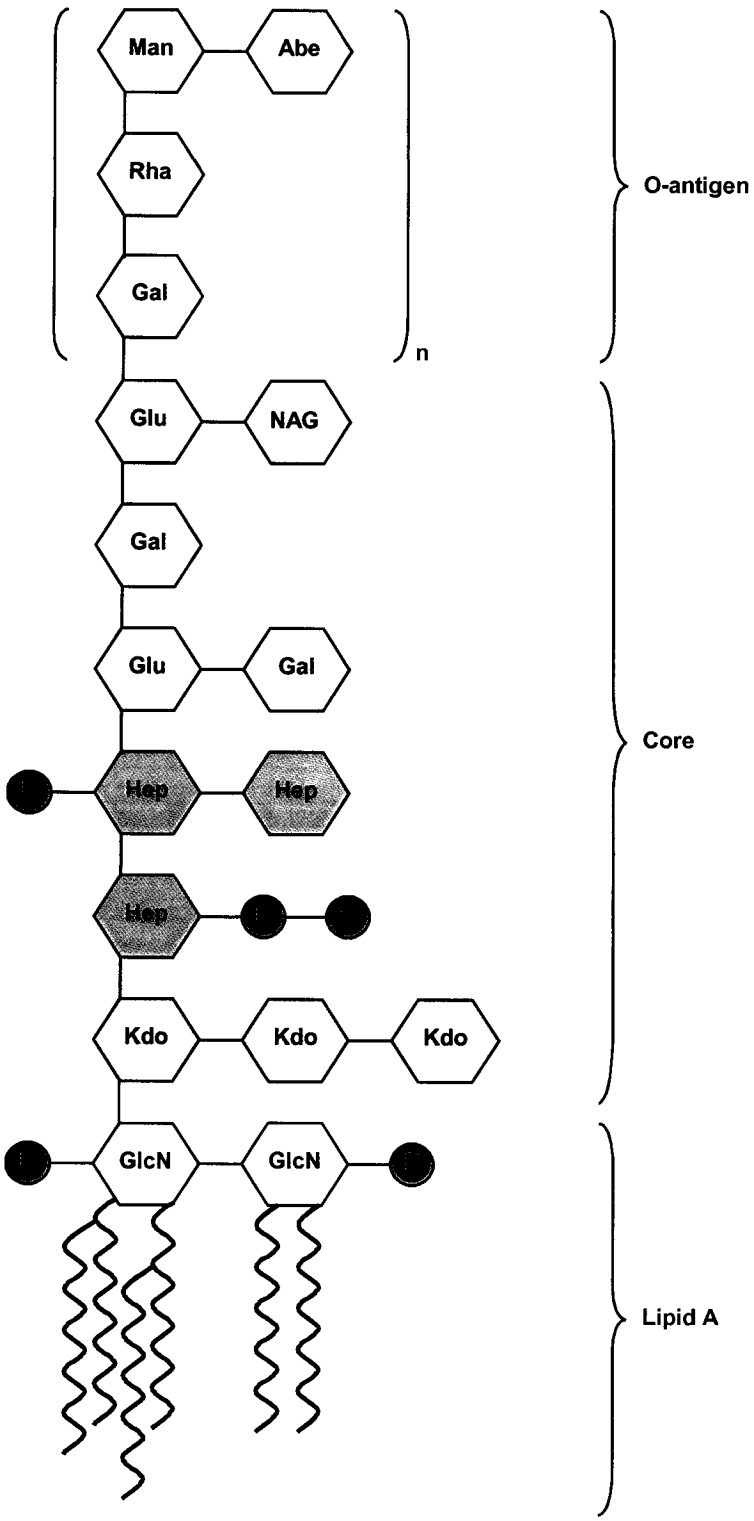
Man
Abe
Rha
Gal
n
O-antigen
Glu
NAG
Gal
Glu
Gal
Hep
Hep
Hep
Kdo
Kdo
Kdo
Core
GlcN
GlcN
Lipid A

Figure 1

result in an unbalanced and massive release of inflammatory mediators, causing a general activation of endothelial cells and leakiness of the capillaries. These conditions can subsequently lead to a dramatic drop in blood pressure, multi-organ dysfunction and failure, as well as other life-threatening complications referred to as septic shock, an increasing clinical condition worldwide (4).

LPS binding protein

In mammals, the detection of LPS is mediated by at least four extracellular and cell surface proteins, LPS-binding protein (LBP), cluster of differentiation 14 (CD14), TLR4 and myeloid differentiation protein 2 (MD-2), referred to as the LPS receptor complex (Figure 2) (5). LPS recognition is initiated by LBP, a 60 kDa lipid transfer protein synthesized by hepatocytes and secreted in the plasma at a concentration of 2-20 μg/mL (6, 7). LBP catalyzes the extraction of LPS monomers from aggregated endotoxin structures or directly from the outer membrane of intact bacteria via specific recognition of the well-conserved lipid anchor region of LPS, lipid A (Figure 1) (8). LPS monomers bound to LBP are subsequently delivered to CD14 and phospholipids, such as high density lipoproteins (HDL) (Figure 2) (9, 10). These two delivery targets lead to opposite outcomes, cellular immune activation through CD14 or neutralization and detoxification of LPS through HDL. Kinetic studies have shown that the transfer of LPS-LBP to CD14 is favoured before its neutralization through HDL, which indicates that immune cells are first activated by LPS before its detoxification, therefore preventing an overzealous immune response and possible septic shock (11).

CD14

CD14 is a high-affinity LPS receptor able to detect picomolar concentrations of endotoxin (12-14). Mutagenesis studies on human CD14 (hCD14) revealed that all the regions involved in

Figure 2. Simplified model of LPS recognition and signaling by the LPS receptor complex. LPS recognition is initiated by the binding of LPS molecules to LBP that catalyzes their transfer to HDL, sCD14 and mCD14. Subsequently, sCD14 neutralizes LPS by transferring it to HDL or induces an immune response by loading LPS on mCD14 or on the dimerized TLR4/MD-2 signaling complex. LPS delivered to mCD14 is subsequently loaded on the TLR4/MD-2 complex. Once bound to TLR4/MD-2, LPS triggers signal transduction by recruiting cytoplasmic adapter proteins with the TIR domain of TLR4. The association of the adapters Mal and MyD88 to TIR leads to the early activation of NF-κB (depicted on the left in purple), whereas recruitment of TRAM and TRIF results in a latter response to LPS, activating the IRF3 and NF-κB transcription factors (presented on the right in green). The activation of these transcription factors induces the expression of numerous pro-inflammatory genes. Legend: HDL, high density lipoprotein; IFN, interferon; IκB, inhibitor κB; IKK, IκB kinase; IL, interleukin; IRAK, interleukin-1 receptor-associated kinase; IRF3, interferon response factor 3; LBP, LPS binding protein; LPS, lipopolysaccharide; LRR, leucine-rich repeat; Mal, MyD88 adapter like; mCD14, membrane-bound CD14; MD-2, myeloid differentiation protein 2; MEKK3, mitogen-activated protein kinase/ERK kinase kinase-3; MyD88, myeloid differentiation factor 88; NEMO, NF-κB essential modulator; NF-κB, nuclear factor κB; RIP, receptor interacting protein; sCD14, soluble CD14; TAB, TAK-1 binding protein; TAK, transforming growth factor-β-activated kinase; TBK1, TANK-binding kinase-1; TIR, Toll/IL-1 receptor homology domain; TLR4, Toll-like receptor 4; TNF, tumor necrosis factor; TRAF6, tumor necrosis factor receptor-associated factor; TRAM, TRIF-related adapter molecule; TRIF, TIR-containing adapter molecule. Figure modified from (15).

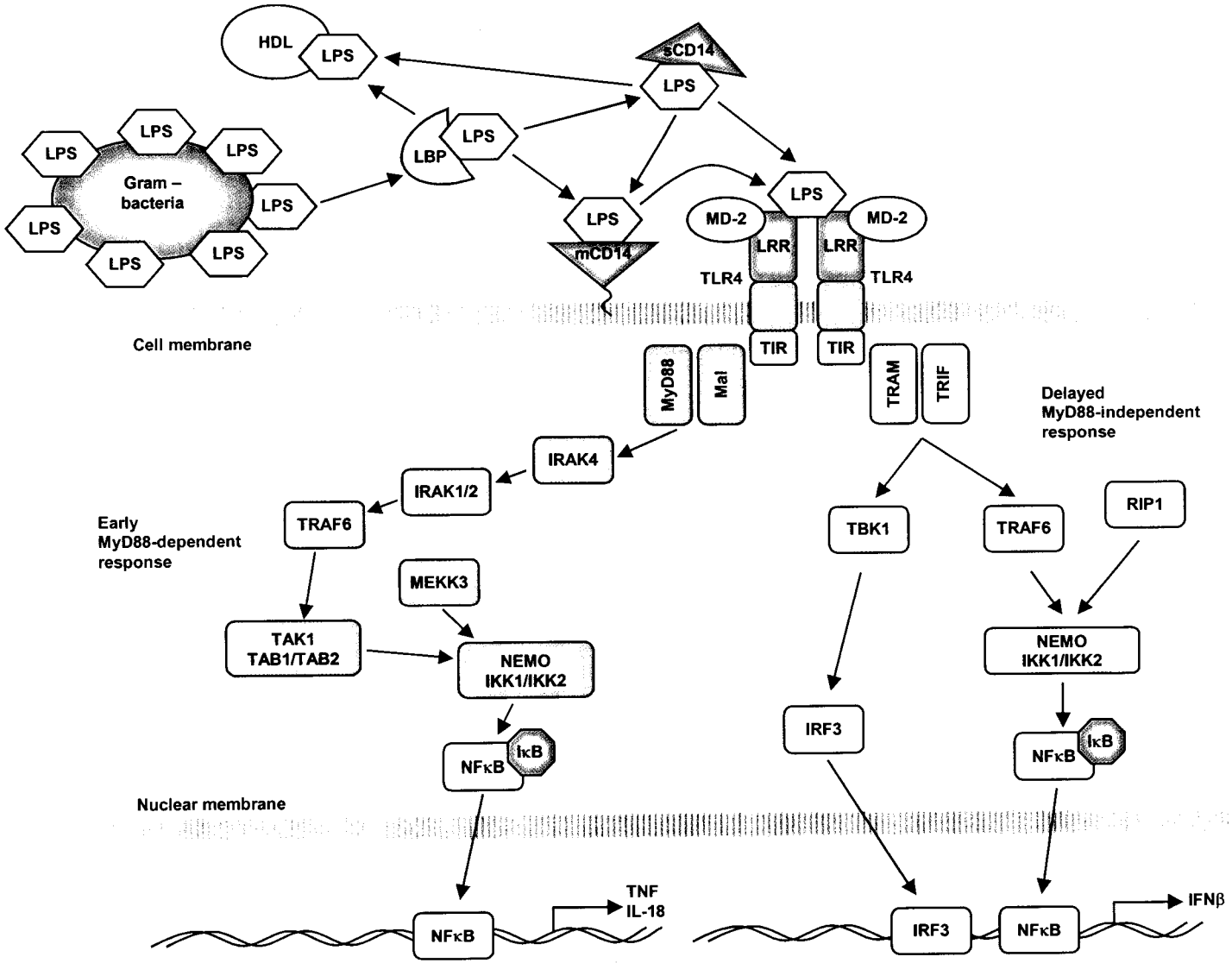
HDL
LPS
sCD14
LPS
LPS
LPS
LPS
LPS
Gram –
bacteria
LPS
LPS
LPS
LBP
LPS
LPS
mCD14
LPS
MD-2
MD-2
LRR
LRR
TLR4
TLR4
Cell membrane
TIR
TIR
MyD88
Mal
TRAM
TRIF
Delayed
MyD88-independent
response
IRAK4
IRAK1/2
TRAF6
Early
MyD88-dependent
response
TBK1
TRAF6
RIP1
MEKK3
TAK1
TAB1/TAB2
NEMO
IKK1/IKK2
NEMO
IKK1/IKK2
IRF3
NFκB
IκB
NFκB
IκB
Nuclear membrane
TNF
IL-18
NFκB
IRF3
NFκB
IFNβ

Figure 2

LPS binding and signaling are located within the N-terminal half of the protein, rendering the C-terminal region beyond amino acid residue 152, non-essential in mediating a LPS response (Figure 3) (16, 17). In addition, the O-linked and N-linked glycans present on CD14 were not found to be essential in mediating LPS signaling (18, 19). However, it was suggested that they could be involved in protein stability (18, 19). In spite of CD14's ability to bind to endotoxin, the reaction occurs at a very low rate due to the amphiphilic nature of the LPS monomers limiting their transfer from LPS aggregates to CD14. However, the transfer rate of LPS to CD14 can be enhanced by 100 to 1,000 times via the lipid transfer action of LBP (20, 21).

CD14 exists in two forms, membrane-bound and soluble. Membrane-bound CD14 (mCD14) is a 55 kDa protein embedded on the plasma membrane of macrophages and polymorphonuclear leukocytes via a glycosylphosphatidylinositol (GPI) anchor (22, 23). LPS can activate myelomonocytic cells after the formation of a ternary complex with LBP and mCD14 (Figure 2) (20, 21).

CD14 also exists as a soluble form (sCD14), found in normal serum (2 to 6 μg/mL) (24) and in numerous secretions and mucosa, such as saliva (25), breast milk (26), lungs (27), intestine (28), urine (29), sperm (30) and amniotic fluid (31, 32). Human serum has two different sCD14 isoforms, one of a low molecular weight (48-50 kDa) and another of high molecular weight (54-56 kDa) (33). These two sCD14 isoforms originate either from the shedding of mCD14 from the cellular surface or from CD14 being directly secreted by the cells. The protease-dependent shedding process occurs when the GPI-anchored mCD14 is cleaved from the cell surface by a membrane-associated serine protease, resulting in the liberated C-terminal truncated 48-50 kDa isoform (34, 35). It has also been suggested that this isoform could be the

Figure 3. Active and structural domains of the hCD14 protein. The 19 amino acid (aa) N-terminal hCD14 signal sequence is cleaved after targeting the preproprotein to the endoplasmic reticulum. mCD14 is embedded on the plasma membrane of myelomonocytic cell via a GPI anchor located at the C-terminus after processing of the spacer domain and the hydrophobic leader peptide. All the LPS binding and signaling domains are located in the N-terminal half of the protein (152 of 326 residues), making the C-terminal half of the protein unnecessary for CD14 biological activity. The four N-linked glycosylation sites are denoted by the symbol N. Figure not drawn to scale. Figure based on references (16-19).

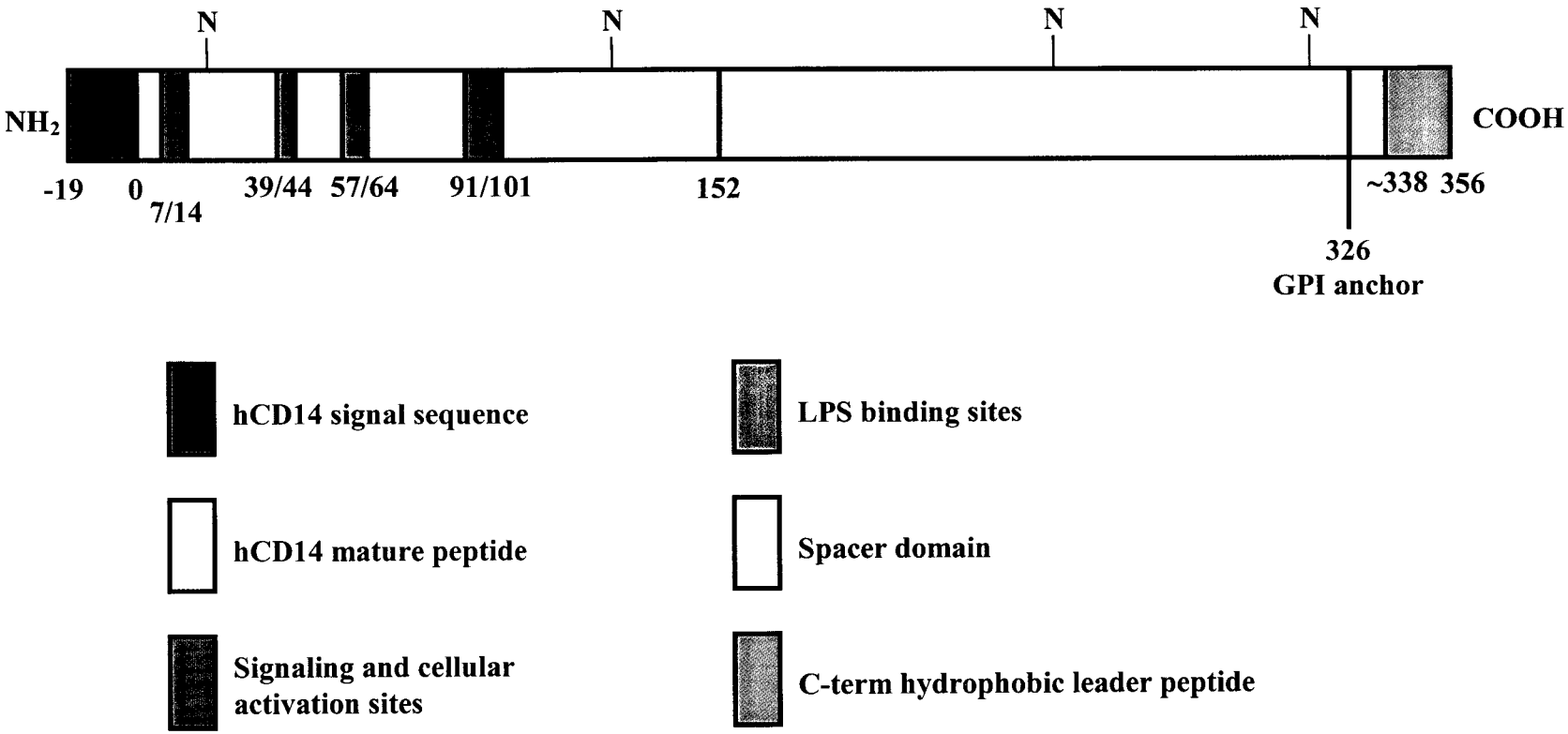
N
N
N
N
NH2
COOH
-19
0
7/14
39/44
57/64
91/101
152
~338
356
326
GPI anchor
hCD14 signal sequence
LPS binding sites
hCD14 mature peptide
Spacer domain
Signaling and cellular activation sites
C-term hydrophobic leader peptide

Figure 3

result of a membrane-bound GPI-specific phospholipase D shedding pathway, as described in the case of the decay-accelerating factor (36). The second pathway, protease-independent, indicates that some CD14 molecules actually bypass the GPI-anchoring mechanism and are directly secreted after biosynthesis, leading to a polypeptide of 54-56 kDa (35). Studies have shown that this latter 54-56 kDa isoform retains its C-terminal leader peptide (Figure 3), being responsible for the higher molecular weight (35).

As for mCD14, sCD14 is able to interact with LPS, a process catalyzed by LBP. Furthermore, sCD14 facilitates the transfer of LPS to mCD14 and TLR4/MD-2 to induce a cytokine response in myelomonocytic cells (Figure 2) (37). In addition to activating macrophages and neutrophils, sCD14 also enables CD14-negative cells, such as endothelial cells, epithelial cells, dendritic cells, smooth muscle cells, and fibroblasts, to respond to low doses of LPS (37-41).

Besides mediating LPS signal transduction, sCD14 is also involved in the detoxification and clearance of LPS in serum by acting as a lipid shuttle (42). Similarly to LBP, sCD14 has the ability to catalyze the transfer of LPS monomers to HDL particles (Figure 2) (43). Furthermore, sCD14 can antagonize the LBP-LPS induced response by competing with mCD14 for LPS binding, resulting in a dampened inflammatory response from myeloid cells (44). The LPS neutralizing abilities of sCD14 are moderate within physiological concentrations (2 to 6 μg/mL serum), but tend to become significant when higher quantities (70 μg/mL) of sCD14 are injected intravenously (45). Experiments on mice demonstrated that sCD14 can save them from the lethality of endotoxin-induced septic shock, suggesting that sCD14 could eventually be used for sepsis therapy in humans (46).

In addition to being the main LPS receptor, CD14 is also involved in the recognition and response to a wide spectrum of microbial PAMP (Table 1) (1, 47). This makes CD14 one of the central PRR of the innate immune system. However, the *in vivo* significance of some of these PAMP-CD14 responses is debated due to the required presence of additional serum factors or to the low sensitivity of CD14 for these ligands (1, 48).

Toll-like receptor 4/myeloid differentiation protein 2

As a GPI-anchored protein, mCD14 cannot transmit the LPS-signal through the plasma membrane due to the lack of transmembrane and cytoplasmic signaling domains. Therefore, another protein is required to act as an endotoxin co-receptor and transmit the CD14-generated signal across the cell membrane. It is now widely recognized that TLR4 is the signaling receptor for LPS, requiring at least two other proteins to accomplish its function, the ligand-binding receptor CD14 and the extracellular adaptor protein MD-2 (49-51). TLR4 is a type 1 receptor composed of extracellular leucine-rich repeats (LRR), a single transmembrane region and an intracellular TIR (Toll/IL-1 receptor) signaling domain (Figure 2). MD-2 is a secretory protein forming a complex with TLR4 on the cell surface. MD-2 is able to bind to LPS and plays a role in ligand recognition by TLR4 (52). Although a direct interaction between CD14 and the TLR4/MD-2 complex has yet to be demonstrated, it has been observed that CD14 is required in loading LPS onto the TLR4/MD-2 signaling complex (51).

Upon binding to the TLR4/MD-2, LPS causes the receptor to homodimerize and triggers at least two separate signals: the early MyD88-dependent response and the delayed MyD88-independent response (Figure 2) (15). These two intracellular signals involve the recruitment of cytoplasmic adapter proteins to the TIR domains of TLR4 to activate intracellular kinase cascades and various transcription factors, such as nuclear factor κB (NF-κB) and interferon regulatory

Table 1. The CD14 PRR recognizes not only LPS of gram-negative bacteria, but also a variety of compounds derived from different microbial and non-microbial sources.[a]

Ligands	Origin	References[b]
LPS	Gram-negative bacteria	(12)
β1,4-*D*-Mannuronic acid (poly M)	*Pseudomonas syringae*	(53)
Peptidoglycan (soluble)	*Staphylococcus aureus*	(54, 55)
Peptidoglycan (insoluble)	*Staphylococcus aureus*	(56)
Lipoteichoic acid (LTA)	Gram-positive bacteria	(57, 58)
Cell walls (insoluble)	Gram-positive bacteria	(59)
Rhamnose-glucose polymer	Streptococcus	(60)
Lipoarabinomannan (LAM)	Mycobacteria	(61, 62)
Lipoprotein, lipopeptide	Spirochetes	(63, 64)
Acylpolygalactosyl	*Klebsiella pneumoniae*	(65)
Poly uronic acid	*Ascophyllum nodosum*	(53)
Chitosans	Arthropods	(66)
WI-1 antigen	*Blastomyces dermatidis*	(67)
Fucoidan	*Fucus vesiculosus*	(68)
Fusion protein	Respiratory syncytial virus	(69)

[a] Adapted from Heumann & Roger (1) and Dziarski *et al.* (47).

[b] Please note that the citation numbering system in figures and tables is in sequence with that of the text.

factor 3 (IRF3) (70). The activation of these transcription factors leads to the expression of numerous pro-inflammatory and immunoregulatory genes and the induction of an innate immune response (15).

In addition to the central action of LBP, CD14, TLR4 and MD-2 in LPS recognition, several additional surface proteins, such as CD11b/CD18, CD16, CD32, CD55, CD64, CD81, heat-shock protein (HSP)-70, HSP-90 and chemokine receptor-4 (CXCR4) have been suggested to form a CD14-dependent receptor cluster within lipid rafts and contribute to endotoxin recognition and signal transduction (71, 72). It has been proposed that the presence of these additional proteins could be involved in ligand-specific cellular responses (71).

The importance of the LPS receptor complex in innate immunity is revealed by its conserved presence throughout the plant and animal kingdoms. LPS has been shown to elicit defence responses in a wide range of plant species (73). Furthermore, the structure of the tomato Cf-9 and the *Arabidopsis* flagellin-sensing (FLS2) receptors have recently been found to share some structural similarity with mammalian CD14 and TLR, respectively (73). The conserved nature and the numerous proteins and signaling pathways involved in the LPS response system reflect its importance to the host in fighting infections.

The work conducted in this thesis aims to further elucidate the fate and function of the LPS receptor complex in the constantly challenged mucosal environment. In the first section, the expression and immune functions of the LPS receptor complex were studied in the directly exposed and easily accessible tear-corneal mucosal interface. In the second section, the persistence and potential functions of breast milk sCD14 were analyzed in the confined and more protected mucosal lumen of the newborn gastrointestinal tract. And thirdly, the production of

hCD14 in transgenic tobacco was envisaged as a promising abundant source of a stable and active CD14.

Chapter 2

Ocular LPS receptor component compartmentalization: a strategy of the eye to limit immune responses to pathogens

Summary

The outer eye is in direct contact with the environment and therefore is in continual exposure with a wide array of microbial pathogens. Consequently, several defence mechanisms have been developed by ocular surfaces against microbial assaults to minimize any loss of corneal integrity and transparency. We analyzed the innate immunity of the tear-corneal interface and identified two proteins in reflex human tears: sCD14 and LBP. Supplementary to tears, the LPS receptor molecules CD14, LBP, TLR4 and MD-2 were found to be spatially and strategically expressed by the different corneal epithelial cell layers to potentially minimize LPS responsiveness against non-pathogenic ocular flora in the intact cornea. Primary and immortalized corneal epithelial cells, representative of the inner epithelial layers of a wounded cornea, showed that tear sCD14 and LBP complemented the LPS receptor complex expressed by the corneal epithelia to mediate in a dose-dependant manner the production of interleukin-6 (IL-6) and IL-8 when challenged with LPS from *Pseudomonas aeruginosa*. This compartmentalized LPS response constitutes another facet of immune privilege evolved with sight to restrict ocular immune responses to corneal epithelial insults by Gram-negative pathogens and limit the sight-threatening consequences of inflammation.

Introduction

The tear film acts as the first protective barrier of the outer eye against the environment. Its continuous flow protects the eye by bathing the ocular surface and flushing foreign particles from the epithelium. In addition to the hydrodynamics, tears contain several immune molecules with bactericidal properties. Of these molecules, secretory IgA (sIgA) opsonizes bacteria and prevents their adherence to the epithelium (74). Another tear component, lactoferrin, limits bacterial growth and biofilm formation by sequestering iron and destabilizing bacterial membranes (75). These defence molecules, along with lysozyme, peroxidase, beta-lysin and various other antimicrobial peptides use tears as a medium to help protect the entire ocular surface (76).

The second barrier contributing to ocular protection is the intact corneal epithelium. Several epithelial features are essential in mediating this protection: tight cell junctions, cell polarity and continuous epithelial turnover (77). Structural integrity is essential in preventing bacterial adherence and infiltration into deeper epithelial layers and subsequent infections (77). However, rather than merely being a passive barrier, there is evidence that corneal epithelial cells actively participate in the ocular immune defence as they express innate immune receptors, such as TLR5 (78), CD14 (79), TLR4 (80) targeted against pathogenic products.

Microbial keratitis is responsible for up to 30% of the prevalence of blindness in less developed countries (81). In tropical and subtropical climates, bacteria account for 50-60% of keratitis cases, whereas for temperate climates, this level rises to 90% (81). Bacterial keratitis is mostly associated with predisposing factors such as extended contact lens wear and LASIK surgery in developed society (82, 83) or trauma in tropical and subtropical communities (84), where *Pseudomonas aeruginosa* remains the primary Gram-negative causative agent (83). In

recent years, a constant increase in keratitis incidence and subsequent treatment costs (83), combined with long-standing occupational insults, has demanded better understanding of the immune defence mechanisms present in the ocular environment to prevent infections.

In this first study, the expression and the immune functions of the LPS receptor proteins, CD14, LBP, TLR4 and MD-2, were investigated in human tears and corneal epithelia. Interestingly, no complementary work is known to have explored the spatial distribution of these molecules across the corneal epithelium and in the protective tear film environment. Given the constraints of working *in ambio* on the human ocular surface, the following experimental design was used to investigate the ocular immune privilege response against LPS: reflex tears, post-mortem corneas, human corneal epithelial cell line, primary corneal epithelial cells, post-surgical and post-mortem lacrimal glands. This experimental data shows that sCD14 and LBP identified in human tears complement the corneal derived repertoire of the LPS receptor complex to induce an innate immune reaction in response to Gram-negative bacterial infiltration of the breached human cornea.

Materials and Methods

Subjects

The study was approved by the Ottawa Hospital Research Ethics Board. Ninety-one healthy volunteers were recruited randomly at the University of Ottawa Eye Institute. The purpose of the research and the experimental procedure were explained to all the participants and their informed consent was obtained before tear collection. The volunteers were chosen based on that they were not taking any ocular medication, had no previous history of eye disease and had

not suffered from dry eye conditions (85). The study included two groups. The first, consisting of 67 healthy non-contact lens wearers included 34 women and 33 men; with a median age of 48 years and a range of 17-86 years. The second group was composed of 24 healthy contact lens wearers, including 13 women and 11 men; with a median age of 27 years and a range of 16-54 years.

Tear fluid collection

Tear production was stimulated by briefly exposing the eye to vapors of freshly minced onions. Tear samples were then collected with 50-μL flamed-polished disposable microcapillaries (VWR, West Chester, PA), while avoiding ocular surface contact. For the continuous incremental tear flow experiment, onion vapor-stimulated tears from 11 individuals were collected as five successive aliquots of 50 μL each and transferred into 5 individual microtubes. All tear samples were frozen at –80°C until analysis.

Human corneal and lacrimal tissues

Ten post-mortem human corneas, sepsis free, stored in Optisol (Chiron Vision, Irvine, CA), were obtained from the Eye Bank of Canada. The mean age of the donors was 44.4 years, with a range of 20 to 74 years. The epithelia from three human corneas were physically isolated for RNA and protein analysis. Briefly, the epithelium was scraped from the cornea with a Gill corneal knife (Storz Instruments, Tuttlingen, Germany) under a dissecting microscope, ensuring that the scraping was confined to the corneal region to minimize any conjunctival or stromal contamination. The isolated epithelia were snap frozen in liquid nitrogen and stored at –80°C until analysis.

For RT-PCR analysis, sepsis free human lacrimal gland biopsies were obtained within 1 h post-surgery from 4 patients (2 men and 2 women, median age of 37 years, range 24-53 years) who had medical conditions requiring surgery (inflammation or tumor). For protein extraction and immunohistological analysis, healthy human lacrimal glands were obtained from the Department of Cellular and Molecular Medicine Anatomy Program (University of Ottawa, ON) within 48 h post-mortem from 4 donors (3 men and 1 woman, median age of 71 years, range 51-89 years). The corneal and lacrimal biopsies were obtained in accordance with the guidelines established by the Ottawa Hospital Research Ethics Board.

Human corneal epithelial cells

The human corneal epithelial cell (HCEC) line immortalized with an SV40 adenovirus recombinant vector (86) was maintained in keratinocyte serum-free medium (KSFM) (Invitrogen, Carlsbad, CA) supplemented with 0.05 mg/mL bovine pituitary extract and 5 ng/mL human recombinant epidermal growth factor (Invitrogen, Carlsbad, CA). Primary corneal epithelial cells derived from progenitors in the limbal-corneal region of human corneas were maintained in complete KSFM, supplemented with 100 U/ml Penicillin, 100 μg/ml streptomycin and 10 μg/ml gentamicin (Invitrogen, Carlsbad, CA). For differentiation, primary corneal epithelial cells or HCEC line were grown to 100% confluence for 2 weeks in supplemented hormonal epithelial medium consisting of DMEM (low glucose):F-12 (Invitrogen, Carlsbad, CA), 15% FBS, 10 ng/mL of epidermal growth factor, 5 μg/mL insulin, 0.1 μg/mL cholera toxin alpha subunit, 5 mM L-glutamine, 0.5% dimethyl sulfoxide and gentamycin. All cells were grown at 37°C in a humid environment containing 5% CO_2, changing the cell culture media every 2 to 3 days. The stratification of primary corneal epithelial cells and HCEC line on an air-liquid interface matrix was performed as previously described (87).

CD14 and LBP protein quantification by ELISA

The collected tear samples were centrifuged for 5 min at 10,000 X g at 4°C to sediment any cellular and insoluble debris. The sCD14 and LBP concentrations in tears, cornea, lacrimal gland, primary cells and HCEC extracts were measured by ELISA (HyCult Biotechnology, Uden, The Netherlands).

RNA isolation and RT-PCR analysis

Messenger RNA was isolated from lacrimal glands, scraped corneal epithelia, confluently grown primary corneal epithelial cells and HCEC line with the RNeasy Mini Kit (Qiagen, Chatsworth, CA). To ensure that all genomic DNA was completely removed from the samples, extracts were subjected to DNase digestion with the RNase-free DNase kit (Qiagen, Chatsworth, CA). The random primed cDNA synthesis was performed with Superscript™ First-Strand Synthesis for RT-PCR (Invitrogen, Carlsbad, CA) as per manufacturer's instructions. Oligonucleotide primers used to amplify CD14, LBP, TLR4 and MD-2 (Table 2) were designed based on the published sequences (GenBank accession numbers: X06882, AF105067, U88880 and AB018549, respectively) and by using the primer design software Gene Runner (version 3.05, Hastings Software Inc., Hastings, NY). PCR was performed using the REDExtract-N-Amp™ PCR Readymix™ (Sigma, St. Louis, MO) and was carried out with 35 cycles of denaturation at 94°C for 45 seconds, annealing at 53°C or 59°C for 45 seconds and extension at 72°C for 45 seconds. The resulting products were resolved by electrophoresis in ethidium bromide-stained 1% low-melt agarose gel. To further confirm the veracity of the RT-PCR products, the amplified sequences were purified with the QIAquick Gel Extraction Kit (Qiagen, Chatsworth, CA) and sequenced by the University of Ottawa Biotechnology Research Institute (Ottawa, ON) using the PCR primers.

Table 2. LPS receptor complex RT-PCR primer sequences.

Gene name	Annealing temperature (°C)	Primer direction	Primer sequence
hCD14	59	Sense	5'-CGCGGAAGATATCACCACGCCAGAACCTTGTGAGCTGGA
		Antisense	5'-GGCATAAGCTTGGATCCTTAGGCAAAGCCCCGGGCCCCT
hLBP	59	Sense	5'-GCTGTTGAACCTCTTCCACAACCAG
		Antisense	5'-CTGAAGTTCAGGAGCGGAGCAGAG
hTLR4	59	Sense	5'-ATGGCCTTCCTCTCCTGCGTGAGAC
		Antisense	5'-TCTGTGCAATAAATACTTTGAATCTTGTTGCTGG
hMD-2	53	Sense	5'-TTCCATATTTACTGAAGCTCAGAAGCAG
		Antisense	5'-GGGCTCCCAGAAATAGCTTCAAC

Immunoblotting

Samples containing CD14 and LBP were resolved by SDS-PAGE electrophoresis under reducing conditions (12% resolving gel) and transferred onto nitrocellulose (Amersham Biosciences, Piscataway, NJ). The membrane was thereafter blocked for 1 h in 5% dried skim milk in TBS with 0.1% Tween-20. CD14 and LBP were probed with the biotinylated polyclonal anti-human CD14 antibody (0.05 μg/mL in TBS-Tween) or with the biotinylated polyclonal anti-human LBP antibody (0.1 μg/mL in TBS-Tween) (R&D Systems, Minneapolis, MN) respectively. After extensive washing, the membrane was incubated for 1 h with the anti-biotin HRP-conjugated antibody (1:1000) (Cell Signaling Technology, Beverly, MA). The antigens were detected using a chemiluminescent system (ECL Western Blotting Detection Reagents, Amersham Biosciences, Piscataway, NJ).

Immunofluorescence staining

Human corneal epithelial cells were grown on a sterile microscope coverslip placed in a 6 well tissue culture plate. After reaching 70 to 80% confluence, cells were fixed with 3.7% paraformaldehyde for 20 min at RT and permeabilized with 0.2% triton X-100 for 20 min at RT. Human corneas and lacrimal glands were fixed overnight at 4°C in 4% paraformaldehyde. Following an overnight equilibration in 30% sucrose, they were incubated at room temperature for 2 h in a 1:1 solutions of 30% sucrose:Optimum Cutting Temperature embedding medium. Samples were flash frozen in sucrose:Optimum Cutting Temperature embedding medium, cryosectioned to 10 μm on a Shandon cryostat (Thermo Electron Corporation, Waltham, MA), and mounted on Superfrost slides (Fisher Scientific, Nepean, ON). After air-drying for 2 h, slides were stored in –80°C until use.

For immunostaining, corneal and lacrimal cryosections were rehydrated in PBS for 10 min. All slides were blocked in 5% normal donkey serum (Jackson ImmunoResearch, West Grove, PA) for 1 h at 37°C. For histological localization of CD14 and LBP, the slides were incubated overnight at 4°C with 27.5 μg/mL mouse monoclonal anti-CD14 antibody (MY4, Beckman Coulter, Miami, FL) in PBS containing 5% normal donkey serum and 0.3% triton-X. The sections were thereafter overlaid with 0.7 μg/mL of anti-LBP rabbit polyclonal antibody (HyCult Biotechnology, Uden, The Netherlands) for 2 h at 37°C. After extensive washing, the slides were incubated for 2 h at 37°C with 30 μg/mL fluorescein isothiocyanate (FITC)-conjugated anti-mouse IgG and 30 μg/mL rhodamine red-X (RRX)-conjugated anti-rabbit IgG antibodies (Jackson ImmunoResearch, West Grove, PA). The corneal sections were further incubated with the 2-minute DAPI fluorescent counterstaining (Innogenex, San Ramon, CA) followed by mounting (Vectashield mounting medium, Vector Laboratories, Burlingame, CA) of the microscope slide. Sections were observed with the Axioskop 2 fluorescent microscope (Carl Zeiss, Thornwood, NY).

The immunohistological localization of TLR4 and MD-2 was performed by blocking the rehydrated cryosections with 5% normal donkey serum (Jackson ImmunoResearch, West Grove, PA). The TLR4 and MD-2 proteins were localized with 2 μg/mL biotinylated goat polyclonal anti-TLR4 antibody (R&D Systems, Minneapolis, MN) and 8 μg/mL rabbit polyclonal anti-MD-2 antibody (FL-160, Santa Cruz Biotechnology, Santa Cruz, CA) incubated for 2 h at 37°C. After 3 washes in PBS, the sections were further incubated for 2 h at 37°C with 32 μg/mL FITC-conjugated mouse monoclonal anti-biotin and 30 μg/mL RRX-conjugated anti-rabbit IgG antibodies (Jackson ImmunoResearch, West Grove, PA). The nuclei were visualized with DAPI staining and the slides were mounted as described above.

LPS biological assays on cultured human corneal epithelial cells

To quantify cytokine production, cultured primary corneal epithelial cells and HCEC line were plated in 24-well flat-bottom tissue culture plates. After reaching approximately 80% confluence, the cells were left untreated or were preincubated with various doses of filter-sterilized pooled human tears, 500 ng/mL recombinant human sCD14 (R&D Systems, Minneapolis, MN), 150 ng/mL recombinant human LBP (R&D Systems, Minneapolis, MN), 10 μg/mL anti-human CD14 monoclonal antibody MY4 (mouse IgG2b; Beckman Coulter, Miami, FL), 10 μg/mL anti-human LBP monoclonal antibody 6G3 (mouse IgG1; HyCult Biotechnology, Uden, The Netherlands); and 10 μg/mL of their isotype-matched controls MOPC-141 and MOPC-21, respectively (Sigma-Aldrich, St. Louis, MO) for 2 h at 37°C. To eliminate any unwanted LPS contaminants affecting cytokine production, the endotoxin levels were measured in all reagents with a gelatin assay of Limulus amebocyte lysate (Associates of Cape Cod, East Falmouth, MA). Any reagent that tested positive for LPS was treated with END-X (Associates of Cape Cod, East Falmouth, MA) to remove any residual endotoxin. With sCD14, LBP, tears and antibodies still present in the medium, LPS derived from *Pseudomonas aeruginosa* 10 (Sigma-Aldrich, St. Louis, MO) was added at a concentration of 100 ng/mL to activate the cells. The medium was harvested after 24 h, centrifuged to remove cellular debris and stored at −70°C until analysis. The culture supernatants were analyzed by ELISA for IL-8 (Sanguin Reagents, Amsterdam, Netherlands) and IL-6 (eBioscience, San Diego, CA).

Statistical analysis

Individual experiments in this study were performed in triplicate to confirm the reproducibility of the results. Values are presented as mean ± standard deviation. The statistical significance of differences between two or more means was evaluated using one-way analysis of

variance (ANOVA), with P values of less than 0.05 (indicated by asterisks) were considered statistically significant.

Results

Quantification of sCD14 and LBP in human tears

Both sCD14 and LBP proteins in onion-vapor stimulated tears from healthy individuals were found to be present in all tear samples (n = 91), with a mean concentration of 561.1 ± 281.6 ng/mL for sCD14 and 135.8 ± 106.6 ng/mL for LBP. Among different individuals, sCD14 and LBP levels varied from 35.4 to 1,249.5 ng/mL and from 23.5 to 307.4 ng/mL, respectively. Linear regression and one-way ANOVA revealed that age, gender, contact lens wear and continuous tear stimulation had no influence on sCD14 and LBP values in reflex tears (Figure 4 and Table 3). Western blotting analysis of representative tear samples showed that sCD14 exhibited an apparent molecular weight of 50 kDa (Figure 5a, lane 4), characteristic of the secretory form of the protein (88). Immunoblotting also revealed the presence of the 60 kDa LBP protein in human tears, which corresponded to the same apparent molecular mass as serum LBP (Figure 5a, lane 4 and 2, respectively).

Human lacrimal glands are the source of tear sCD14 and LBP

Immunoblotting analysis was performed on human lacrimal gland extracts (n = 4) to determine the source of these tear immune proteins. Two polypeptides of molecular mass of 50 and 55 kDa were detected with the anti-CD14 antibody, while a 60 kDa protein was identified as LBP with the anti-LBP antibody (Figure 5a, lane 3). CD14 and LBP expression was further

Figure 4. CD14 and LBP innate immune proteins are abundant in onion-vapor stimulated human tears. To investigate the effects of age on tear sCD14 **(a)** and LBP **(b)** concentration, both proteins were quantified by ELISA in tears of 67 non-contact lens wearers. Linear regression and correlation coefficient were calculated using Microsoft Excel. **(c)** Five successive 50 μL tear aliquots from 11 donors were analyzed by ELISA to determine if tear sCD14 and LBP levels vary with time after stimulation. Results are expressed as means ± SD.

a

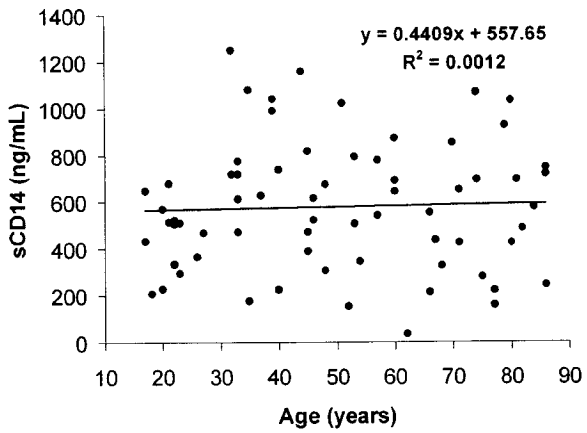
y = 0.4409x + 557.65
R² = 0.0012
sCD14 (ng/mL)
1400
1200
1000
800
600
400
200
0
10 20 30 40 50 60 70 80 90
Age (years)

b

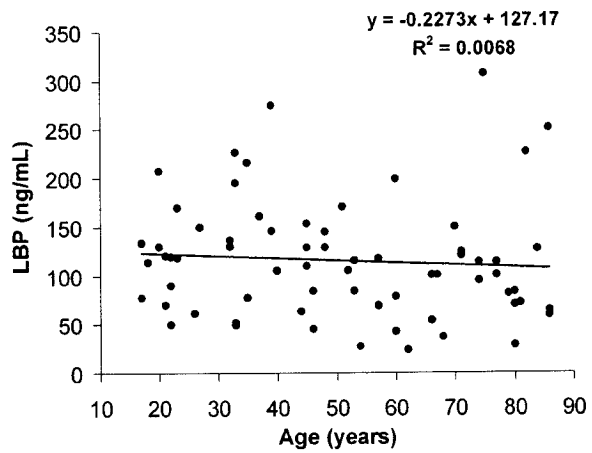
y = -0.2273x + 127.17
R² = 0.0068
LBP (ng/mL)
350
300
250
200
150
100
50
0
10 20 30 40 50 60 70 80 90
Age (years)

c

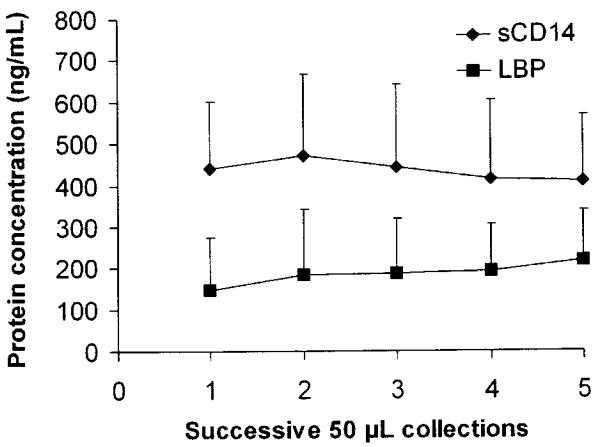
sCD14
LBP
Protein concentration (ng/mL)
800
700
600
500
400
300
200
100
0
0 1 2 3 4 5
Successive 50 µL collections

Figure 4

Table 3. Levels of sCD14 and LBP in human tears according to gender and contact lens wear.

Study groups[a]	sCD14[b] (ng/mL)	LBP[b] (ng/mL)
Women (n=34)	562 ± 337	140 ± 132
Men (n=33)	597 ± 194	125 ± 90
Non contact lens wearers (n=67)	579 ± 274	133 ± 113
Contact lens wearers (n=24)	509 ± 300	143 ± 90

[a] The first study group was composed of 67 healthy non-contact lens wearers, 34 women and 33 men; with a median age of 48 years and a range of 17-86 years. The second group was composed of 24 healthy contact lens wearers, including 13 women and 11 men; with a median age of 27 years and a range of 16-54 years. Tear production was stimulated by onion vapors and reflex tears were collected with flamed-polished disposable microcapillaries.

[b] The quantification of sCD14 and LBP in tears was performed by ELISA using commercially available kits. Results are expressed as means ± SD.

Figure 5. The LPS receptor complex proteins, CD14, LBP, TLR4 and MD-2 are expressed by the lacrimal gland and the corneal epithelia. **(a)** Lacrimal gland, tears and corneal epithelium were analyzed by western immunoblotting with the biotinylated anti-human CD14 or biotinylated anti-human LBP polyclonal antibodies followed by the anti-biotin HRP-linked antibody. **(b)** Detection of CD14, LBP, TLR4 and MD-2 mRNAs by RT-PCR from human lacrimal gland, isolated corneal epithelium, cultured corneal epithelial primary cells and the immortalized human corneal epithelial HCEC cell line. The reactions were performed with and without the reverse-transcriptase (RT) step to confirm the cDNA origin of the amplification.

a

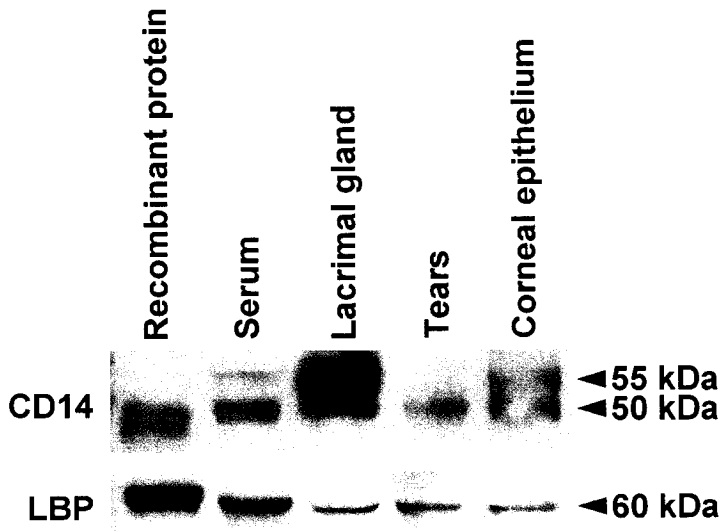
Recombinant protein
Serum
Lacrimal gland
Tears
Corneal epithelium
CD14
LBP
55 kDa
50 kDa
60 kDa

b

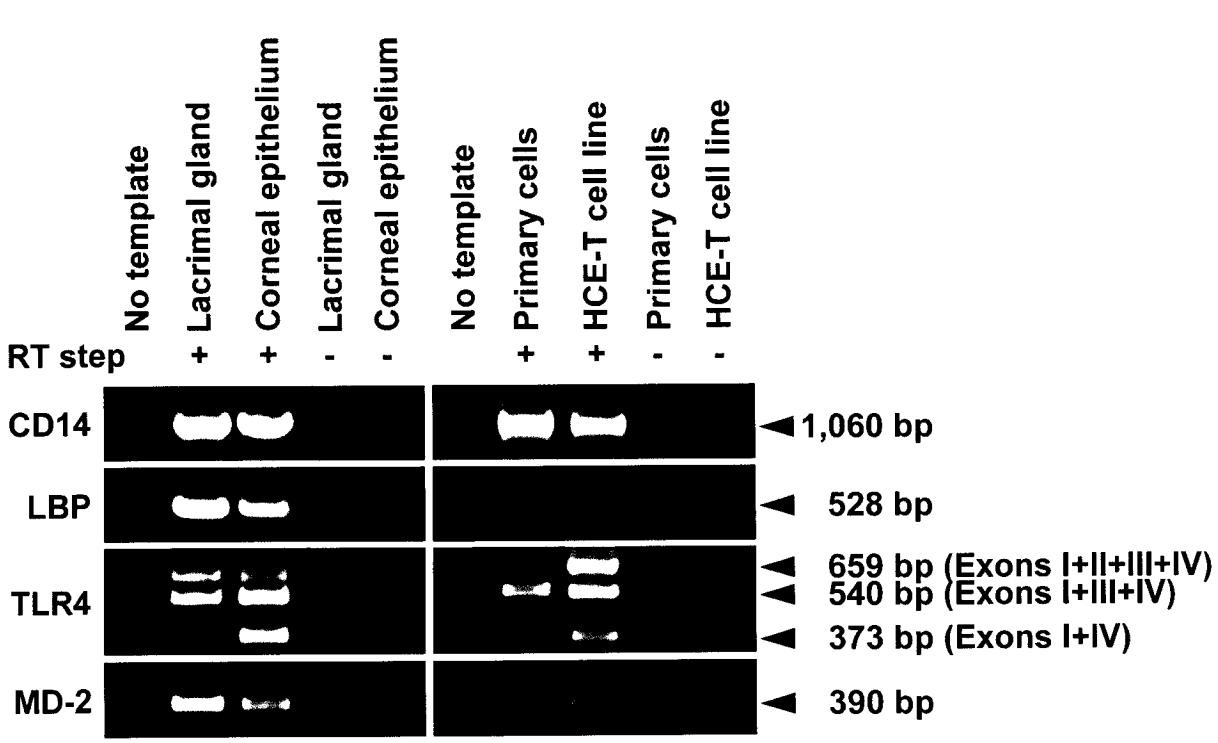
No template
+ Lacrimal gland
+ Corneal epithelium
- Lacrimal gland
- Corneal epithelium
No template
+ Primary cells
+ HCE-T cell line
- Primary cells
- HCE-T cell line
RT step
CD14
LBP
TLR4
MD-2
1,060 bp
528 bp
659 bp (Exons I+II+III+IV)
540 bp (Exons I+III+IV)
373 bp (Exons I+IV)
390 bp

Figure 5

detected in human lacrimal glands by the amplification of both transcripts by RT-PCR (Figure 5b) using human gene specific primers. Sequencing of the RT-PCR products correlated to the CD14 and LBP published sequence (GenBank accession numbers X06882 and AF105067, respectively) (Figure 6 a,b). Immunofluorescence detection of both proteins in human lacrimal glands (n = 4) showed CD14 and LBP to be co-localized in the cytoplasm of acinar cells constituting the alveoli of the serous gland (Figure 7 a-c). Control sections omitting primary antibodies and, cross-reactivity analysis of the secondary antibodies confirmed the specificity of labelling (Figure 7 i-p).

Lacrimal acinar cells also express TLR4 and MD-2

Besides synthesizing and secreting sCD14 and LBP in tears, lacrimal acinar cells were found to express TLR4 and MD-2, as shown by RT-PCR (Figure 5b). For TLR4, however, three products were amplified using primers flanking the region between exons I and IV of the gene. Sequencing of the amplified fragments confirmed the nature of the three splicing variants of human TLR4 (Figure 8). The TLR4 transcript containing exons I, III and IV, encoding the proper functional TLR4 (89), was predominant in human lacrimal gland (Figure 5b). The other two less abundant alternative splicing forms were unlikely to encode a functional TLR4 due to premature translational termination of the protein (89). In the lacrimal acinar cells, both TLR4 and MD-2 proteins were found to be co-localized *in situ* by immunofluorescence (Figure 7 e-g).

Human corneal epithelium expresses the LPS-receptor complex

To examine whether the cornea exhibits a failsafe backup system for its supply of LPS receptor proteins, the expression of these proteins was investigated in this stratified tissue. Immunohistological analysis of human corneas (n = 7) revealed that LBP is strongly expressed in

Figure 6. Nucleotide sequences of human CD14, LBP and MD-2 amplified from human lacrimal gland total mRNA. The identity of the CD14 **(a)**, LBP **(b)** and MD-2 **(c)** products amplified by RT-PCR from human lacrimal gland total mRNA (Figure 5b) were confirmed by sequencing. The sequencing results correspond to: **(a)** nucleotides 370 to 1,034 of the 1,570 nucleotide sequence of CD14 (GenBank accession number X06882), **(b)** nucleotides 627 to 1,072 of the 1,463 nucleotide sequence of LBP mRNA (GenBank accession number AF105067) and **(c)** nucleotides 266 to 551 of the 624 nucleotide sequence of MD-2 mRNA (GenBank accession number AB018549).

a

```
CCCGACTGGT CCGAAGCCTT CCAGTGTGTG TCTGCAGTAG AGGTGGAGAT  50
CCATGCCGGC GGTCTCAACC TAGAGCCGTT TCTAAAGCGC GTCGATGCGG 100
ACGCCGACCC GCGGCAGTAT GCTGACACGG TCAAGGCTCT CCGCGTGCGG 150
CGGCTCACAG TGGGAGCCGC ACAGGTTCCT GCTCAGCTAC TGGTAGGCGC 200
CCTGCGTGTG CTAGCGTACT CCCGCCTCAA GGAACTGACG CTCGAGGACC 250
TAAAGATAAC CGGCACCATG CCTCCGCTGC CTCTGGAAGC CACAGGACTT 300
GCACTTTCCA GCTTGCGCCT ACGCAACGTG TCGTGGGCGA CAGGGCGTTC 350
TTGGCTCGCC GAGCTGCAGC AGTGGCTCAA GCCAGGCCTC AAGGTACTGA 400
GCATTGCCCA AGCACACTCG CCTGCCTTTT CCTGCGAACA GGTTCGCGCC 450
TTCCCGGCCC TTACCAGCCT AGACCTGTCT GACAATCCTG GACTGGGCGA 500
ACGCGGACTG ATGGCGGCTC TCTGTCCCCA CAAGTTCCCG GCCATCCAGA 550
ATCTAGCGCT GCGCAACACA GGAATGGAGA CGCCCACAGG CGTGTGCGCC 600
GCACTGGCGG CGGCAGGTGT GCAGCCCCAC AGCCTAGACC TCAGCCACAA 650
CTCGCTGCGC GCCAC                                       664
```

b

```
TCGGTGTCCT CCGATCTACA GCCTTATCTC CAAACTCTGC CAGTTACAAC  50
AGAGATTGAC AGTTTCGCCG ACATTGATTA TAGCTTAGTG GAAGCCCCTC 100
GGGCAACAGC CCAGATGCTG GAGGTGATGT TTAAGGGTGA AATCTTTCAT 150
CGTAACCACC GTTCTCCAGT TACCCTCCTT GCTGCAGTCA TGAGCCTTCC 200
TGAGGAACAC AACAAAATGG TCTACTTTGC CATCTCGGAT TATGTCTTCA 250
ACACGGCCAG CCTGGTTTAT CATGAGGAAG GATATCTGAA CTTCTCCATC 300
ACAGATGACA TGATACCGCC TGACTCTAAT ATCCGACTGA CCACCAAGTC 350
CTTCCGACCC TTCGTCCCAC GGTTAGCCAG GCTCTACCCC AACATGAACC 400
TGGAACTCCA GGGATCAGTG CCCTCTGCTC CGCTCCTGAA CTTCAG     446
```

c

```
TGTTAACCCC TGTATAGAAT TGAAAGGATC CAAAGGATTA TTGCACATTT  50
TCTACATTCC AAGGAGAGAT TTAAAGCAAT TATATTTCAA TCTCTATATA 100
ACTGTCAACA CCATGAATCT TCCAAAGCGC AAAGAAGTTA TTTGCCGAGG 150
ATCTGATGAC GATTACTCTT TTTGCAGAGC TCTGAAGGGA GAGACTGTGA 200
ATACAACAAT ATCATTCTCC TTCAAGGGAA TAAAATTTTC TAAGGGAAAA 250
TACAAATGTG TTGTTGAAGC TATTTCTGGG AGCCCA               286
```

Figure 6

Figure 7. Immunolocalization of CD14, LBP, TLR4 and MD-2 in human lacrimal glands. **(a,b)** Double immunofluorescence labeling using the monoclonal anti-CD14 (MY4) and the polyclonal anti-LBP antibodies. **(c)** CD14 and LBP merged staining, where the arrows indicate the acinar cell nuclei and the arrowhead refers to the tear duct in the centre of the alveoli. **(d)** The phase contrast image of the tissue confirming the section integrity. **(e,f)** Double-labeling experiment using the biotinylated anti-TLR4 and the polyclonal anti-MD-2 antibodies. **(g,h)** TLR4 and MD-2 merged staining and phase contrast image of the tissue. **(i-p)** Secondary antibody controls were performed by omitting the primary antibodies and the cross-reactivity controls were done by incubating the mouse primary antibody with the anti-rabbit secondary antibody and vice-versa. Original magnification x 400.

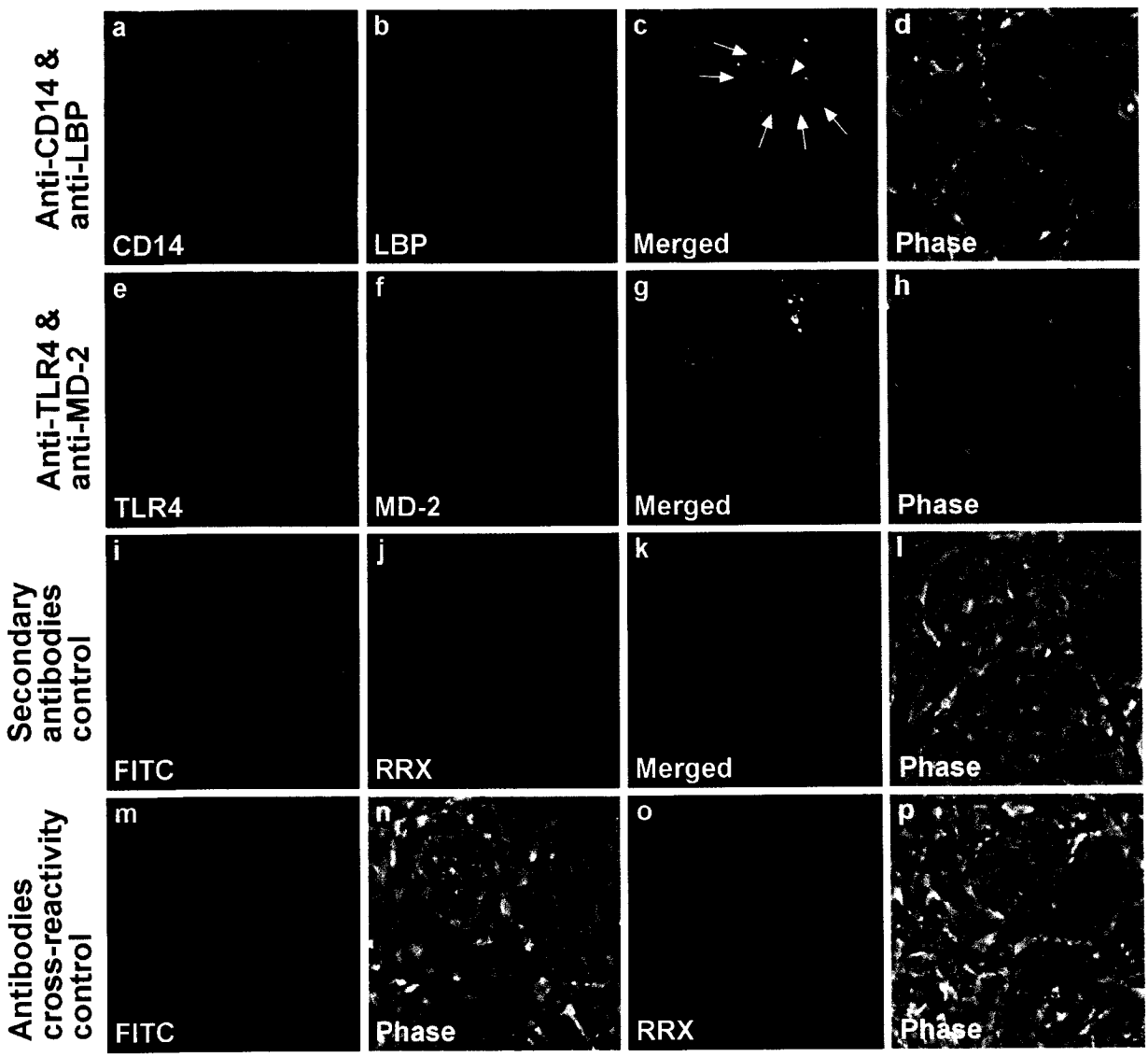
Anti-CD14 & anti-LBP
a
CD14
b
LBP
c
Merged
d
Phase
Anti-TLR4 & anti-MD-2
e
TLR4
f
MD-2
g
Merged
h
Phase
Secondary antibodies control
i
FITC
j
RRX
k
Merged
l
Phase
Antibodies cross-reactivity control
m
FITC
n
Phase
o
RRX
p
Phase

Figure 7

Figure 8. Nucleotide sequences of human TLR4 amplified from human lacrimal gland total mRNA. The identity of the TLR4 products: 659 bp **(a)**, 540 bp **(b)** and 373 bp **(c)** amplified by RT-PCR from human lacrimal gland total mRNA (figure 5b) were confirmed by sequencing. The RT-PCR amplified region covered the three splicing sites of the human TLR4 gene where the four resulting exons are color indicated and their position within the 3,811 nucleotide sequence of TLR4 mRNA (GenBank accession number U88880) is indicated in brackets: **exon 1 in black** (nucleotides 91 to 137), (nucleotides 138 to 258), **exon 3 in blue** (nucleotides 259 to 424) and **exon 4 in red** (nucleotides 425 to 705).

a

```
CCTTCCTCTC CTGCGTGAGA CCAGAAAGCT GGGAGCCCTG CGTGGAG          50
                                                            100
                                                            150
                    GTG GTTCCTAATA TTACTTATCA ATGCATGGAG    200
CTGAATTTCT ACAAAATCCC CGACAACCTC CCCTTCTCAA CCAAGAACCT      250
GGACCTGAGC TTTAATCCCC TGAGGCATTT AGGCAGCTAT AGCTTCTTCA      300
GTTTCCCAGA ACTGCAGGTG CTGGATTTAT CCAGGTGTGA AATCCAGACA      350
ATTGAAGATG GGGCATATCA GAGCCTAAGC CACCTCTCTA CCTTAATATT      400
GACAGGAAAC CCCATCCAGA GTTTAGCCCT GGGAGCCTTT TCTGGACTAT      450
CAAGTTTACA GAAGCTGGTG GCTGTGGAGA CAAATCTAGC ATCTCTAGAG      500
AACTTCCCCA TTGGACATCT CAAAACTTTG AAAGAACTTA ATGTGGCTCA      550
CAATCTTATC CAATCTTTCA AATTACCTGA GTATTTTTCT AATCTGACCA      600
ATCTAGAG                                                   608
```

b

```
CCTTCCTCTC CTGCGTGAGA CCAGAAAGCT GGGAGCCCTG CGTGGAGGTG      50
GTTCCTAATA TTACTTATCA ATGCATGGAG CTGAATTTCT ACAAAATCCC      100
CGACAACCTC CCCTTCTCAA CCAAGAACCT GGACCTGAGC TTTAATCCCC      150
TGAGGCATTT AGGCAGCTAT AGCTTCTTCA GTTTCCCAGA ACTGCAGGTG      200
CTGGATTTAT CCAGGTGTGA AATCCAGACA ATTGAAGATG GGGCATATCA      250
GAGCCTAAGC CACCTCTCTA CCTTAATATT GACAGGAAAC CCCATCCAGA      300
GTTTAGCCCT GGGAGCCTTT TCTGGACTAT CAAGTTTACA GAAGCTGGTG      350
GCTGTGGAGA CAAATCTAGC ATCTCTAGAG AACTTCCCCA TTGGACATCT      400
CAAAACTTTG AAAGAACTTA ATGTGGCTCA CAATCTTATC CAATCTTTCA      450
AATTACCTGA GTATTTTTCT AATCTGACCA ATCTAGAGCA CTTGG           495
```

c

```
CCTTCCTCTC CTGCGTGAGA CCAGAAAGCT GGGAGCCCTG CGTGGAGGTG      50
TGAAATCCAG ACAATTGAAG ATGGGGCATA TCAGAGCCTA AGCCACCTCT      100
CTACCTTAAT ATTGACAGGA AACCCCATCC AGAGTTTAGC CCTGGGAGCC      150
TTTTCTGGAC TATCAAGTTT ACAGAAGCTG GTGGCTGTGG AGACAAATCT      200
AGCATCTCTA GAGAACTTCC CCATTGGACA TCTCAAAACT TTGAAAGAAC      250
TTAATGTGGC TCACAATCTT ATCCAATCTT TCAAATTACC TGAGTATTTT      300
TCTAATCTGA CCAATCTAGA G                                    321
```

Figure 8

the squamous superficial epithelium and sparsely expressed in the columnar basal cells (Figure 9b). Negligible LBP staining was observed among wing cells composing the intermediate layer of the corneal epithelium. Corneal CD14 expression was sparse and mainly limited to the basal epithelial cells with an absence of staining in the superficial and wing cells (Figure 9a). In the basal epithelium, LBP and CD14 were not co-localized suggesting they were expressed by different epithelial cells (Figure 9c). Both CD14 and LBP could also be detected by western blotting in isolated corneal epithelia (Figure 5a, lane 5), thus further confirming the immunofluorescence results. In contrast, TLR4 and MD-2 expression was polarized with ubiquitous staining along the basal and wing epithelial cells, with little or no expression in the superficial differentiated epithelium (Figure 9 e,f). Image overlay indicated that both proteins were expressed by the same cells (Figure 9g). To elucidate the origin of these proteins, the respective CD14, LBP, TLR4 and MD-2 mRNAs were detected by RT-PCR in the isolated human corneal epithelia (n = 3) (Figure 5b). The three splicing forms of human TLR4 were amplified from corneal epithelial cDNA, with the functional transcript composed of exons I, III and IV being the most abundant.

Primary human corneal epithelial cells and HCEC line do not express the entire LPS receptor complex *in vitro*

HCEC line may complement tear sCD14 and LBP to reconstitute the LPS complex *in ambio*. To test this hypothesis, their expression was analyzed *in vitro*. CD14 mRNA was amplified by RT-PCR from freshly isolated primary corneal epithelial cells and from the HCEC line (Figure 5b). LBP mRNA was not detected in both primary and HCEC cells (Figure 5b). These results were supported by immunofluorescence, where CD14, but not LBP, showed some reactivity in both HCEC (Figure 10 a-c) and primary corneal epithelial cells (data not shown).

Figure 9. Immunolocalization of CD14, LBP, TLR4 and MD-2 in human corneal epithelium. **(a,b)** Double immunofluorescence labeling using the monoclonal anti-CD14 MY4 and the polyclonal anti-LBP antibodies. **(c)** CD14 and LBP staining were merged with the DAPI stained nuclei. **(d)** The phase contrast image of the tissue, where the corneal organization is indicated as follows: S, superficial epithelial cells; W, wing epithelial cells; B, basal epithelial cells; BM, Bowman's membrane and ST, stroma. **(e,f)** Double-labelling experiment using the biotinylated anti-TLR4 and the polyclonal anti-MD-2 antibodies. **(g,h)** Merged staining of TLR4 and MD-2 with DAPI, and phase contrast image of the tissue. **(i-p)** Secondary antibody controls and the cross-reactivity controls were performed as previously described. Original magnification x 400.

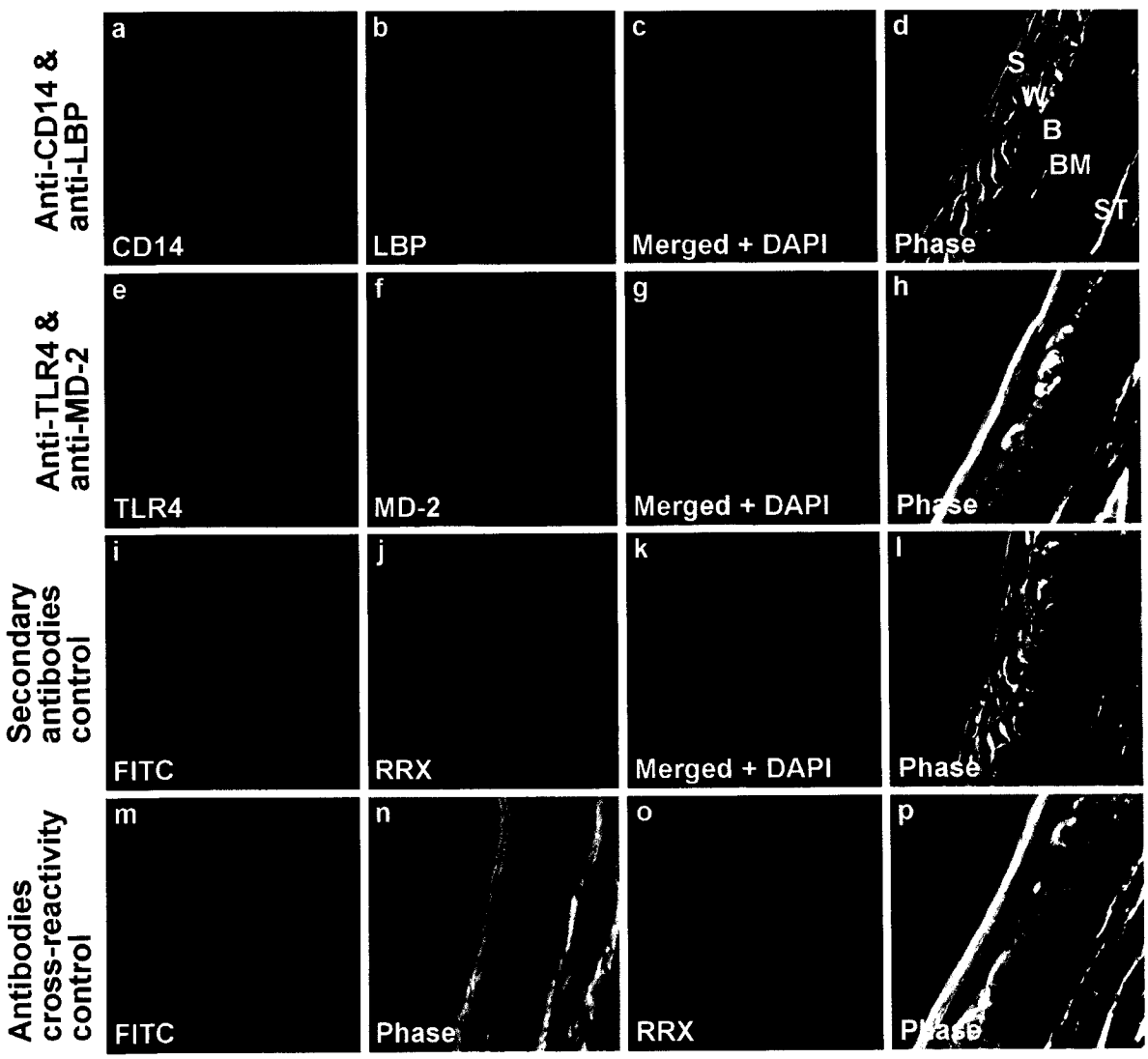
Anti-CD14 & anti-LBP
a
CD14
b
LBP
c
Merged + DAPI
d
S
W
B
BM
ST
Phase
Anti-TLR4 & anti-MD-2
e
TLR4
f
MD-2
g
Merged + DAPI
h
Phase
Secondary antibodies control
i
FITC
j
RRX
k
Merged + DAPI
l
Phase
Antibodies cross-reactivity control
m
FITC
n
Phase
o
RRX
p
Phase

Figure 9

Figure 10. Immunolocalization of CD14, LBP, TLR4 and MD-2 in the human corneal epithelial cell line HCEC. **(a,b)** Double immunofluorescence labeling using the monoclonal anti-CD14 (MY4) and the polyclonal anti-LBP antibodies. **(c,d)** CD14 and LBP merged staining and phase contrast image. **(e,f)** Double-labelling experiment using the biotinylated anti-TLR4 and the polyclonal anti-MD-2 antibodies. **(g,h)** TLR4 and MD-2 merged staining and phase contrast image. **(i-p)** Secondary antibody controls and the cross-reactivity controls were performed as previously described. Similar expression pattern of the LPS receptor complex was observed with primary corneal epithelial cells (data not shown). Original magnification x 400.

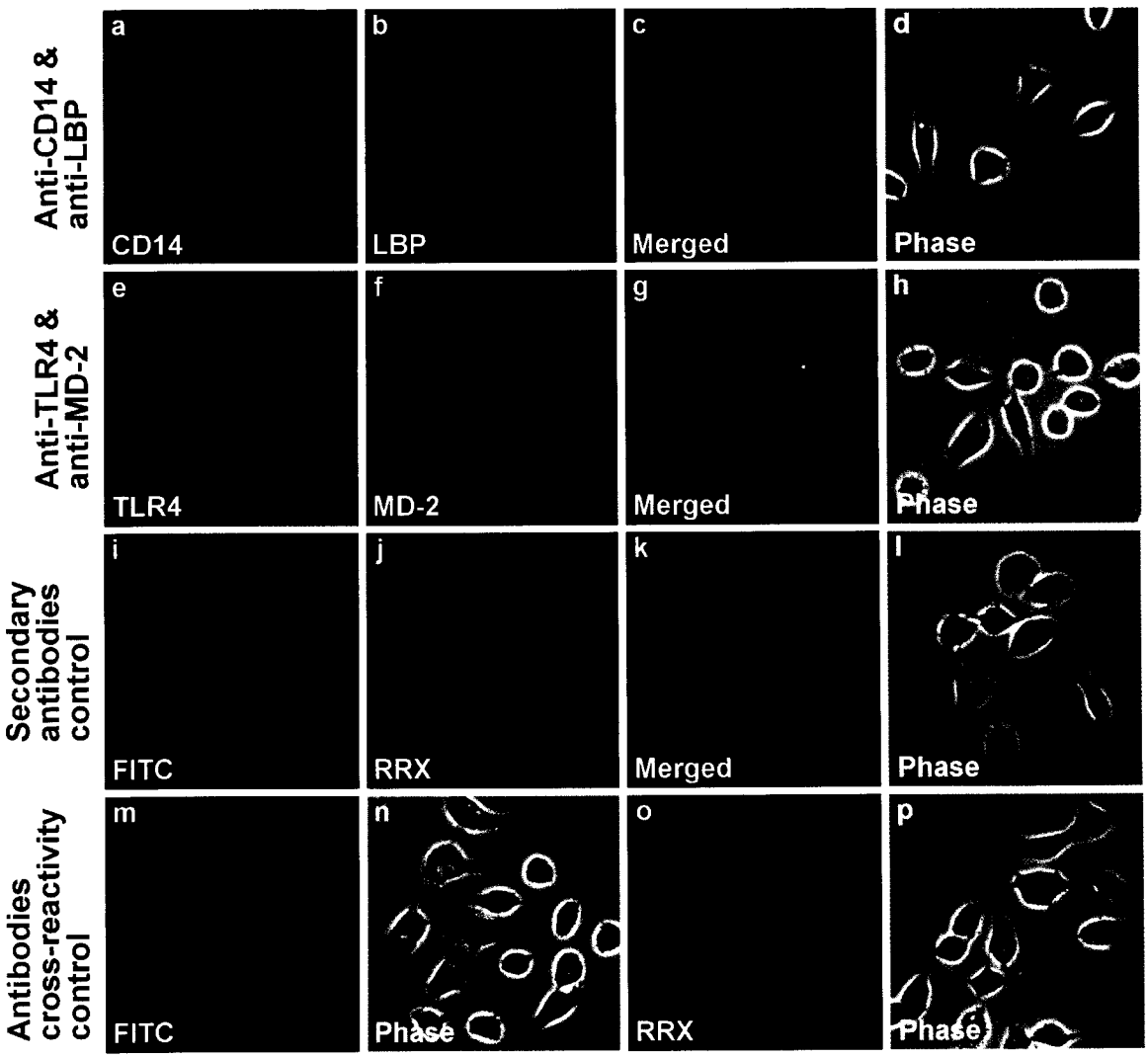
Anti-CD14 & anti-LBP
a
CD14
b
LBP
c
Merged
d
Phase
Anti-TLR4 & anti-MD-2
e
TLR4
f
MD-2
g
Merged
h
Phase
Secondary antibodies control
i
FITC
j
RRX
k
Merged
l
Phase
Antibodies cross-reactivity control
m
FITC
n
Phase
o
RRX
p
Phase

Figure 10

ELISA on total cell lysate and culture supernatant indicated that CD14 was expressed by corneal epithelial cells but was not secreted, as the media showed no CD14 reactivity with the ELISA kit (data not shown). LBP was not detected by ELISA in corneal epithelial cell lysate or culture supernatant, which suggested that it was not expressed by primary and HCEC cells *in vitro*. Cultures of primary corneal epithelial cells and HCEC differentiated in supplemented hormonal epithelial medium or stratified on an air-liquid interface matrix failed to induce LBP expression (data not shown). On the other hand, both TLR4 and MD-2 were expressed *in vitro* as confirmed by RT-PCR (Figure 5b) and immunofluorescence (Figure 10 e-g).

Primary human corneal epithelial cells and HCEC line respond to LPS in the presence of tear sCD14 and LBP

To assess the biological relevance of tear sCD14 and LBP in the initiation of an endotoxin immune response, the production of proinflammatory molecules was analyzed in primary human corneal epithelial cells and HCEC line challenged with *Pseudomonas*-derived LPS in the presence of sCD14, LBP and human tears. *In vitro* cultures of primary corneal epithelial cells and HCEC line had expression patterns of the LPS receptor complex (Figure 5b, and 10 a-h) similar to those of basal and wing epithelial cells *in vivo* (Figure 9 a-h). Therefore, primary and HCEC cells represent an adequate *in vitro* model of the inner epithelial layers of a breached cornea to study LPS responsiveness in amplifying cells. LPS alone had little effect on IL-6 and IL-8 secretion by primary corneal epithelial cells (Figure 11 a,b) and HCEC line (Figure 11 c,d) as previously observed (79, 80), whereas the addition of recombinant sCD14 or LBP increased IL-6 and IL-8 production (Figure 11). However, no major difference was detected in IL-6 or IL-8 production whether sCD14 and LBP were added alone or combined. This indicated that the two soluble proteins increased, individually or in concert, the efficiency of the

Figure 11. Enhanced LPS response of primary corneal epithelial cells and HCEC line in presence of sCD14 and LBP. Primary corneal epithelial cells **(a,b)** and HCEC line **(c,d)** were pretreated with sCD14 and LBP (500 ng/mL and 150 ng/mL respectively, the average concentrations found in human tears), anti-CD14 monoclonal antibody MY4 (10 μg/mL), anti-LBP monoclonal antibody 6G3 (10 μg/mL) and their isotype-matched controls (IgG2b and IgG1 respectively at 10 μg/mL each) before addition of LPS from *P. aeruginosa* (100 ng/mL). Secretion of IL-6 and IL-8 proinflammatory cytokines in the cell culture media was assessed by ELISA. Results are expressed as means ± SD of triplicate cultures of one experiment representative of three. Statistically significant differences were determined using one-way ANOVA, with probabilities $*P < 0.05$ and $**P < 0.005$.

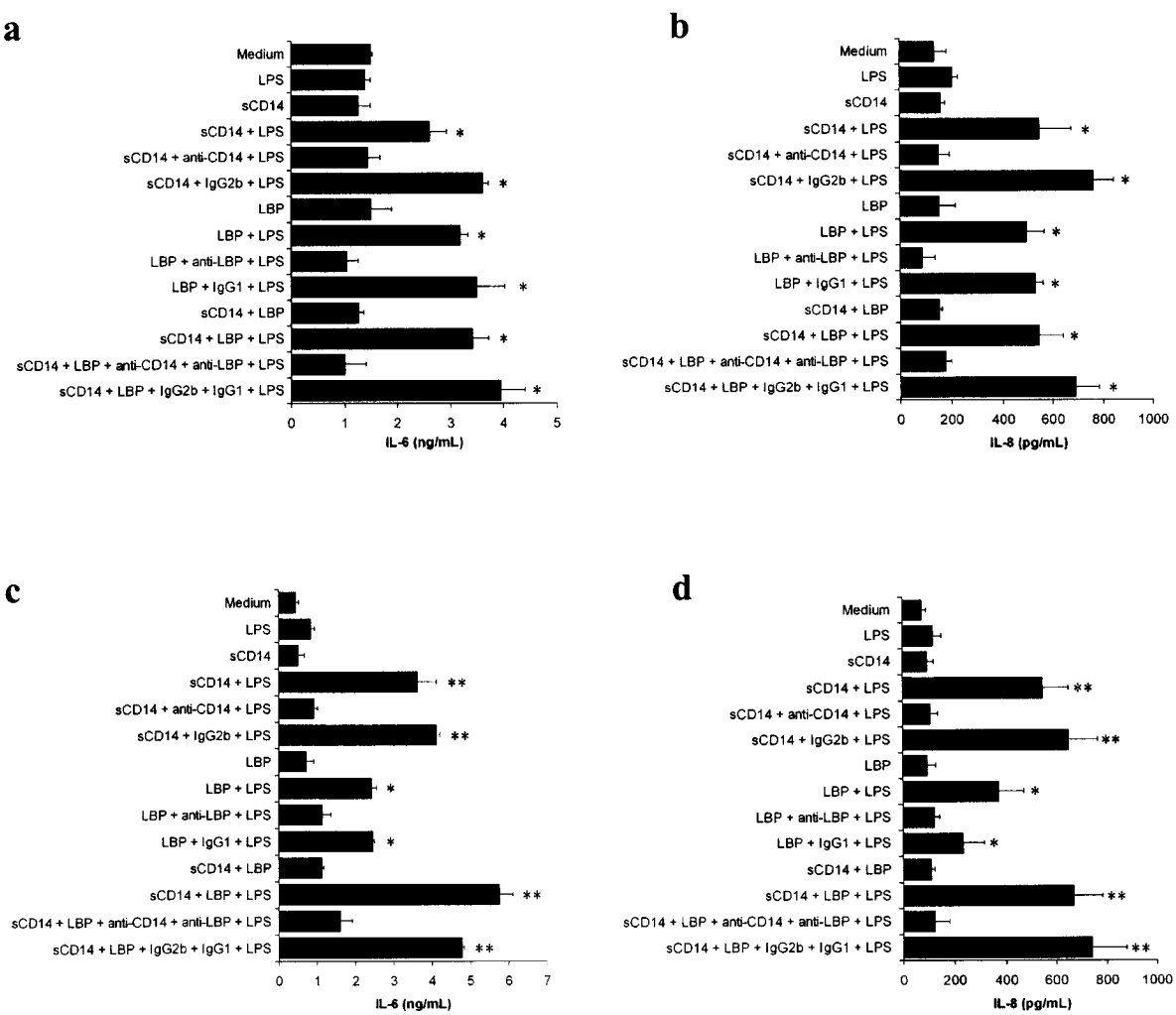
a
Medium
LPS
sCD14
sCD14 + LPS
sCD14 + anti-CD14 + LPS
sCD14 + IgG2b + LPS
LBP
LBP + LPS
LBP + anti-LBP + LPS
LBP + IgG1 + LPS
sCD14 + LBP
sCD14 + LBP + LPS
sCD14 + LBP + anti-CD14 + anti-LBP + LPS
sCD14 + LBP + IgG2b + IgG1 + LPS
0 1 2 3 4 5
IL-6 (ng/mL)
b
Medium
LPS
sCD14
sCD14 + LPS
sCD14 + anti-CD14 + LPS
sCD14 + IgG2b + LPS
LBP
LBP + LPS
LBP + anti-LBP + LPS
LBP + IgG1 + LPS
sCD14 + LBP
sCD14 + LBP + LPS
sCD14 + LBP + anti-CD14 + anti-LBP + LPS
sCD14 + LBP + IgG2b + IgG1 + LPS
0 200 400 600 800 1000
IL-8 (pg/mL)
c
Medium
LPS
sCD14
sCD14 + LPS
sCD14 + anti-CD14 + LPS
sCD14 + IgG2b + LPS
LBP
LBP + LPS
LBP + anti-LBP + LPS
LBP + IgG1 + LPS
sCD14 + LBP
sCD14 + LBP + LPS
sCD14 + LBP + anti-CD14 + anti-LBP + LPS
sCD14 + LBP + IgG2b + IgG1 + LPS
0 1 2 3 4 5 6 7
IL-6 (ng/mL)
d
Medium
LPS
sCD14
sCD14 + LPS
sCD14 + anti-CD14 + LPS
sCD14 + IgG2b + LPS
LBP
LBP + LPS
LBP + anti-LBP + LPS
LBP + IgG1 + LPS
sCD14 + LBP
sCD14 + LBP + LPS
sCD14 + LBP + anti-CD14 + anti-LBP + LPS
sCD14 + LBP + IgG2b + IgG1 + LPS
0 200 400 600 800 1000
IL-8 (pg/mL)

Figure 11

LPS-induced response. The recombinant sCD14 and LBP-mediated activation was significantly abrogated by the neutralizing anti-CD14 MY4 and the anti-LBP 6G3 antibodies, thus suggesting that both proteins contributed to this activity (Figure 11). Pooled human tears were also tested for enhancing LPS-mediated cytokine production. Tear sCD14 and LBP mediated the activation of primary and HCEC cells by endotoxin in a dose-dependant manner to produce IL-6 and IL-8 (Figure 12). The tear induced production of IL-6 and IL-8 in primary corneal epithelial cells (Figure 12 a,b) and HCEC line (Figure 12 c,d) was significantly inhibited by the anti-CD14 MY4 and the anti-LBP 6G3 antibodies, but not by their isotype-antibody matched controls, therefore supporting the biological activity of sCD14 and LBP in tears for mediating innate immunity.

Figure 12. Enhanced LPS response of primary corneal epithelial cells and HCEC line in presence of human tears. Primary corneal epithelial cells **(a,b)** and HCEC **(c,d)** were pretreated with various concentrations of pooled human tears, anti-CD14 monoclonal antibody MY4 (10 μg/mL), anti-LBP monoclonal antibody 6G3 (10 μg/mL) and their isotype-matched controls (IgG2b and IgG1 respectively at 10 μg/mL each) before addition of LPS from *P. aeruginosa* (100 ng/mL). Secretion of IL-6 and IL-8 proinflammatory cytokines in the cell culture media was assessed by ELISA. Results are expressed as means ± SD of triplicate cultures of one experiment representative of three. Statistically significant differences were determined using one-way ANOVA, with probabilities $*P < 0.01$.

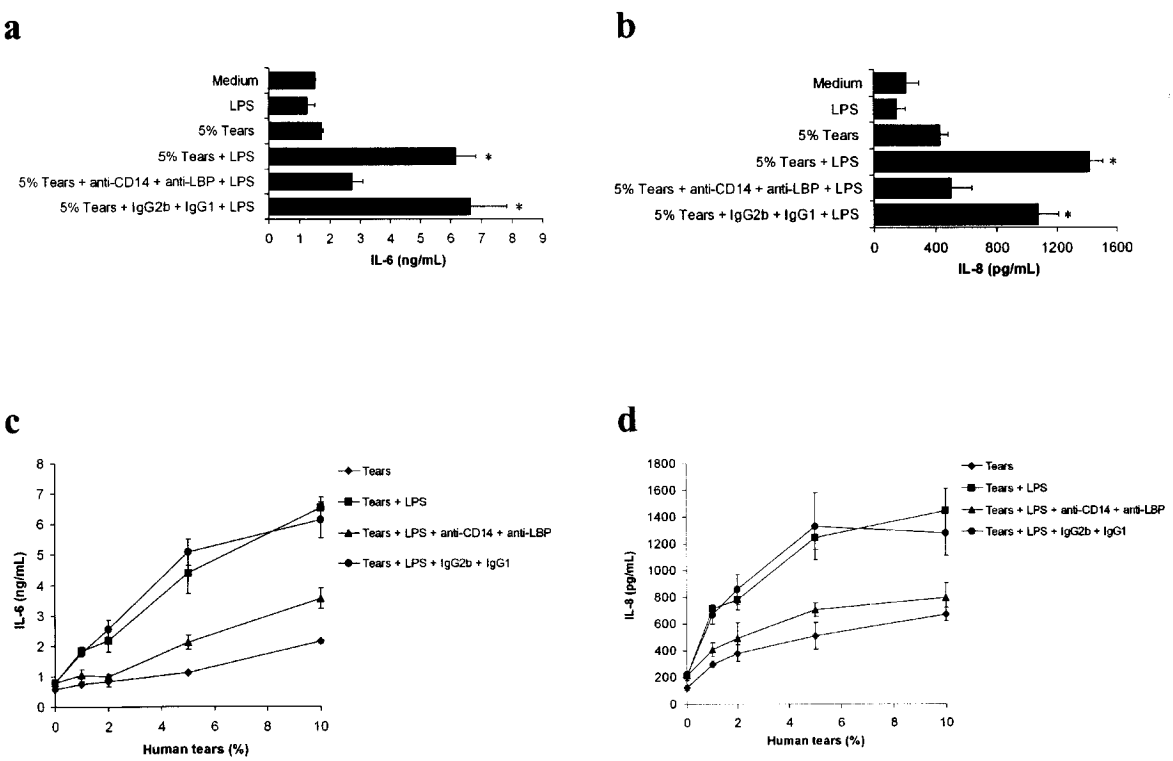
a
Medium
LPS
5% Tears
5% Tears + LPS
5% Tears + anti-CD14 + anti-LBP + LPS
5% Tears + IgG2b + IgG1 + LPS
0 1 2 3 4 5 6 7 8 9
IL-6 (ng/mL)
b
Medium
LPS
5% Tears
5% Tears + LPS
5% Tears + anti-CD14 + anti-LBP + LPS
5% Tears + IgG2b + IgG1 + LPS
0 400 800 1200 1600
IL-8 (pg/mL)
c
IL-6 (ng/mL)
Human tears (%)
Tears
Tears + LPS
Tears + LPS + anti-CD14 + anti-LBP
Tears + LPS + IgG2b + IgG1
d
IL-8 (pg/mL)
Human tears (%)
Tears
Tears + LPS
Tears + LPS + anti-CD14 + anti-LBP
Tears + LPS + IgG2b + IgG1

Figure 12

Discussion

In this study, the LPS from *P. aeruginosa* induced an innate immune response in basal corneal epithelial cells due its interaction with two LPS receptor proteins, sCD14 or LBP, discovered in tears bathing the surface of the eye. The detection of sCD14 in reflex tears supports the presence of the protein in other human secretory fluids (25, 26, 29, 30). However, the presence of LBP in tears is remarkable, as it was undetectable in other secretions, such as urine (29), seminal fluid (30) and saliva (25), with the exception of breast milk where trace amounts of the protein were found (26). The dual presence of sCD14 and LBP in tears could be attributed to the extremely delicate structure of the cornea, requiring more sensitive detection of Gram-negative bacteria to eliminate any potential sight threatening damages caused by infections. Since non-stimulated basal tears contain higher or equivalent amounts of lactoferrin, sIgA and lysozyme compared to stimulated reflex tears (90), the levels of sCD14 and LBP in basal tears may therefore be higher or equivalent to those measured in reflex tears. The broad concentration range of both proteins among different individuals and the unchanged sCD14 and LBP levels between age groups, gender, and contact lens wear are characteristics shared by other tear innate immune proteins, such as lactoferrin (91) or lysozyme (92), thus confirming the innate nature of both CD14 and LBP for ocular protection.

The mRNA and protein detection of CD14 and LBP in the lacrimal gland suggests that acinar epithelial cells are a main source of both proteins in human tears. In addition, the sole presence of the 50 kDa sCD14 isoform in human tears makes any contributions from serum exudate unlikely due to the presence of two serum sCD14 isoforms: 50 kDa and 55 kDa (93). The 50 kDa sCD14 isoform in tears is likely to originate from the cleavage of a 55 kDa precursor (93) which was present, in addition to the 50 kDa soluble isoform, in the lacrimal protein extract. Another potential source of LBP in tears is the superficial corneal epithelial cells, as they were

shown by immunofluorescence to express the protein. The fact, however, that reflex tears flow voluminously and quickly could suggest that such a contribution by superficial corneal epithelial cell may be secondary.

At least four potential roles of tear sCD14 and LBP are foreseen: (i) protection of the lacrimal gland against Gram-negative infections, (ii) opsonization of Gram-negative bacteria and LPS to prevent their adherence on the intact corneal epithelium, (iii) efficient delivery of LPS to the exposed inner epithelial layers of the breached corneal epithelium, and (iv) protection of the downstream lacrimal sac and nasal epithelium against infection via tear sCD14 and LBP drainage through the nasolacrimal duct:

The infrequency of lacrimal gland infections (94) could be in part attributed to the abundance and variety of antimicrobial products synthesized and secreted by this serous gland. Besides expressing sCD14 and LBP, acinar cells were also shown to express TLR4 and MD-2, therefore enabling them to respond to Gram-negative insults threatening to compromise the essential ocular function of this organ (Figure 13a).

Due to its anatomical localization, the corneal epithelium is constantly exposed to microorganisms and their virulence factors. In keratitis, *P. aeruginosa* adheres to corneal epithelial cells through adhesins, such as LPS that binds to specific corneal epithelial molecules, like asialo GM_1 glycolipids (95), galectin-3 (96) and cystic fibrosis transmembrane conductance regulator (CFTR) (97). An inflammatory response against pathogens, although beneficial in other organs, may affect corneal transparency. The infiltrating polymorphonuclear leukocytes (PMN) and plasma proteins in the cornea can diffract and obstruct the visual axis, thus causing the

Figure 13. Distribution and potential functions of the LPS receptor complex in the human lacrimal-corneal environment. **(a)** Lacrimal acinar cells express the entire LPS receptor complex and should therefore be able to initiate an innate immune response against Gram-negative insults. **(b)** On the normal intact cornea, an endotoxin induced immune response is uncommon or non-existent. This lack of immune response is attributed to the opsonizing capacity of tear sCD14 and LBP on Gram-negative bacteria and the limited expression of the LPS receptor complex by superficial corneal epithelial cells. **(c)** In the hypothetical model of wounding where mechanical damage has breached the corneal epithelium, the tear film provides sCD14 and LBP to deliver the LPS signal more efficiently to wing and basal epithelial cells. The activated epithelial cells recruit and activate PMNs to the site of infection by releasing IL-6, IL-8 and other cytokines. The adjacent table summarizes data from ELISA, RT-PCR, western blotting and microscopic analysis of the distribution of the LPS receptor components in the ocular environment and is represented as follows: +, ubiquitous presence; +/-, sparse presence and -, absence. Cartoon modified after (98).

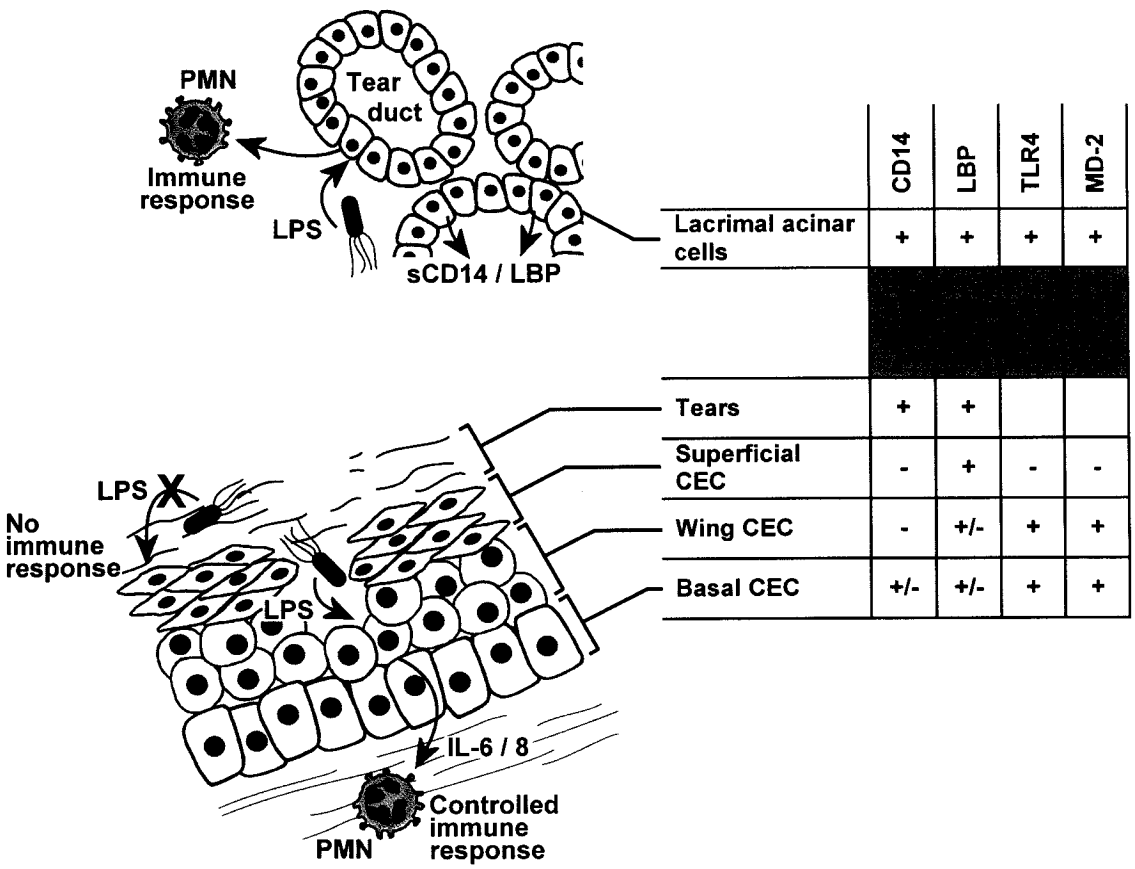

	CD14	LBP	TLR4	MD-2
Lacrimal acinar cells	+	+	+	+
Tears	+	+		
Superficial CEC	-	+	-	-
Wing CEC	-	+/-	+	+
Basal CEC	+/-	+/-	+	+

Figure 13

focused image to be cast away from the retina (99). Persisting inflammation may also lead to permanent corneal destruction by scarring, perforation and blindness (83). Immune privilege is the evolutionary solution of the eye to ensure ocular immune protection against pathogens while limiting immunogenic inflammation (99). The first step in preventing sight-distorting events such as infection and inflammation is to inhibit the adherence of ocular pathogens, such as *P. aeruginosa*, to the corneal epithelium. LBP and CD14 are known to have opsonizing activities (42, 100, 101), so tear sCD14 and LBP could inhibit the adherence of *P. aeruginosa* to the cornea by binding and neutralizing LPS on the surface of the bacteria (Figure 13b). In a similar mechanism, superficial corneal epithelial cells expressing LBP could prevent *P. aeruginosa* adherence by releasing LBP in the outer corneal environment and saturating the LPS adhesins of the bacteria. Furthermore, tear sCD14 and LBP could prevent shedded LPS monomers from interacting with the intact corneal epithelium by transferring them to lactoferrin (102) or lipoproteins (42, 103), two proteins also found in human tears (75, 104). The lactoferrin- and lipoprotein-bound LPS would no longer be available to interact with corneal epithelial cells and could be removed from the ocular surface via tears, eyelid blinking and hydrodynamic flushing. Also, LBP alone could mediate LPS detoxification by forming large LBP-LPS complexes that could subsequently be washed away with tears (105). The corneal epithelium itself strategically expresses the LPS receptor complex to minimize LPS responsiveness on its intact structure. Indeed, all the LPS receptor constituents required for an endotoxin response were expressed by basal and wing epithelial cells located in the inner corneal epithelial layers, with no CD14, TLR4 and MD-2 expression found in the squamous apical layers (Figure 9). Such polarized expression has been noted for TLR5 (78) and was proposed to contribute to ocular immune privilege by preventing host detrimental inflammatory responses of the corneal epithelium against non-pathogenic ocular flora.

Although the ocular surface is relatively resistant to microbial invasions, corneal surface injury disrupts the epithelial integrity allowing the infiltration of pathogens into the epithelium (83). Our *in vitro* model of the inner epithelial layers of a damaged cornea, primary and HCEC cell stimulation, revealed that the presence of tear sCD14 and LBP was required for an efficient delivery of endotoxin to the LPS receptor molecules expressed on corneal epithelial cells and for the release of IL-6 and IL-8 cytokines (Figure 13c). The observed minute cytokine response mediated exclusively by LPS correlated with previous findings (79, 80). This could be attributed to the limited presence of CD14 or TLR4 on the surface of corneal epithelial cells (79, 80) or to their intracellular localization (80), therefore limiting their biological response to LPS. Extracellular LBP and sCD14, provided by natural tears for example, are known to complement and facilitate the transfer of LPS to CD14 and TLR4/MD-2 (20, 37) now shown to be also expressed by corneal epithelial cells. This compartmentalized activation is another facet of immune privilege evolved with sight to restrain ocular immune responses to corneal epithelial insults by Gram-negative pathogens. LBP expressed by the apical epithelial layer of the cornea could also play an important role in LPS recognition in the injured corneal surface. Similarly to IL-1a (106), LBP stored in the cytoplasm of superficial epithelial cells could be passively released by the rupture of the cellular membrane caused by pathogens or trauma. LBP released by the damaged superficial cells could increase the LBP concentration in the wound microenvironment and improve LPS delivery to the exposed wing and basal epithelial cells to trigger an innate immune response.

This first thesis project suggests that the combined roles of tear sCD14 and LBP along with the polarized expression of the LPS receptor complex in the corneal epithelium could explain ways in which corneal epithelial cells discriminate between pathogenic and nonpathogenic Gram-negative bacteria, hence contributing to ocular immune privilege by limiting redundant

inflammation while ensuring immune protection. Further understanding of the molecular interactions among tear sCD14 and LBP, Gram-negative pathogens and corneal epithelial cells may lead to the development of efficient treatments to enhance ocular innate immune defences and prevent the sight threatening consequences of severe Gram-negative infections.

Chapter 3

Killing the messenger in the nick of time: persistence of breast milk sCD14 in the neonatal gastrointestinal tract

Summary

Human breast milk contains several proteins that supplement and stimulate the newborn immune system to prevent gastrointestinal infections. To deliver their immune benefits to the neonate, these proteins would have to survive the passage through the gastrointestinal tract and retain their biological activity. We analyzed the presence of breast milk sCD14 in the neonatal digestive system and found breast milk sCD14 to be undetectable in stools of breast-fed infants. *In vitro* digestion analysis with simulated gastric and pancreatic fluids revealed that sCD14 is likely to survive the pepsin digestion but is more prone to been nicked and digested by pancreatin. These findings suggest that the presence of intact breast milk sCD14 in the upper digestive system could promote innate immunity in this low bacteria density lumen. The low concentration of sCD14 in the LPS-rich environment of the distal gastrointestinal tract (i.e. commensal microflora) could be a strategy to prevent excessive and complicative inflammation.

Introduction

At birth, the human immune system is not fully developed and the neonatal intestine does not yet harbor its beneficial commensal flora (107, 108). These mucosal weaknesses make human neonates particularly vulnerable to infections and gastrointestinal illnesses (109). Necrotizing enterocolitis and diarrhea are such gastrointestinal disorders that can occur during the bacterial colonization of the intestine and are annually responsible for millions of infant deaths worldwide (110-112).

Besides its nutritional role, breast milk is known to supplement and stimulate the infant's developing immune system with immunologically active factors that prevent and fight gastrointestinal infections (113). Such factors include immunocompetent cells, immunoglobulins, growth factors, cytokines, lysozyme, lactoferrin and complement (114). However, these immunologically important molecules would have to remain intact and active throughout the gastrointestinal tract to provide immune benefits for the newborn. Some of these breast milk immune proteins, such as sIgA (115, 116) and lactoferrin (117, 118), have been shown to survive the passage through the infant digestive system, with observed faecal excretion rates of 160 mg/day and 14.3 mg/day, respectively (116).

Recently, another immune messenger, sCD14, has been found in significant quantities (15 μg/mL) in the milk of lactating mothers (26, 119, 120). In the digestive tract, the LPS co-receptor components TLR4 and MD-2 have been shown to be expressed by gastric (121, 122) and intestinal epithelial cells (123, 124). The TLR4/MD-2 co-receptor, in conjunction with CD14, has been shown to enable gastric and intestinal epithelial cells to respond to LPS *in vitro* (26, 119, 121). Consequently, several immune functions have been proposed for breast milk sCD14 in the neonatal intestinal environment: modulation of selective intestinal immune

responses to commensal and pathogenic microorganisms during postnatal intestinal bacterial colonization (119, 125), induction of B cell growth, differentiation and IgM secretion to stimulate the newborn immune system (126) and down-regulation of IgE secretion by neonatal B cells resulting in a reduced risk of atopy and eczema development (32, 127). Despite all the beneficial roles envisaged for sCD14, the *in vivo* physiological significance of this milk-borne innate immune protein remains to be elucidated: does breast milk sCD14 persist throughout the suckling neonatal digestive tract to deliver valuable immune protection?

In this second study, the daily intake and excretion, the digestive stability, the intestinal absorption and the proteolytic susceptibility of breast milk sCD14 were investigated in the human newborn gastrointestinal tract. Given the constraints of working *in ambio* in the human neonatal intestine, the following experimental design was used to investigate the fate of breast milk sCD14: faeces and urine of exclusively breast-fed neonates and formula-fed neonates, and *in vitro* digestion of human breast milk with simulated gastric and pancreatic fluids. This experimental data shows that breast milk sCD14 is susceptible to pancreatin proteolysis *in vivo* and therefore, its absence from the newborn distal gastrointestinal tract prevents complicative inflammation during colonization by LPS-bearing microflora.

Materials and Methods

Subjects

The study was approved by the Ottawa Hospital Research Ethics Board. Two groups of neonates (n = 28), born at the Ottawa Hospital – General Campus, were enrolled within one day after birth when the purpose of the research and the experimental procedure were explained to the parents and their informed consent was obtained. The first group was composed of 15 newborns (7 girls and 8 boys) who were exclusively breast-fed for at least one month after birth. All the nursing mothers were healthy and had no medical complications. The second group consisted of 13 newborns (6 girls and 7 boys) whose mothers planned to exclusively formula-feed for at least the first month of life of their newborn, using the commercial milk formula of their choice (Enfalac, Similac, Similac Advance or Nestlé Good Start; with or without iron). All infants were healthy and born at term (38-42 weeks) with a birth weight ranging between 3.1-4.1 kg. Given that all the neonates were born within a normal range, the groups of patients studied constitute an adequate representation of the population.

Sample collection

Three 24 h collections were performed on each newborn in their own home at 1 week (6-9 days), 2 weeks (12-16 days) and 4 weeks (26-32 days) of age. For each collection, the participants were asked to collect for a period of 24 h the infant faeces and urine using Kushies® diaper liners (D.D.F. Inc., Stoney Creek, ON). The diaper liners soiled with faeces or urine were placed in their respective sterile containers and were immediately frozen (-20°C) in the family personal freezer. Milk intake of each infant was measured for 24 h on each collection day using the difference in body weight before and after each nursing. Infants were weighed by their mothers on a Seca 725 mechanical paediatric baby scale (Seca Corporation, Hamburg, Germany)

without altering the normal feeding pattern. The weight of milk was converted to volume using its specific gravity of 1.031 g/mL (128). On each day of collection, breast-feeding mothers hand-expressed a small milk sample into a sterile plastic container, whereas formula-feeding mothers provided a small sample of the commercial formula milk fed to the infant. Milk samples were immediately frozen (-20°C) until analysis. A urine sample from human adult (male, 26 years old) was collected to study the *in vivo* secretion of urinary sCD14 and IgA. All the samples were collected as directed by the families. In the studied groups, no concerns or problems that would have affected the samples or their storage occurred during the collection days.

Sample preparation and analysis

Diaper liners containing urine were gently squeezed and the extracted urine was frozen until analysis. Diaper liners containing faecal material were weighed and the faeces were scraped from the diaper liners. The faeces were thereafter homogenized in PBS (1:2) containing a protease inhibitor cocktail (Sigma-Aldrich, St. Louis, MO) and incubated on ice for 30 min to extract any soluble proteins. The extract was then centrifuged at 10,000 X *g* for 20 min at 4°C to sediment any insoluble material and the supernatant was used for analysis. Milk samples were centrifuged at 5,000 X *g* to remove fat and heavy cellular components and stored at –80°C until analysis. The quantification of sCD14 and sIgA proteins in milk, urine and stool extracts was performed in duplicate by ELISA according to the manufacturer's instructions.

Reagents

The quantification of sCD14 and sIgA proteins was performed using the human sCD14 ELISA kit (HyCult Biotechnology, Uden, The Netherlands) and the human IgA ELISA quantification kit (Bethyl Laboratories Inc., Montgomery, TX), respectively. Commercial recombinant human CD14 (rhCD14) (R&D Systems, Inc., Minneapolis, MN) and purified breast

milk human sIgA (Serotec Ltd., Oxford, UK) served as controls in the *in vitro* digestion analysis. Immunodetection was performed using the biotinylated polyclonal anti-human CD14 antibody (R&D Systems, Minneapolis, MN) and the biotinylated alpha chain-specific anti-human IgA antibody (Caltag Laboratories, Burlingame, CA). Human AB serum used as a loading control in immunoblotting was purchased from Sigma-Aldrich, St. Louis, MO.

***In vitro* digestion of purified sCD14, purified sIgA and breast milk**

The procedure was slightly modified from that developed by Rudloff *et al* (129). For the pepsin digestion procedure, control rhCD14 or sIgA were prepared at a concentration of 10 ng/mL in phosphate-buffered saline (PBS). The pH of the rhCD14, sIgA and human breast milk samples was adjusted to 4.5 with 1M hydrochloric acid. The rhCD14, sIgA and human breast milk samples were each aliquoted in four microtubes and pepsin (from porcine gastric mucosa, 800-2500 U/mg of protein, Sigma, St. Louis, MO) was added to the desired concentration. The samples were kept in the dark and incubated at 37°C for 30 min with occasional shaking. The reaction was halted by diluting the samples in SDS gel-loading buffer and boiling them for 5 min.

The pancreatin digestion was performed by adjusting the pH of breast milk, control sIgA (10 ng/mL) and rhCD14 (10 ng/mL) to 7.0 with 1M HCl or 1M $NaHCO_3$. The rhCD14, sIgA and human breast milk samples were each aliquoted in four microtubes and pancreatin (from porcine pancreas, 4X USP specifications, Sigma, St. Louis, MO) was added to the desired concentration. The samples were digested at 37°C for 1 h as described above.

The sequential digestions of control rhCD14, sIgA and breast milk with simulated gastric and pancreatic fluids were performed by adjusting the pH of breast milk, sIgA (10 ng/mL) and

rhCD14 (10 ng/mL) to 4.5 with 1M HCl. The rhCD14, sIgA and human breast milk samples were each aliquoted in four microtubes and pepsin was added to a concentration of 1 mg/mL. The samples were kept in the dark and incubated at 37°C for various periods (30-60 min) with occasional shaking. After the pepsin digestion, the pH of each sample was increased gradually during 10 min to 7.0 with 1M $NaHCO_3$ and pancreatin was added to a concentration of 1 mg/mL. The samples were kept in the dark and incubated at 37°C for various periods of time (60-120 min) with occasional shaking. The reaction was halted by diluting the samples in SDS gel-loading buffer and boiling them for 5 min. Each *in vitro* digestion experiment was performed in triplicate on breast milk samples from different mothers.

Immunoblotting

To monitor the intact breast milk immune proteins, samples were resolved by SDS-PAGE electrophoresis under reducing conditions (11% resolving gel) and transferred onto nitrocellulose (Amersham Biosciences, Piscataway, NJ). The membrane was blocked for 1 h in 5% dried skim milk in TBS with 0.1% Tween-20. The sCD14 and sIgA proteins were probed with the biotinylated polyclonal anti-human CD14 antibody (0.05 μg/mL in TBS-Tween) or with the biotinylated alpha chain-specific anti-human IgA antibody (0.07 μg/mL in TBS-Tween), respectively. After extensive washing, the membrane was incubated for 1 h with the anti-biotin HRP-conjugated antibody (1:1,000) (Cell Signaling Technology, Beverly, MA). The antigens were detected using a chemiluminescent system (ECL Western Blotting Detection Reagents, Amersham Biosciences).

Statistical analysis

Individual experiments in this study were performed in triplicate to confirm the reproducibility of the results. Values are presented as mean ± standard deviation. The statistical

significance of differences between two or more means was evaluated using one-way ANOVA, where *P* values of less than 0.05 (indicated by asterisks) were considered statistically significant.

Results

Contrary to sIgA, breast milk sCD14 is not excreted by the newborn

To analyze the stability of breast milk sCD14 in the newborn digestive system, the input (breast milk) and the output (faeces and urine) levels of sCD14 were measured by ELISA and compared to sIgA, a breast milk antibody known for its gastrointestinal persistence (115, 116). To ensure that the output levels of sCD14 and sIgA did not originate from *in vivo* gastrointestinal synthesis by the newborn, formula-fed neonates were recruited as a control group, since sCD14 and sIgA could not be detected in any commercial milk formulas (Table 4 and 5). The lack of detection of sCD14 and sIgA in commercial milk formulas could be attributed to the absence or extremely low concentration of these proteins in the commercial preparations or to the inability of the ELISA kits and antibodies to detect the bovine sCD14 and sIgA proteins. In the study group, both sCD14 and sIgA could be observed in all breast milk samples, with sIgA levels being on average 30 times higher than sCD14 (Table 4 and 5). The output faecal and urinary levels of sCD14 were similar between breast-fed and formula-fed neonates (Table 4). However, sIgA was present in higher concentration, one thousand fold and ten fold respectively, in faeces and urine samples from breast-fed neonates when compared to those of formula-fed newborns (Table 5). To rule out any presence of aggregated or adsorbed sCD14 proteins in the stool matrix that would be non-extractable with PBS, harsher extraction techniques with detergents were performed on stool samples. These stronger extraction procedures generated similar faecal sCD14 levels to those of the PBS extraction, with no significant difference observed between the two techniques

Table 4. CD14 concentration in breast milk, in milk formula, and in the urine and faeces of breast-fed and formula-fed infants.

	Breast-fed neonates (n=15)			Formula-fed neonates (n=13)		
Samples / Age (weeks)	Breast milk (ng/mL)[a]	Urine (ng/mL)[a]	Faeces (ng/g_{fw})[a]	Milk formula (ng/mL)[a]	Urine (ng/mL)[a]	Faeces (ng/g_{fw})[a]
1	29,500 ± 15,400[b]	47.8 ± 86.3	4.1 ± 9.6	0.4 ± 0.7	37.6 ± 69.8	11.7 ± 27.3
2	25,100 ± 11,900[b]	1.6 ± 3.4	8.0 ± 15.0	0.6 ± 1.8	10.2 ± 10.3	3.8 ± 4.6
4	22,300 ± 14,000[b]	8.4 ± 12.5	2.9 ± 5.0	0.2 ± 0.5	22.9 ± 35.3	2.0 ± 4.1

[a] The quantification of CD14 in the collected samples was performed by ELISA using a commercially available kit.

Results are expressed as means ± SD of triplicate cultures of one experiment representative of three. Statistically significant differences between samples from breast-fed and formula-fed newborns were determined using one-way ANOVA, with probabilities: [b] $P < 0.0001$.

Table 5. IgA concentration in breast milk, in milk formula, and in the urine and faeces of breast-fed and formula-fed infants.

	Breast-fed neonates (n=15)			Formula-fed neonates (n=13)		
Samples / Age (weeks)	Breast milk (ug/mL)[a]	Urine (ug/mL)[a]	Faeces (ug/g_{fw})[a]	Milk formula (ug/mL)[a]	Urine (ug/mL)[a]	Faeces (ug/g_{fw})[a]
1	991 ± 682[b]	3.9 ± 9.6	1,559 ± 999[b]	0 ± 0	0 ± 0	2.1 ± 1.6
2	831 ± 624[b]	2.0 ± 2.2[c]	1,569 ± 988[b]	0 ± 0	0.1 ± 0.1	14.7 ± 27.3
4	499 ± 181[b]	4.1 ± 5.6[c]	1,299 ± 756[b]	0 ± 0	0.2 ± 0.2	20.1 ± 27.5

[a] The quantification of IgA in the colleted samples was performed by ELISA using a commercially available kit.

Results are expressed as means ± SD of triplicate cultures of one experiment representative of three. Statistically significant differences between samples from breast-fed and formula-fed newborns were determined using one-way ANOVA, with probabilities: [b] $P < 0.0005$; [c] $P < 0.01$.

(data not shown). Furthermore, stool homogenate spiked with rhCD14 to give a final rhCD14 concentration of 8 ng/mL, revealed that the constituents of the stool extract did not impede the reactivity of the CD14 antigens with the commercial ELISA kit, since a rhCD14 concentration of 8.7 ± 0.5 ng/mL was detected in the spiked stool homogenate. The daily intake and excretion of sCD14 and sIgA per unit body weight showed that breast-fed infants excreted considerably higher quantities of sIgA (1,800 ± 1,700 μg/Kg/day) when compared to formula-fed infants (15 ± 27 μg/Kg/day) (Figure 14). Despite the significant difference in sCD14 intake between breast-fed (3,300 ± 2,300 μg/Kg/day) and formula-fed (0.05 ± 0.15 μg/Kg/day) infants, the daily excretory levels of sCD14 were similar (0.005 ± 0.009 μg/Kg/day for breast-fed and 0.007 ± 0.014 μg/Kg/day for formula-fed) between the two groups, albeit the minute faecal concentration (Figure 14).

To estimate whether sCD14 and sIgA proteins passed intact through the gastrointestinal tract, immunoblotting analysis was performed on samples collected from breast-fed and formula-fed babies. Two polypeptides of molecular mass of 48 and 52 kDa were detected with the anti-CD14 antibody in breast milk and serum, whereas only a 52 kDa polypeptide was observed in the urine of breast-fed and formula-fed infants, corresponding to the size of sCD14 detected in the adult urine sample (Figure 15a). Immunoblot analysis also revealed the presence of the 60 kDa heavy chain polypeptide of sIgA in breast milk as well as in the stool and urine of breast-fed newborns, which corresponded to the same apparent molecular mass of the heavy chain of serum IgA (Figure 15b). Smaller polypeptides, that likely represent digested fragments of the sIgA heavy chain, were also detected by the anti-IgA antibody in faecal samples of breast-fed infants (Figure 15b).

Figure 14. Daily intake and faecal excretion of sCD14 **(a)** and sIgA **(b)** in exclusively breast-fed (BF) (n=15) or formula-fed (FF) (n=13) infants. The quantification of sCD14 and sIgA in milk and newborn stool homogenate was performed by ELISA using commercially available kits. The daily intake was calculated by converting the weight of milk consumed within the 24 h collection period to volume, multiplying it with the CD14 or IgA concentration measured and dividing it with the neonate's body weight. The daily excretion was calculated by multiplying the weight of faeces recovered within the 24 h collection period with the CD14 or IgA concentration measured and dividing it with the neonate's body weight. Results are expressed as means ± SD.

a

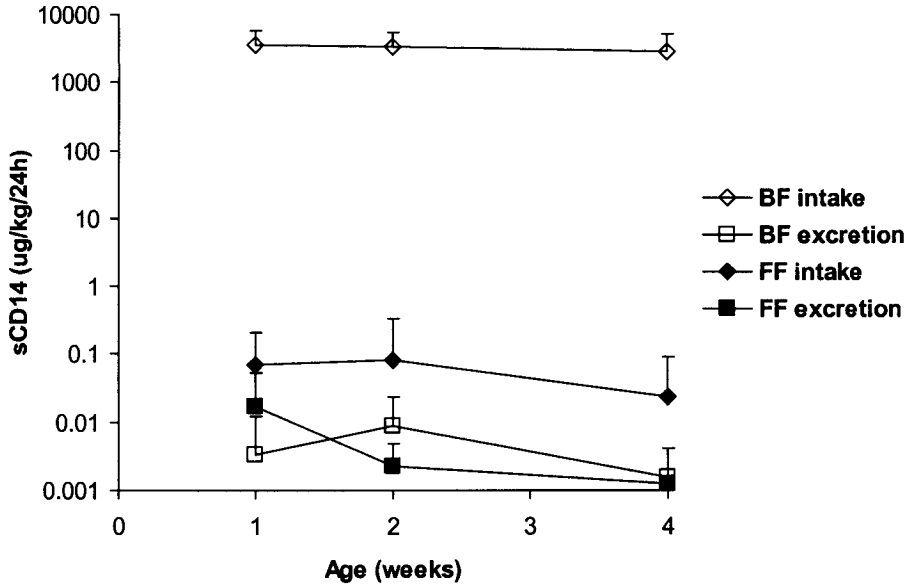
10000
1000
100
10
1
0.1
0.01
0.001
sCD14 (ug/kg/24h)
0
1
2
3
4
Age (weeks)
BF intake
BF excretion
FF intake
FF excretion

b

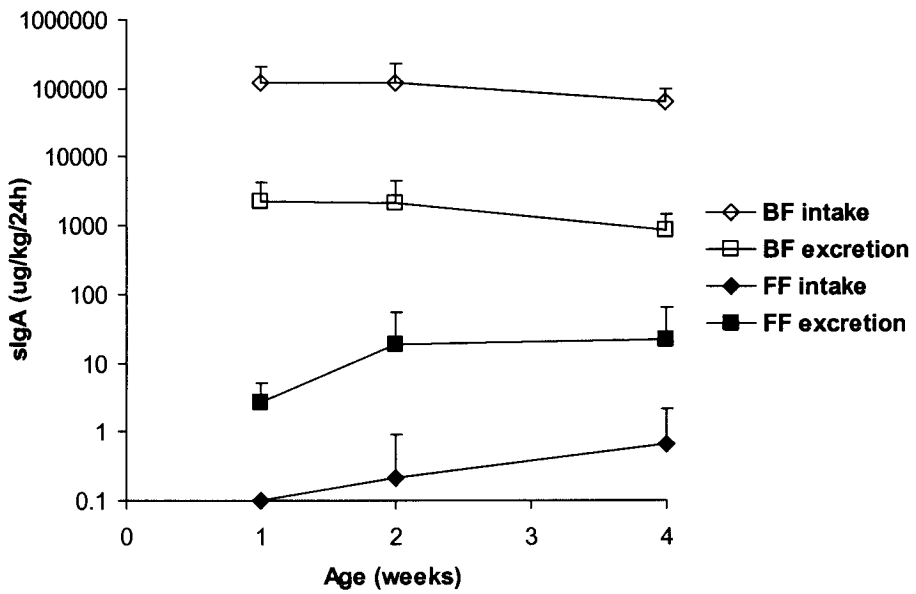
1000000
100000
10000
1000
100
10
1
0.1
sIgA (ug/kg/24h)
0
1
2
3
4
Age (weeks)
BF intake
BF excretion
FF intake
FF excretion

Figure 14

Figure 15. Immunodetection of human sCD14 **(a)** and sIgA **(b)** in various samples from breast-fed and formula-fed infants. Breast-fed (BF) and formula-fed (FF) infant samples along with serum and adult urine controls were subjected to western blotting with the biotinylated anti-CD14 polyclonal antibody **(a)** or the biotinylated anti-IgA polyclonal antibody (α chain specific) **(b)**, followed by the anti-biotin HRP-linked antibody. The immunoblots are representative of three different mother-neonate groups.

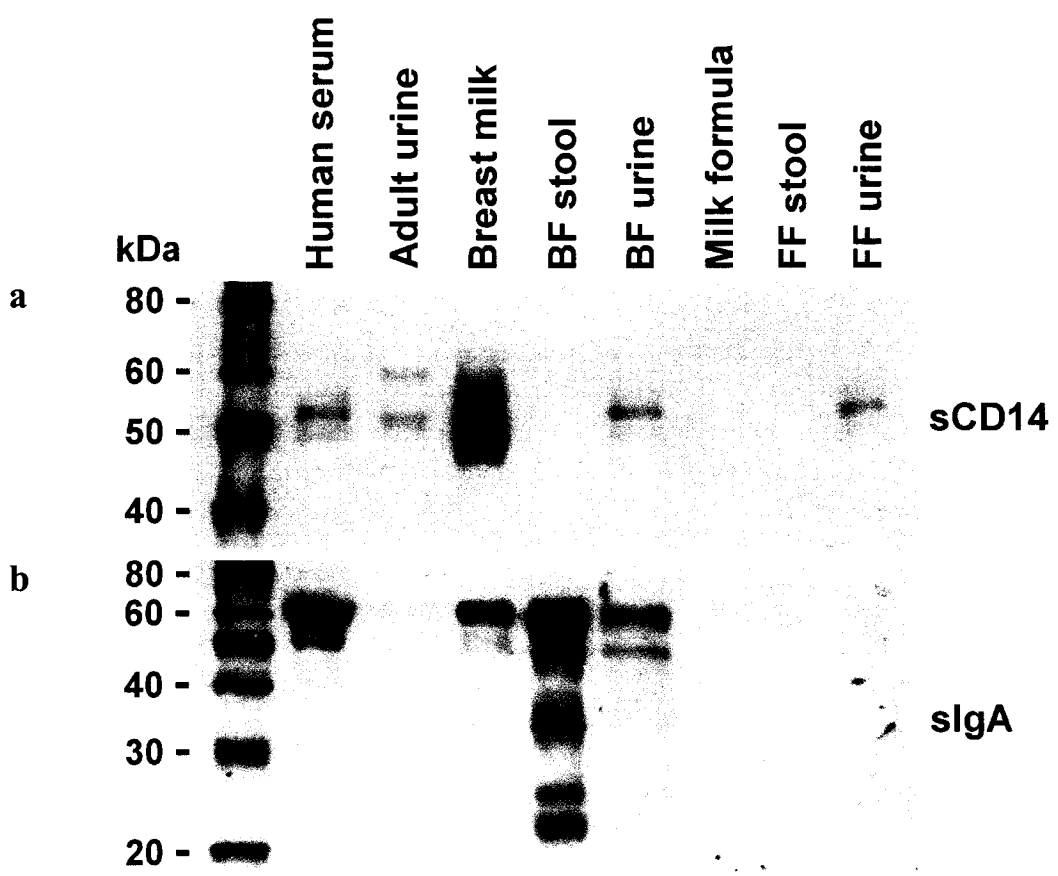
Human serum
Adult urine
Breast milk
BF stool
BF urine
Milk formula
FF stool
FF urine
kDa
a
80
60
50
40
b
80
60
40
30
20
sCD14
sIgA

Figure 15

Breast milk sCD14 is more susceptible to *in vitro* pancreatin digestion than pepsin digestion

To investigate the susceptibility of sCD14 to digestion in comparison to sIgA along the gastrointestinal tract, both proteins (10 ng/mL) were subjected separately to *in vitro* proteolysis with porcine pepsin and pancreatin enzymes. Both sCD14 and sIgA, in their recombinant or purified forms and naturally present in breast milk, showed a similar resistance to pepsin digestion (Figure 16). All the breast milk samples continued to show the intact molecular weight of both proteins after the 10 mg/mL pepsin digestion (Figure 16). For the pancreatin digestions, control rhCD14 and sIgA also had a similar and high susceptibility to the enzyme, with no protein detectable after the 0.1 mg/mL pancreatin digestion (Figure 17). In the breast milk milieu however, sIgA showed more resistance to porcine pancreatin than did sCD14, where no sCD14 survived the 10 mg/mL digestion (Figure 17, lane 10). During the sequential pepsin and pancreatin digestions, both control proteins were proteolyzed, whereas in the breast milk environment, sIgA clearly showed a stronger resistance to proteolysis when compared to sCD14 (Figure 18). Approximately half of breast milk sCD14 proteins were degraded in the shortest digestion period (30 min pepsin and 60 min pancreatin) and no protein remained after the longest digestion period (60 min pepsin and 120 min pancreatin) (Figure 18), as judged by visual examination of the western blot signal. For breast milk sIgA, the sequential digestions were less effective, where approximately one quarter of the original amount of the protein was still remaining after the longest sequential gastric and pancreatic digestion (60 min pepsin and 120 min pancreatin) (Figure 18). The multiple smaller bands detected on the blots likely represent digested products of sCD14 or sIgA heavy chain, which were absent in non-digested samples (Figure 16, 17 and 18). In general, the sCD14 and sIgA proteins in breast milk showed a higher resistance to pepsin and pancreatin digestions than the control proteins (Figure 16, 17 and 18).

Figure 16. Western analysis of pepsin digested human breast milk, control rhCD14 **(a)** and sIgA **(b)**. The control proteins, rhCD14 and sIgA (10 ng/mL), and breast milk were digested *in vitro* with the indicated concentrations of pepsin for 30 min at 37°C, pH 4.5 and subjected to western blotting with the biotinylated anti-CD14 polyclonal antibody **(a)** or the biotinylated α chain specific anti-IgA polyclonal antibody **(b)**, followed by the anti-biotin HRP-linked antibody. Lane P represents porcine pepsin (10 mg/mL) in PBS as a loading control. The immunoblots are representative of three independent digestions performed on different breast milk samples.

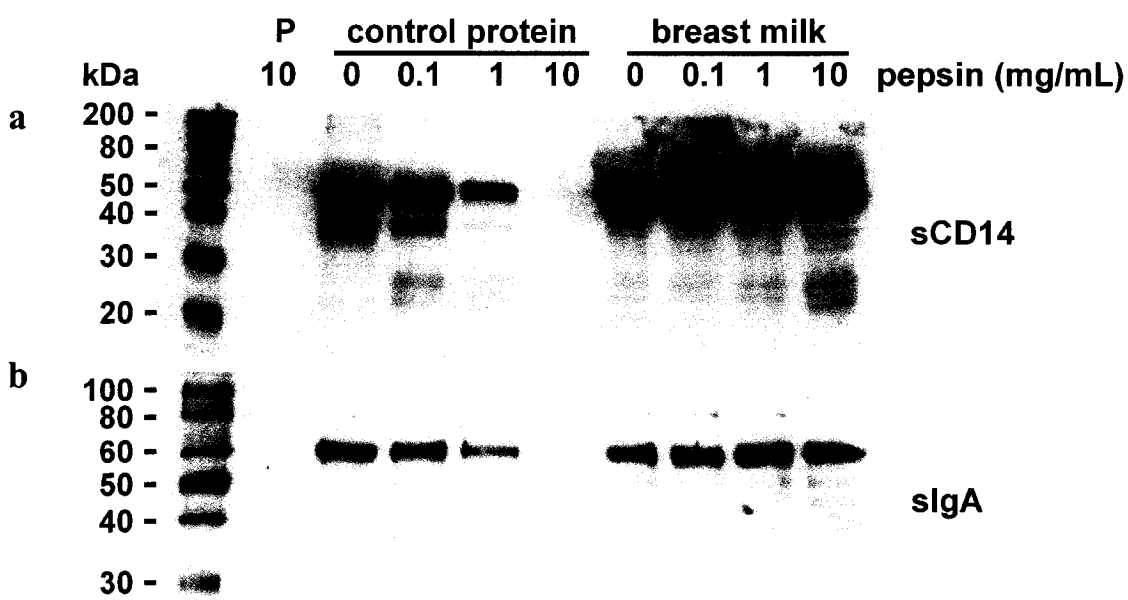
P
control protein
breast milk
kDa
10
0
0.1
1
10
0
0.1
1
10
pepsin (mg/mL)
a
200
80
50
40
30
20
sCD14
b
100
80
60
50
40
30
sIgA

Figure 16

Figure 17. Western analysis of pancreatin digested human breast milk, control rhCD14 **(a)** and sIgA **(b)**. The control proteins, rhCD14 and sIgA (10 ng/mL), and breast milk were digested *in vitro* with the indicated concentrations of pancreatin for 60 min at 37°C, pH 7.0 and subjected to western blotting with the biotinylated anti-CD14 polyclonal antibody **(a)** or the biotinylated α chain specific anti-IgA polyclonal antibody **(b)**, followed by the anti-biotin HRP-linked antibody. Lane P represents porcine pancreatin (10 mg/mL) in PBS as a loading control. The immunoblots are representative of three independent digestions performed on different breast milk samples.

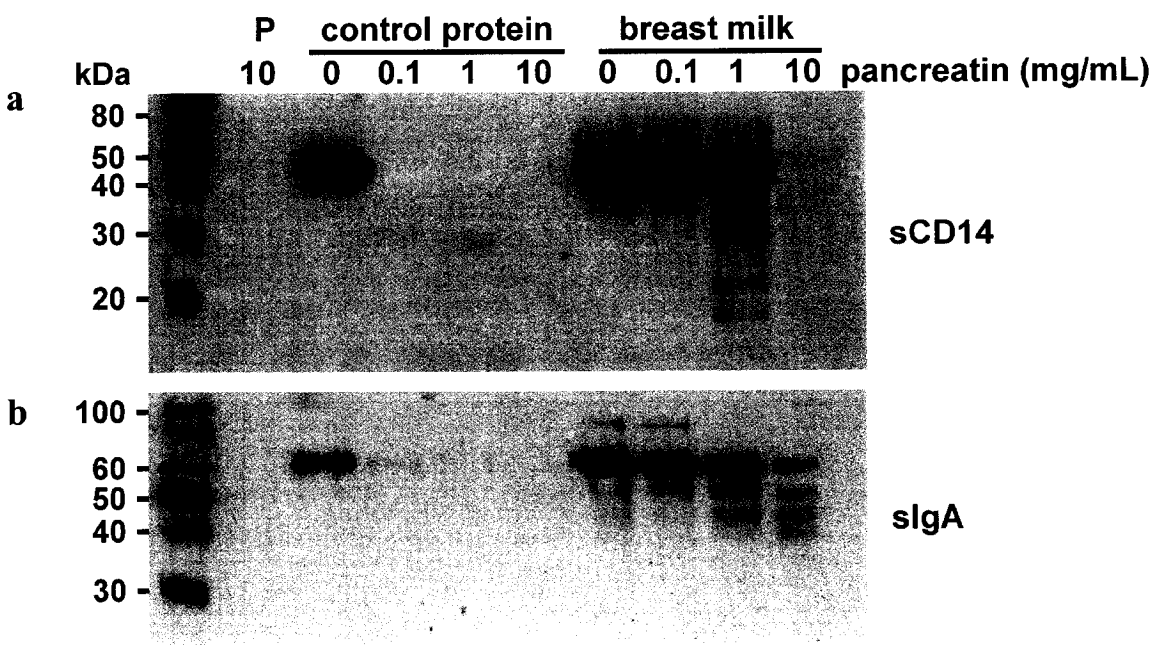
P
control protein
breast milk
kDa
10
0
0.1
1
10
0
0.1
1
10
pancreatin (mg/mL)
a
80
50
40
30
20
sCD14
b
100
60
50
40
30
sIgA

Figure 17

Figure 18. Western analysis of sequential digestion of human breast milk, control rhCD14 **(a)** and sIgA **(b)** with simulated gastric and pancreatic fluids. The control proteins, rhCD14 and sIgA (10 ng/mL), and breast milk were digested *in vitro* at various incubation times with pepsin (1 mg/mL) at 37°C, pH 4.5 followed by a pancreatin digestion (1 mg/mL) at 37°C, pH 7.0 and subjected to western blotting with the biotinylated anti-CD14 polyclonal antibody **(a)** or the biotinylated α chain specific anti-IgA polyclonal antibody **(b)**, followed by the anti-biotin HRP-linked antibody. Lane P represents porcine pepsin (1 mg/mL) and pancreatin (1 mg/mL) in PBS as a loading control. The immunoblots are representative of three independent digestions performed on breast milk samples from different nursing mothers.

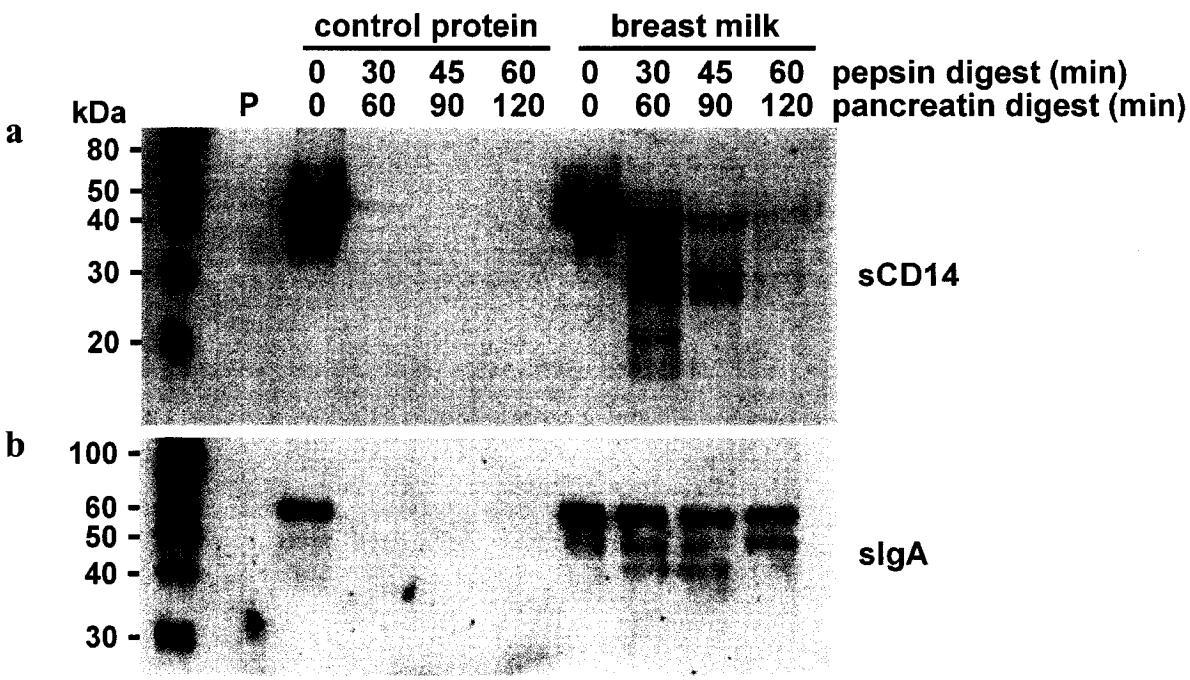
control protein
breast milk
0 30 45 60 0 30 45 60 pepsin digest (min)
kDa P 0 60 90 120 0 60 90 120 pancreatin digest (min)
a
80
50
40
30
20
sCD14
b
100
60
50
40
30
sIgA

Figure 18

Discussion

The results presented in this study suggest that breast milk sCD14 protein does not persist the newborn gastrointestinal tract. This finding is supported by the trace excretory levels (5.4 ± 11.0 ng/g) of sCD14 observed in feces of both exclusively breast-fed (intake of 25.6 ± 13.8 μg/mL of sCD14) and formula-fed neonates (virtually no intake of sCD14). These observations were constant at three weekly time points during the first month of life of the human newborn, when the gastrointestinal tract is maturing. Furthermore, the trace levels of faecal sCD14 measured in both breast-fed and formula-fed infants could result from endogenous intestinal synthesis of sCD14 (28) or could be related to analytical variations at the lower limit of detection of the ELISA kit. However, the minute concentrations of faecal sCD14 measured from formula-fed neonates suggest that the endogenous intestinal secretion of sCD14 is very limited or its intestinal fate restricts its detection in stool.

By contrast, breast milk sIgA was detected in high quantity in the stools of breast-fed newborns ($1{,}500 \pm 900$ μg/g), confirming its persistence in the gastrointestinal tract (115, 116). The gastrointestinal persistence of sIgA is largely attributed to its high degree of glycolysation and to the presence of the secretory chain, rendering this dimeric antibody inherently resistant to luminal proteolysis (130). This faecal sIgA difference observed between breast-fed and formula-fed neonates validates the methodology used to measure the passage of intact breast milk proteins in the newborn gastrointestinal tract.

The lack of detection of breast milk sCD14 in stools of breast-fed infants suggests two possible fates of sCD14 in the gastrointestinal tract: (i) efficient transport, in an intact and active form, through the intestinal mucosa to contribute to the serum pool of sCD14, and/or (ii) digestion

and degradation by the gastrointestinal enzymes to restrict its biological activity along the newborn intestinal tract.

The first potential fate of breast milk sCD14 was investigated by analyzing the levels of sCD14 in the urine of breast-fed and formula-fed neonates. The quantification of urinary proteins is a suitable technique to estimate the serum concentration of specific proteins in the newborn without having to resort to invasive procedures (131-133). In both groups of breast-fed and formula-fed neonates, the urinary sCD14 detected by immunoblot had a similar electrophoretic mobility to sCD14 found in human adult urine (29). However, the similar urinary sCD14 levels between breast-fed and formula-fed newborns measured by ELISA do not support the notion of its absorption through the intestinal mucosa and its subsequent renal excretion. Even within the first week of age, when the small intestine is known to have an enhanced permeability to macromolecules coming in contact with its mucosa (134), no differences in urinary sCD14 levels were observed. In contrast, breast milk sIgA has been shown to be absorbed by the newborn intestinal mucosa within the first week of life and to contribute to the serum IgA pool (134), which was reflected with higher urinary sIgA levels (131). These results suggest that sCD14 observed in urine samples is endogenous in origin and is unlikely to originate from intact breast milk sCD14 absorbed by the small intestine.

Secondly, the digestibility of breast milk sCD14 was investigated *in vitro* with simulated gastric juices and revealed that the protein is resistant to pepsin digestion. This gastric resistance can be attributed to the low secretion of hydrochloric acid in the neonatal stomach, resulting in a pH of 3.5-5, far higher than the optimal pH conditions of pepsin (135). In this study, the conditions of the *in vitro* model of gastric digestion (pH 4.5 for 30-60 min) were designed to reflect the neonatal gastric environment (129). The relative abundance of sCD14 in breast milk

(25.6 ± 13.8 μg/mL), when compared to its serum concentration (3 μg/mL) (26), and its relative resistance to pepsin digestion, may allow significant amounts of the intact protein to reach the duodenum. Furthermore, the enhanced proteolytic resistance observed for both sCD14 and sIgA naturally present in breast milk, in comparison to their purified forms, may be attributed to the breast milk abundance of alternate substrates for digestive enzymes and to the presence in milk of protease inhibitors, such as α_1-antitrypsin and antichymotrypsin (136, 137). These protective properties of breast milk could contribute to some proteolytic resistance of sCD14 during its upper gastrointestinal passage. The first N-terminal half of sCD14 has been shown to contain all the active domains to trigger biological responses against LPS (Figure 3) (16). As a result, partially digested forms of sCD14, in addition to its undigested form, could offer immune protection to the upper digestive tract (oral cavity, esophagus, stomach and duodenum), where low bacterial density is found (138). Besides inducing an intestinal LPS-immune response (26, 119), breast milk sCD14 could also modulate this LPS-response by interacting with other breast milk immune proteins, such as lactoferrin (102) and TLR2 (139), and prevent excessive immune reactions and inflammation. Breast milk sCD14 could reduce the luminal bioavailability of free LPS monomers by transferring them to lactoferrin (102) and prevent the interaction of endotoxin with intestinal epithelial cells. Another CD14 co-receptor, soluble TLR2, recently found in breast milk, could also interact with sCD14 to avoid excessive local inflammation against Gram-positive bacteria and mycobacteria present in the neonatal intestinal tract (139). This modulated sCD14 activation was investigated in another delicate environment, the tear-cornea interface, one which also requires fine-tuned immune responses in order to fully accomplish its biological functions while remaining infection- and inflammation-free.

The increased proteolytic susceptibility of breast milk sCD14 to pancreatic fluids, when compared to breast milk sIgA, suggests that only a minute fraction of sCD14 ingested by the

neonate may persist the duodenal passage. These results could explain the relative absence of breast milk sCD14 in the stools of breast-fed neonates. Furthermore, breast milk sCD14 proteins could be subjected to additional hydrolysis during their jejunum, ileum and colon transit by proteolytic enzymes of bacterial and intestinal origin (140). The absence or trace amounts of sCD14 in the distal small intestine and colon could be a solution in preventing uncontrolled and detrimental immune responses in this heavily colonized environment (138). Indeed, by binding to LPS, sCD14 cannot discriminate between harmful pathogenic and beneficial commensal Gram-negative bacteria and therefore could trigger inflammation in the distal bowel. In contrast, the gastrointestinal persistence of breast milk sIgA is considered beneficial to the newborn due to its specificity in targeting pathogens to which the nursing mother has been exposed and consequently preventing their penetration through the neonatal intestinal mucosa (113, 141). Similarly, the persistence of breast milk lactoferrin and lysozyme in the neonatal intestine is also considered advantageous due to the fact that they reduce and control bacterial proliferation and colonization without triggering inflammation and immune responses (142, 143). These results suggest that breast milk sCD14 is absent or has a very limited presence in the distal gastrointestinal tract to avoid excessive mucosal inflammation in this densely colonized environment.

This second thesis project suggests that breast milk sCD14 is particularly susceptible to pancreatin digestion and is not excreted in feces. This non-ubiquitous gastrointestinal presence may allow sCD14 to contribute to immune protection against Gram-negative pathogens in the upper digestive tract while reducing its inflammatory activity in the LPS-rich environment of the distal bowel.

Chapter 4

Human CD14 expressed in seeds of transgenic tobacco displays similar proteolytic resistance and bioactivity with its mammalian-produced counterpart

Summary

Human CD14 plays an important role in innate immunity by being the key receptor of LPS found on Gram-negative bacteria. The recently discovered widespread localization of CD14 in secretions and mucosal surfaces, such as breast milk, tears and the cornea, reveals its extensive anti-microbial properties and numerous potential medical applications. To produce active rhCD14 for massive distribution, transgenic tobacco plants were successfully generated to express rhCD14 in the seed endosperm under the control of two versions of the rice glutelin Gt-1 promoter. Plant-made rhCD14 reached a concentration of 16 μg/g of seeds and showed stability, proteolytic resistance and ability to induce the release of pro-inflammatory cytokines in presence of LPS. The expression of plant rhCD14 in tobacco seeds constitutes a promising low-cost and abundant supply of this immune protein to further investigate its roles in, impacts on and potential medical applications for the innate immune system.

Introduction

Plants have been used as medicine since the earliest stages of civilization. Nearly 80% of the world population still depends on traditional herbal medicine for primary health care, while close to one quarter of prescription drugs used in developed countries are of plant origin (144). In recent years, biotechnology has extended the medicinal use of plants by improving the expression of endogenous medicinal compounds and also by introducing foreign health enhancing genes (145-147). Compared to other organisms, plants offer several advantages in producing important medicinal proteins. They carry appropriate post-translational modifications and lack mammalian viruses, pathogens or oncogenes. In addition, mass production of biopharmaceutical proteins becomes commercially feasible by scaling up to agricultural field production, while maintaining low costs (148). Furthermore, when the expression of recombinant proteins is targeted into edible seeds, these proteins can be safely stored in protein bodies of endosperm cells for oral delivery, without requiring processing or purification (149). This combination of advantages has allowed the expression, in edible plant organs, of a wide diversity of biopharmaceutical proteins with preventive, diagnostic and therapeutic potential (150).

Another promising candidate for plant-made pharmaceuticals is human CD14. As mentioned in the general introduction, sCD14 is present in serum as well as several secretions and mucosa, such as tears, cornea (79), saliva (25), breast milk (26), lungs (27), intestine (28), urine (29), sperm (30) and amniotic fluid (31, 32). The widespread localization of sCD14 in body fluids and mucosa reflects the important roles played by this protein, as a first line of defence against Gram-negative pathogens, in these constantly challenged mucosal environments.

Through its widespread mucosal presence, several preventive and clinical usages have been suggested for sCD14 (151). Soluble CD14 is known to detoxify and eliminate LPS in serum

by transferring them to HDL particles and plasma membranes (Figure 2) (42, 43). Therefore, intravenously administered sCD14 may compete with mCD14 for LPS, dampening the LPS-mediated responses of myeloid cells and preventing the lethal consequences of endotoxin-induced septic shock (46). Similarly, intra-mammary administered sCD14 may reduce the severity of bovine mastitis by increasing the recruitment of immune cells to the site of infection (152). Due to potential opportunities of sCD14 in prevention and treatment of Gram-negative infections, several attempts relying on recombinant DNA technology have been carried to produce CD14, such as mammalian cell lines (153, 154), insect cell cultures (45), *E. coli* (155), as well as yeast (156). The production of rhCD14 in tobacco callus suspension culture was also attempted (157). However, obstacles were encountered with the secretion of the protein and its stability (157).

In mammalian cells, secretory organelles, such as the Weibel-Palade bodies of endothelial cells, play a key role in homeostasis and inflammation by regulating the storage and secretion of various regulatory proteins, such as the homeostatic von Willebrand factor and the leukocyte receptor P-selectin (158). Similarly, plant biotechnology take advantage of the storage and delivery properties of proteins bodies by using specific promoters to target cytokines, vaccine candidates, growth hormones and other biopharmaceuticals to the seed endosperm, a natural protein deposition site (145, 159, 160). In this third study, the accumulation of rhCD14 protein was explored in transgenic tobacco seeds. The full-length and truncated rice glutelin Gt-1 promoters were used to successfully direct CD14 expression to the tobacco seed endosperm. This experimental data shows that plant-produced rhCD14 was stable, proteolytic resistant and biological active in presence of LPS.

Materials and methods

Reagents

Human genomic DNA isolated from blood samples was kindly provided by Dr. Alex MacKenzie (Children's Hospital of Eastern Ontario, Ottawa, ON). Commercial Chinese hamster ovary cell (CHO) produced rhCD14 (R&D Systems, Inc., Minneapolis, MN) was used as a control in western blotting, in pepsin and pancreatin *in vitro* digestions and in biological assays.

Transgene construction and tobacco transformation

The hCD14 coding sequence was isolated by polymerase chain reaction (PCR) from human genomic DNA. Two primers covering the hCD14 coding sequence, but excluding the hCD14 signal sequence (Figure 3), were designed based on the published sequence (161). The 5' primer (5'-CGCGGAAGATATCACCACGCCAGAACCTTGTGAGCTGGA-3') was designed with an *Eco*R V restriction site (underlined), whereas the 3' primer (5'-GGCATAAGCTTGGATCC**TTA** GGCAAAGCCCCGGGCCCCT-3') contained *Hin*d III and *Bam*H I restriction sites (underlined) and a stop codon (bold). PCR was performed using $Vent_R$ DNA Polymerase Kit (New England Biolabs, Mississauga, ON) and 35 cycles of denaturation at 94°C for 1 min; annealing at 61°C for 1 min and extension at 72°C for 1 min. The resulting PCR products were subjected to 3' end A-tailing by using *Taq* DNA polymerase (Promega Corporation, Madison, WI) following the manufacturer's instructions. The A-tailed PCR product was cloned into the pGEM-T Easy Vector (Promega Corporation, Madison, WI) and the construct was named pCD14WT (Figure 19). To target seed specific expression, the hCD14 coding sequence was cloned under the control of the 1.8 kb or 5.1 kb rice glutelin Gt-1 promoter (162), the rice glutelin Gt-1 signal sequence and the nopaline synthase termination of transcription signal (145) (Figure 19 and 20). To confirm the integrity of the hCD14 coding sequence, DNA sequencing was performed on the pCD-1WT

Figure 19. Construction of the pWT1.8 expression cassette containing the hCD14 coding sequence under the control of the truncated 1.8 Kb rice glutelin seed-specific Gt-1 promoter. The hCD14 coding sequence lacking the human signal sequence was subcloned from pCD14WT into pPH3 using the *Nae* I and *Eco*R V blunt-end restriction enzymes as well as *Hin*d III. The glutelin Gt-1 signal sequence (Gt-1/SS) fused to the hCD14 coding sequence was thereafter subcloned into the pPH3/GM-CSF/Nos-ter construct. The generated pCD-2WT construct was subcloned into the pRD400 transformation vector to generate the pWT1.8 expression construct. Legend: hCD14, human CD14 coding sequence lacking the human CD14 signal sequence; Gt-1 promoter, glutelin-1 promoter; Gt-1/SS, glutelin-1 signal sequence; LB, left border; Nos-ter, nopaline synthase gene polyadenylation signal; npt II, neomycin phosphotransferase II gene; RB, right border.

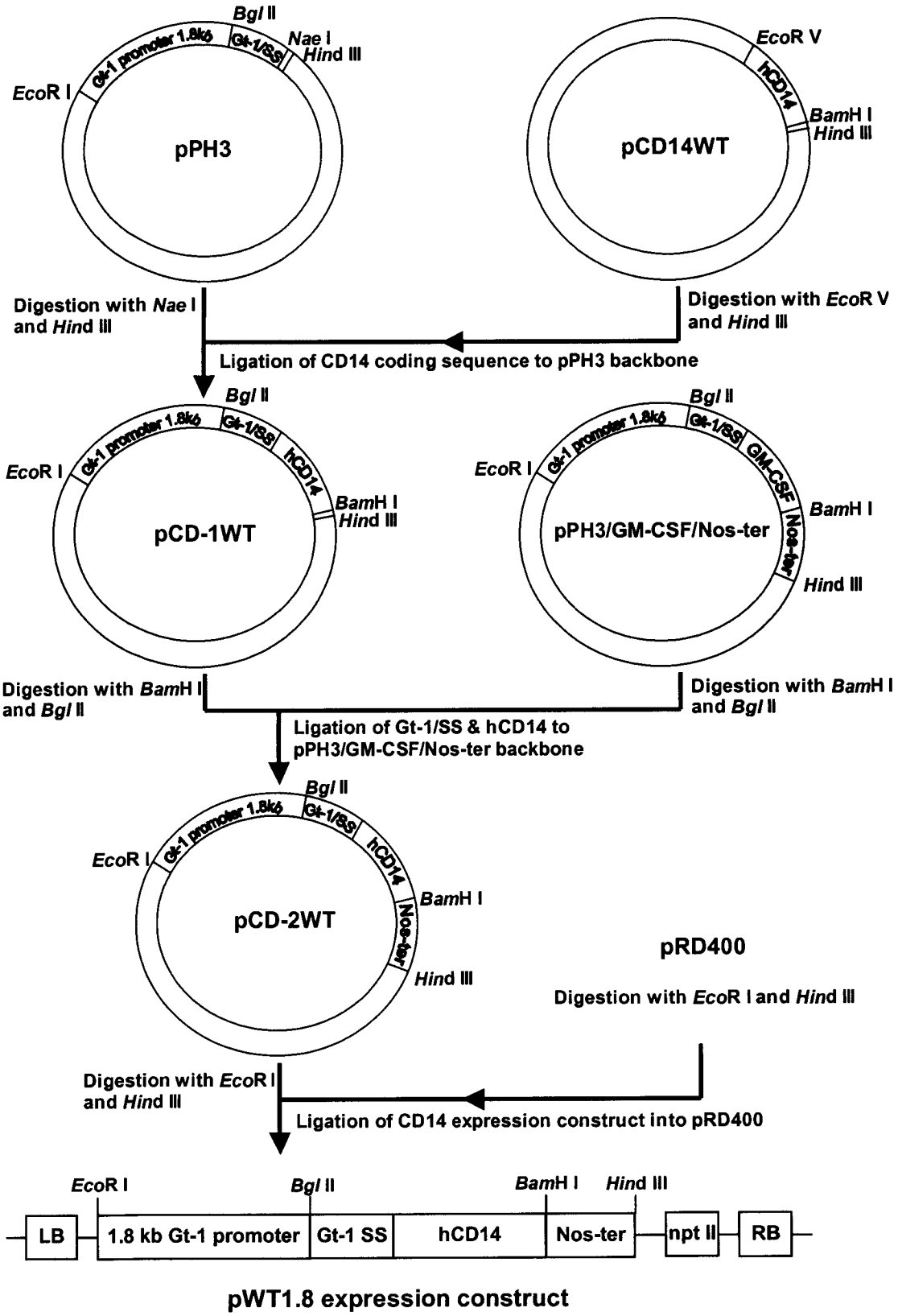
Bgl II
Nae I
Hind III
EcoR I
Gt-1 promoter 1.8kb
Gt-1/SS
pPH3
EcoR V
hCD14
BamH I
Hind III
pCD14WT
Digestion with Nae I and Hind III
Digestion with EcoR V and Hind III
Ligation of CD14 coding sequence to pPH3 backbone
pCD-1WT
pPH3/GM-CSF/Nos-ter
GM-CSF
Nos-ter
Digestion with BamH I and Bgl II
Ligation of Gt-1/SS & hCD14 to pPH3/GM-CSF/Nos-ter backbone
pCD-2WT
pRD400
Digestion with EcoR I and Hind III
Ligation of CD14 expression construct into pRD400
LB
1.8 kb Gt-1 promoter
Gt-1 SS
hCD14
Nos-ter
npt II
RB
pWT1.8 expression construct

Figure 19

Figure 20. Construction of the pWT5.1 expression cassette containing the hCD14 coding sequence under the control of the full-length 5.1 Kb rice glutelin seed-specific Gt-1 promoter. The expression construct of pCD-2WT was subcloned into the pPCR-Script Amp SK(+) using the *Ssp* I and *Hin*c II blunt-end restriction enzymes as well as *Hin*d III to introduce a *Kpn* I restriction site upstream of the 1.8 kb Gt-1 promoter. The full-length 5.1 kb Gt-1 promoter was thereafter subcloned from pGt1 into pCD-3WT to replace the truncated 1.8 kb Gt-1 promoter and generated pCD-4WT. The pCD-4WT construct was subcloned into the pRD400 transformation vector to generate the pWT5.1 expression construct. Legend: hCD14, human CD14 coding sequence lacking the human CD14 signal sequence; Gt-1 promoter, glutelin-1 promoter; Gt-1/SS, glutelin-1 signal sequence; LB, left border; Nos-ter, nopaline synthase gene polyadenylation signal; npt II, neomycin phosphotransferase II gene; RB, right border.

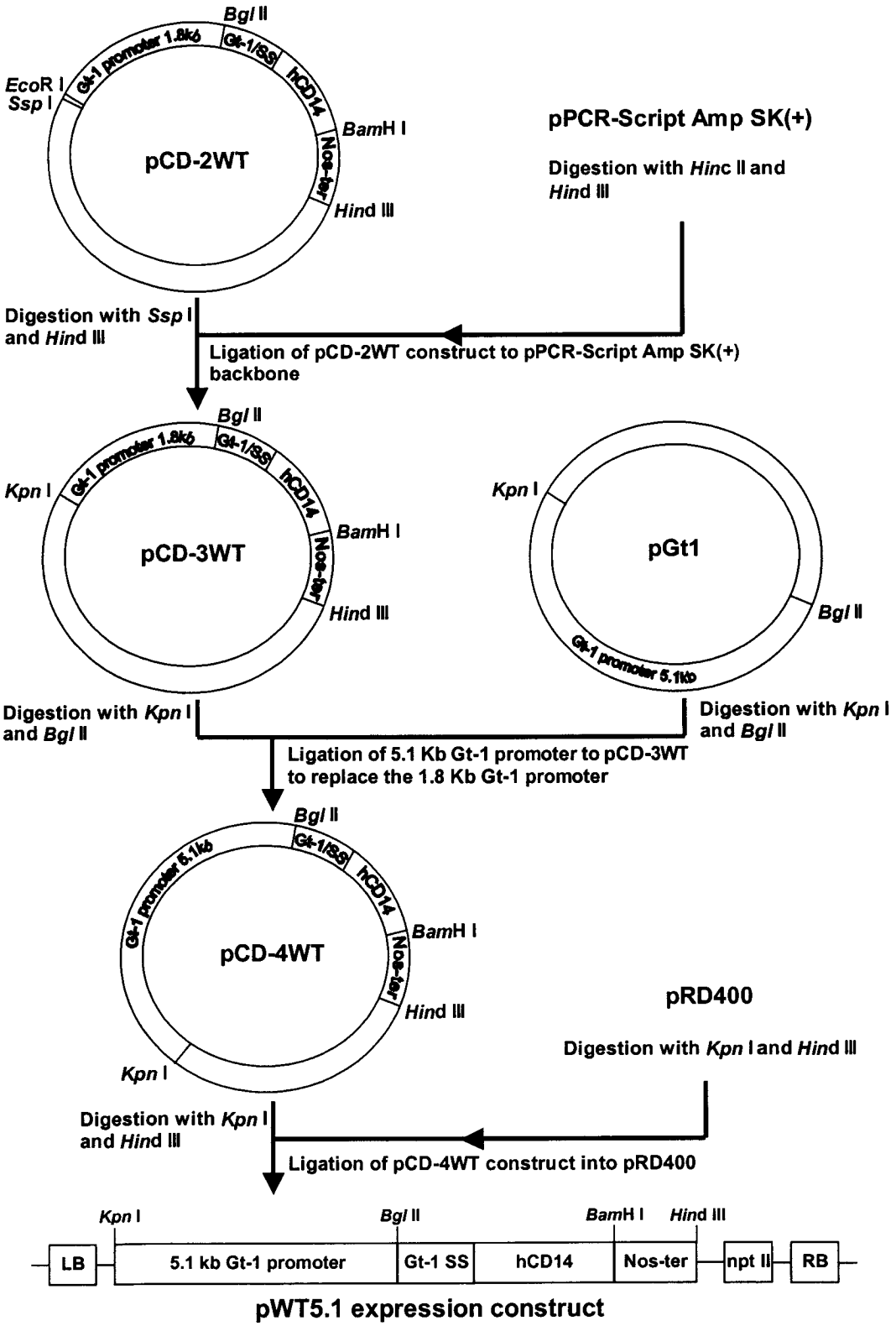
Bgl II
Gt-1 promoter 1.8kb
Gt-1/SS
hCD14
Nos-ter
EcoR I
Ssp I
BamH I
Hind III
pCD-2WT
pPCR-Script Amp SK(+)
Digestion with Hinc II and Hind III
Digestion with Ssp I and Hind III
Ligation of pCD-2WT construct to pPCR-Script Amp SK(+) backbone
Kpn I
pCD-3WT
pGt1
Gt-1 promoter 5.1kb
Digestion with Kpn I and Bgl II
Ligation of 5.1 Kb Gt-1 promoter to pCD-3WT to replace the 1.8 Kb Gt-1 promoter
pCD-4WT
pRD400
Digestion with Kpn I and Hind III
Ligation of pCD-4WT construct into pRD400
LB
5.1 kb Gt-1 promoter
Gt-1 SS
hCD14
Nos-ter
npt II
RB
pWT5.1 expression construct

Figure 20

plasmid, using the following primers: 5'-dGCACGATGATTTCTCATTG, 5'-dGCTCAGCTACTGGTAGGCG, and 5'-dACGCCCACAGGCGTGTGC. The two transgene expression cassettes were further cloned into the *Agrobacterium* binary vector pRD400 (163) to generate the pWT1.8 and pWT5.1 expression constructs (Figure 19 and 20). The pWT1.8 and pWT5.1 vectors were introduced into the *Agrobacterium tumefaciens* strain LBA4404 (Gibco/BRL, Mississauga, ON) by cold-shock transformation (164). *Agrobacterium*-mediated transformation was performed on leaf disk tissue of *Nicotiana tabacum* cultivar Xanthi as previously described (165). Kanamycin (300 mg/L) was used to select transformants, defined as T0 lines. The first generation (T1) lines were progeny lines derived from self-pollination of the T0 primary events.

PCR, Southern analyses and RT-PCR

Tobacco genomic DNA was extracted from young leaves of transformed and non-transformed plants as previously described (166). For PCR, the hCD14 coding sequence was amplified using the REDExtract-N-Amp^{TM} Plant PCR kit (Sigma-Aldrich, St. Louis, MO) with the same primers and PCR conditions as described above.

Southern blotting was performed as previously described (167). Briefly, 40 μg of plant genomic DNA was digested with the appropriate restriction enzymes (New England BioLabs Inc., Mississauga, ON). The restriction-digested DNA fragments were separated on a 0.7% agarose gel, denatured and transferred onto Hybond-N+ nylon membrane (Amersham Biosciences, Piscataway, NJ). The membrane was probed with the [^{32}P] labeled *Bgl* II - *Bam*H I fragment corresponding to the Gt-1 signal sequence and hCD14 coding sequence from the pWT1.8 expression construct (Figure 19). The radiolabelling was performed using the Ready-to-go DNA Labelling kit (Pharmacia, Baie d'Urfé, Québec). The hybridizations were incubated overnight at

68°C. The blots were then subjected twice to 15 min washes in 2X SSC containing 0.1% SDS at room temperature, followed by two 30 min washes in a 0.1X SSC, 0.5% SDS solution at 37°C and 68°C, respectively. Kodak Biomax MS-1 Films (Amersham Biosciences, Piscataway, NJ) were exposed to the nylon membranes for 16-24 h at –70°C before being developed.

For RT-PCR, RNA was extracted from developing seeds (6-11 days after pollination) using the RNeasy Plant Mini kit and the RNase-free DNase kit (Qiagen Inc., Mississauga, ON). First strand cDNA synthesis was performed with the Superscript™ First-Strand Synthesis for RT-PCR (Invitrogen Life Technologies, Carlsbad, CA). The hCD14 coding sequence was amplified using the REDExtract-N-Amp™ PCR Readymix™ (Sigma-Aldrich, St. Louis, MO) with the same primers and PCR conditions as described above. The resulting products were resolved by electrophoresis in ethidium bromide-stained 1% low-melt agarose gel. To further confirm the veracity of the RT-PCR products, the amplified sequences were purified with the QIAquick Gel Extraction kit (Qiagen Inc., Mississauga, ON) and sequenced by the University of Ottawa Biotechnology Research Institute (Ottawa, ON) using the PCR primers.

ELISA and western blotting

Mature tobacco seeds (16-20 days after pollination) were grounded in liquid nitrogen with a mortar and pestle and their proteins were extracted as previously described (145). The rhCD14 concentration in protein extracts was measured using ELISA plates (HyCult Biotechnology, Uden, The Netherlands). For western immunoblotting, total soluble protein extracts were resolved by SDS-PAGE electrophoresis under reducing conditions (11% resolving gel) and transferred onto nitrocellulose (Amersham Biosciences, Piscataway, NJ). The membrane was blocked for 1 h in 5% dried skim milk in TBS with 0.1% Tween-20. The rhCD14 protein was probed with the biotinylated polyclonal anti-human CD14 antibody (0.05 μg/mL in TBS-Tween).

After extensive washing, the membrane was incubated for 1 h with the anti-biotin HRP-conjugated antibody (1:1,000) (Cell Signaling Technology, Beverly, MA). The antigens were detected using a chemiluminescent system (ECL Western Blotting Detection Reagents, Amersham Biosciences, Piscataway, NJ).

Pepsin and pancreatin digestion analyses and biological assays

For *in vitro* digestion susceptibility experiments and biological assays, rhCD14 from total seed protein extract was partially purified and concentrated by ammonium sulfate precipitation. Briefly, ammonium sulfate was added to the total protein extract to a final concentration of 40% (w/v). The mixture was incubated on ice for 1 h with occasional shaking and centrifuged at 10,000g for 10 min at 4°C. Ammonium sulfate was further added to the supernatant to give a final concentration of 55% (w/v). The solution was incubated on ice for 1 h with occasional shaking and centrifuged at 10,000g for 10 min at 4°C. The pellet was resuspended in PBS, dialyzed against the same buffer and concentrated using the Centriprep YM-10 Centrifugal Filter Unit (Millipore, Billerica, MA).

In vitro digestions of transgenic tobacco soluble seed proteins extracts, breast milk and commercial CHO rhCD14 with porcine pepsin and pancreatin enzymes were performed as described in chapter 3. Biological assays were performed on primary corneal epithelial cells and the HCEC line as they were previously shown to react to LPS in presence of sCD14 (Figure 11). The cells were plated in 24-well flat-bottom tissue culture plates and after reaching approximately 80% confluence, they were left untreated or were preincubated with tobacco seed rhCD14 protein fraction (500 ng/mL of CD14), non-transgenic (NT) tobacco seed protein extract, 500 ng/mL CHO rhCD14, 10 μg/mL anti-human CD14 monoclonal antibody MY4 (mouse IgG2b; Beckman Coulter, Miami, FL), and 10 μg/mL of its isotype-matched control IgG2b MOPC-141 (Sigma-

Aldrich, St. Louis, MO) for 2 h at 37°C. To eliminate any unwanted LPS contaminants affecting cytokine production, the endotoxin levels were measured in all reagents with a gelatin assay of *Limulus* amebocyte lysate (Associates of Cape Cod, East Falmouth, MA). Any reagent that tested positive for LPS was treated with END-X (Associates of Cape Cod, Falmouth, MA) to remove any residual endotoxin. With rhCD14 and antibodies still present in the medium, LPS derived from *Pseudomonas aeruginosa* 10 (Sigma-Aldrich, St. Louis, MO) was added at a concentration of 100 ng/mL to activate the cells. The medium was harvested after 24 h, centrifuged to remove cellular debris and stored at –70°C until cytokine analysis. To verify the rhCD14 bioactivity, the culture supernatants were analyzed by ELISA for IL-8 (Sanguin Reagents, Amsterdam, Netherlands) and IL-6 (eBioscience, San Diego, CA).

Statistical analysis

Individual experiments in this study were performed in triplicate to confirm the reproducibility of the results. Values are presented as mean ± standard deviation. The statistical significance of differences between two or more means was evaluated by using one-way ANOVA; P values of less than 0.05 (indicated by asterisks) were considered to be statistically significant.

Results

Generation and identification of stable transgenic tobacco lines

To express hCD14 in tobacco, transgene expression vectors were constructed, in which the hCD14 coding sequence was cloned under the control of the 1.8 kb or 5.1 kb rice glutelin Gt-1 promoter, the rice glutelin Gt-1 signal sequence and the nopaline synthase termination of transcription signal (Figure 19 and 20). The sequencing of the hCD14 coding sequence cloned in pCD-1WT (Figure 19) revealed that the 72 bp Gt-1 signal sequence was fused in-frame of the 5'end of the mature hCD14 coding sequence (Figure 21). The stop codon was also present in-frame at the 3'end of the hCD14 coding sequence (Figure 21). DNA sequencing revealed no mutations in the Gt-1 signal sequence, nor in the hCD14 coding sequence (161, 168).

After *Agrobacterium*-mediated transformation, transgenic plantlets containing the hCD14 transgene were first selected by kanamycin resistance and then screened for the hCD14 coding sequence (1.1 kb) by genomic PCR (Figure 22a). In total, eight WT1.8 and nine WT5.1 independent transgenic plants were chosen for further investigation. Genome integration of the entire and intact expression cassette was confirmed by Southern blot analysis, where both the 3.2 and 6.5 kb restriction-digested fragments corresponding to the entire pWT1.8 and pWT5.1 expression cassettes were detected in the transformed plants (Figure 22c). Southern blotting revealed the genomic organization of independent transgenic events. The tested transgenic lines contained between one and four transgene copies in their genomes (Figure 22b). PCR and Southern analysis confirmed that the hCD14 transgene was stably inherited to the successive T1 generation (Figure 23). The overall horticultural traits and development of these two generations of transgenic plants were similar to those of NT plants.

Figure 21. Nucleotide sequence of the hCD14 coding sequence fused to the Gt-1 signal sequence. The entire hCD14 coding sequence fused to the Gt-1 signal sequence and cloned into the pCD-1WT vector (Figure 19) was sequenced as described in the materials and methods section. The 72 nucleotides glutelin-1 signal sequence (**red**) was found to be in-frame at the 5'end of the 1,071 nucleotides mature hCD14 coding sequence (**black**) ending with a stop codon (**blue**).

```
ATGGCATCCA TAAATCGCCC CATAGTTTTC TTCACAGTTT GCTTGTTCCT    50
CTTGTGCGAT GGCTCCCTAG CCACCACGCC AGAACCTTGT GAGCTGGACG   100
ATGAAGATTT CCGCTGCGTC TGCAACTTCT CCGAACCTCA GCCCGACTGG   150
TCCGAAGCCT TCCAGTGTGT GTCTGCAGTA GAGGTGGAGA TCCATGCCGG   200
CGGTCTCAAC CTAGAGCCGT TTCTAAAGCG CGTCGATGCG GACGCCGACC   250
CGCGGCAGTA TGCTGACACG GTCAAGGCTC TCCGCGTGCG GCGGCTCACA   300
GTGGGAGCCG CACAGGTTCC TGCTCAGCTA CTGGTAGGCG CCCTGCGTGT   350
GCTAGCGTAC TCCCGCCTCA AGGAACTGAC GCTCGAGGAC CTAAAGATAA   400
CCGGCACCAT GCCTCCGCTG CCTCTGGAAG CCACAGGACT TGCACTTTCC   450
AGCTTGCGCC TACGCAACGT GTCGTGGGCG ACAGGGCGTT CTTGGCTCGC   500
CGAGCTGCAG CAGTGGCTCA AGCCAGGCCT CAAGGTACTG AGCATTGCCC   550
AAGCACACTC GCCTGCCTTT TCCTACGAAC AGGTTCGCGC CTTCCCGGCC   600
CTTACCAGCC TAGACCTGTC TGACAATCCT GGACTGGGCG AACGCGGACT   650
GATGGCGGCT CTCTGTCCCC ACAAGTTCCC GGCCATCCAG AATCTAGCGC   700
TGCGCAACAC AGGAATGGAG ACGCCCACAG GCGTGTGCGC CGCACTGGCG   750
GCGGCAGGTG TGCAGCCCCA CAGCCTAGAC CTCAGCCACA ACTCGCTGCG   800
CGCCACCGTA AACCCTAGCG CTCCGAGATG CATGTGGTCC AGCGCCCTGA   850
ACTCCCTCAA TCTGTCGTTC GCTGGGCTGG AACAGGTGCC TAAAGGACTG   900
CCAGCCAAGC TCAGAGTGCT CGATCTCAGC TGCAACAGAC TGAACAGGGC   950
GCCGCAGCCT GACGAGCTGC CCGAGGTGGA TAACCTGACA CTGGACGGGA  1000
ATCCCTTCCT GGTCCCTGGA ACTGCCCTCC CCCACGAGGG CTCAATGAAC  1050
TCCGGCGTGG TCCCAGCCTG TGCACGTTCG ACCCTGTCGG TGGGGGTGTC  1100
GGGAACCCTG GTGCTGCTCC AAGGGGCCCG GGGCTTTGCC TAA         1143
```

Figure 21

Figure 22. Identification and molecular characterization of T0 transgenic tobacco. **(a)** The PCR amplification of the CD14 coding sequence from tobacco genomic DNA was performed to reveal the transgenic nature of the transformed plants. **(b)** Southern analysis was performed to determine the genomic organization of independent transgenic events. Genomic DNA (40 μg) was digested with *Bgl* II and probed with the 1.1 kb [^{32}P] radiolabelled *Bgl* II – *Bam*H I fragment (corresponding to the Gt-1 signal sequence and hCD14 coding sequence) from the pWT1.8 construct (Figure 19). **(c)** Southern blotting was conducted to verify that no transgene rearrangements occurred during the genomic insertion of the expression construct. Genomic DNA (40 μg) from selected transgenic tobacco transformed with the WT1.8 or WT5.1 transgene was digested with *Eco*R I + *Hin*d III or *Kpn* I + *Hin*d III, respectively and probed as indicated above. Transgenic plant lines are identified by number and are grouped by the expression construct (WT1.8 or WT5.1) inserted into their genome. Non-transgenic tobacco (NT) was used as a non-transformed negative control, while the digested full-lenght pWT1.8 (*Eco*R I – *Hin*d III fragment) (Figure 19) and pWT5.1 (*Kpn* I – *Hin*d III fragment) (Figure 20) expression contructs were used as positive controls (+) where their respective size is indicated with the arrowhead.

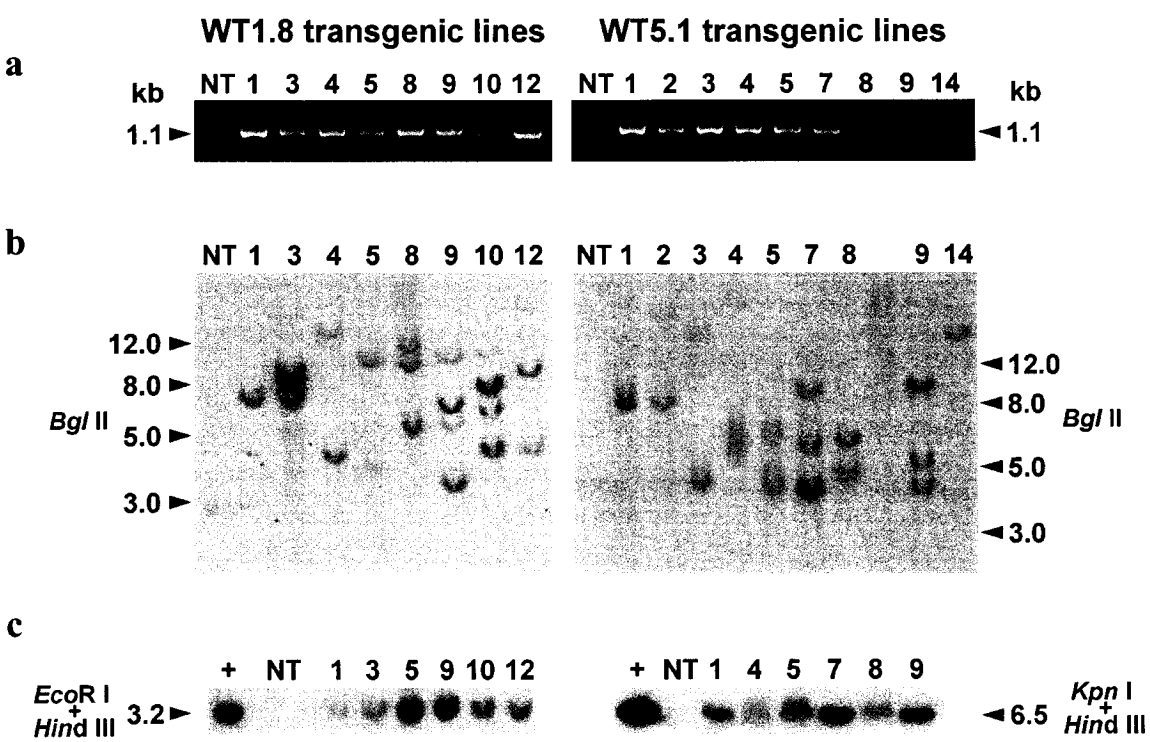
a
WT1.8 transgenic lines
WT5.1 transgenic lines
kb
NT 1 3 4 5 8 9 10 12
NT 1 2 3 4 5 7 8 9 14
kb
1.1
1.1
b
NT 1 3 4 5 8 9 10 12
NT 1 2 3 4 5 7 8 9 14
12.0
8.0
Bgl II
5.0
3.0
12.0
8.0
Bgl II
5.0
3.0
c
+ NT 1 3 5 9 10 12
+ NT 1 4 5 7 8 9
EcoR I + Hind III
3.2
6.5
Kpn I + Hind III

Figure 22

Figure 23. Identification and molecular characterization of T1 transgenic tobacco. **(a)** The PCR amplification of the CD14 coding sequence from selected T1 tobacco genomic DNA was performed to confirm the transgenic nature of the plants. **(b)** Southern analysis was performed to compare the genomic organization between T0 and T1 transgenic plants. Genomic DNA (40 μg) was digested with *Bgl* II and probed with the 1.1 kb [^{32}P] radiolabelled *Bgl* II – *Bam*H I fragment (corresponding to the Gt-1 signal sequence and hCD14 coding sequence) from the pWT1.8 construct (Figure 19). Transformed plants are identified by number and expression construct (WT1.8 or WT5.1). Non-transgenic tobacco (NT) was used as a non-transformed negative control.

a

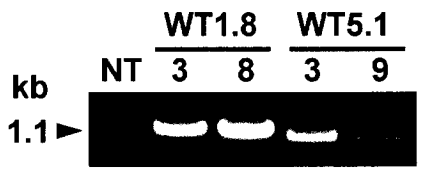
WT1.8
WT5.1
NT
3
8
3
9
kb
1.1

b

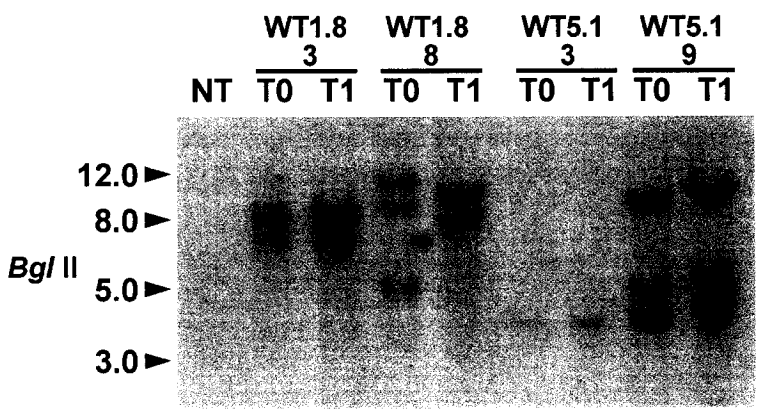
WT1.8
3
WT1.8
8
WT5.1
3
WT5.1
9
NT
T0
T1
T0
T1
T0
T1
T0
T1
12.0
8.0
Bgl II
5.0
3.0

Figure 23

CD14 is specifically expressed in seeds of transgenic tobacco

To determine the hCD14 transgene expression in T0 and T1 transgenic tobacco, RT-PCR, ELISA and immunoblotting were performed on seeds and other plant tissues. CD14 expression was detected in developing seeds of both T0 and T1 plants by RT-PCR amplification of the transgenic transcript using human gene specific primers (Figure 24a). Sequencing of the RT-PCR products (Figure 25) correlated to the hCD14 published sequence (161). To support the RT-PCR findings and to estimate the structural integrity of rhCD14 proteins, immunoblotting was performed on the seed protein extracts. One polypeptide of apparent molecular mass of 46 kDa was detected with the polyclonal anti-CD14 antibody in representative seed samples, and was slightly lower than the molecular weight of the CHO rhCD14 protein (50 kDa) (Figure 24b). Western blotting analysis of various plant tissues showed the presence of the rhCD14 protein to be limited to seed tissue (Figure 24c). The rhCD14 seed-specific expression was also supported by ELISA performed on different plant tissues (data not shown).

The concentration of rhCD14 protein in mature tobacco seeds was assessed by ELISA. The protein was detected in seed extracts of all tested transgenic plants and their progeny (n = 25), with a mean concentration of 2.19 ± 1.69 μg/g seeds for WT1.8-T0 and 1.39 ± 0.68 μg/g seeds for WT5.1-T0 transgenic plants (Figure 26). One-way ANOVA analysis revealed that the full-length (5.1 kb) or the truncated (1.8 kb) Gt-1 promoters had no influence on rhCD14 seed expression and that the seed rhCD14 levels were similar between T0 and T1 generations. Seed protein extracts of NT plants showed no immunoreactive material (Figure 26).

Figure 24. Expression of rhCD14 in T0 and T1 transgenic tobacco. **(a)** RT-PCR detection of CD14 transcripts in developing seeds (6-11 days after pollination) of transgenic tobacco. The reactions were performed with (+) or without (-) the reverse-transcriptase (RT) step to confirm the cDNA origin of the amplification. Non-transgenic tobacco (NT) was used as a non-transformed negative control, while the pWT5.1 expression construct was used as a positive control. **(b)** Western blot analysis of seed protein extracts from selected transgenic plants. The seed extracts were subjected to western immunoblotting with the biotinylated anti-CD14 polyclonal antibody followed by the anti-biotin HRP-linked antibody. NT plant and commercially available CHO produced rhCD14 (CHO CD14) were used as negative and positive controls. **(c)** Western blot analysis of tissue specific expression of CD14 in the wt1.8-3 T0 transgenic tobacco. The seed specific expression analysis is representative of three independent experiments performed on tissue extracts from different transgenic tobacco plants (WT1.8-3 T0, WT5.1-3 T0 and WT1.8-3 T1).

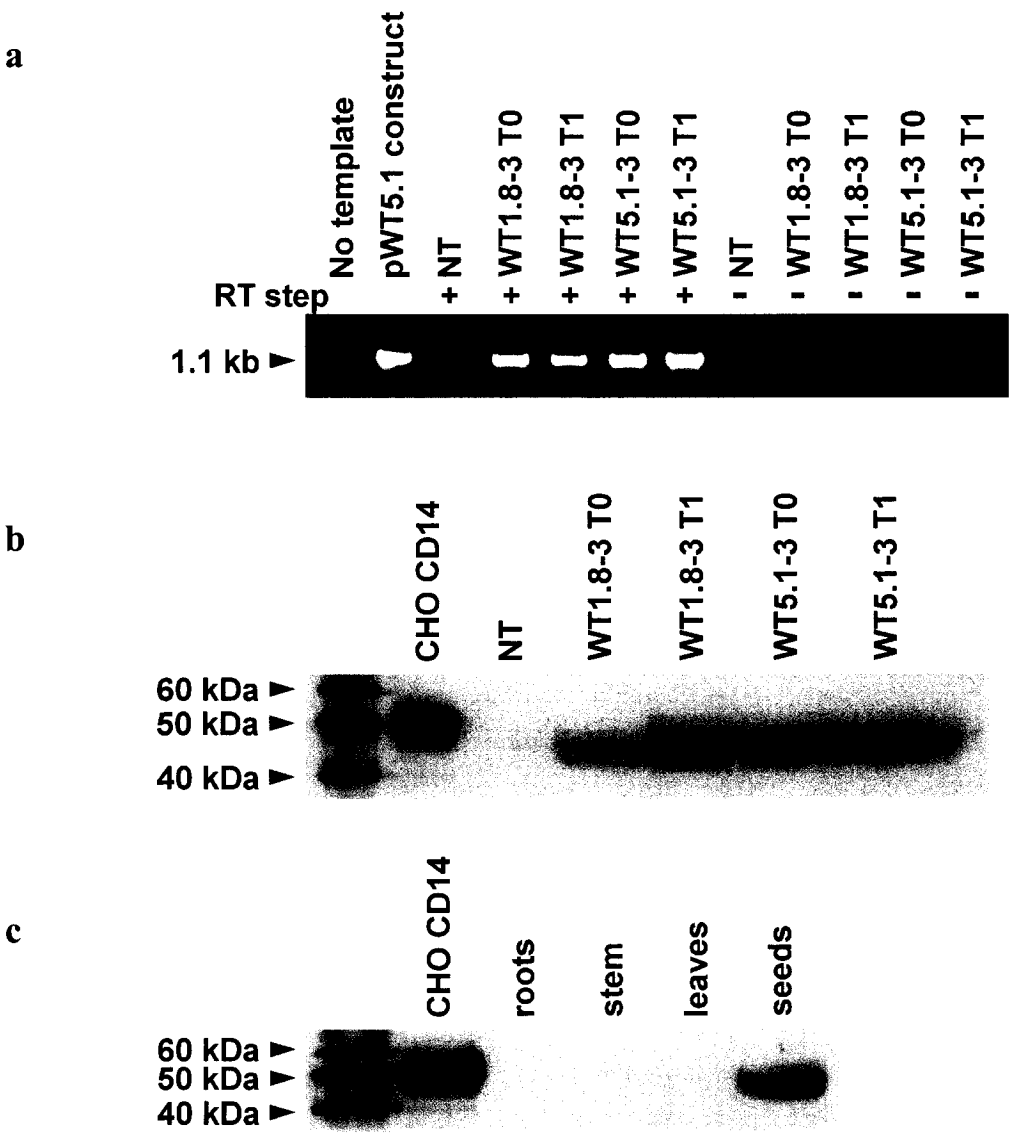
a
RT step
No template
pWT5.1 construct
+ NT
+ WT1.8-3 T0
+ WT1.8-3 T1
+ WT5.1-3 T0
+ WT5.1-3 T1
- NT
- WT1.8-3 T0
- WT1.8-3 T1
- WT5.1-3 T0
- WT5.1-3 T1
1.1 kb
b
CHO CD14
NT
WT1.8-3 T0
WT1.8-3 T1
WT5.1-3 T0
WT5.1-3 T1
60 kDa
50 kDa
40 kDa
c
CHO CD14
roots
stem
leaves
seeds
60 kDa
50 kDa
40 kDa

Figure 24

Figure 25. Nucleotide sequence of the rhCD14 RT-PCR product amplified from WT1.8-3 T0 transgenic tobacco. RNA was extracted from developing seeds (6-11 days after pollination) of the transgenic tobacco line WT1.8-3 T0, was subjected RT-PCR to amplify hCD14 coding sequence (Figure 24a) and the resulting products were sequenced. The sequencing result corresponds to nucleotides 159 to 913 of the 1,143 nucleotides constituting the Gt1 signal sequence fused to the hCD14 coding sequence (Figure 21).

```
CTTCCAGTGT GTGTCTGCAG TAGAGGTGGA GATCCATGCC GGCGGTCTCA  50
ACCTAGAGCC GTTTCTAAAG CGCGTCGATG CGGACGCCGA CCCGCGGCAG 100
TATGCTGACA CGGTCAAGGC TCTCCGCGTG CGGCGGCTCA CAGTGGGAGC 150
CGCACAGGTT CCTGCTCAGC TACTGGTAGG CGCCCTGCGT GTGCTAGCGT 200
ACTCCCGCCT CAAGGAACTG ACGCTCGAGG ACCTAAAGAT AACCGGCACC 250
ATGCCTCCGC TGCCTCTGGA AGCCACAGGA CTTGCACTTT CCAGCTTGCG 300
CCTACGCAAC GTGTCGTGGG CGACAGGGCG TTCTTGGCTC GCCGAGCTGC 350
AGCAGTGGCT CAAGCCAGGC CTCAAGGTAC TGAGCATTGC CCAAGCACAC 400
TCGCCTGCCT TTTCCTACGA ACAGGTTCGC GCCTTCCCGG CCCTTACCAG 450
CCTAGACCTG TCTGACAATC CTGGACTGGG CGAACGCGGA CTGATGGCGG 500
CTCTCTGTCC CCACAAGTTC CCGGCCATCC AGAATCTAGC GCTGCGCAAC 550
ACAGGAATGG AGACGCCCAC AGGCGTGTGC GCCGCACTGG CGGCGGCAGG 600
TGTGCAGCCC CACAGCCTAG ACCTCAGCCA CAACTCGCTG CGCGCCACCG 650
TAAACCCTAG CGCTCCGAGA TGCATGTGGT CCAGCGCCCT GAACTCCCTC 700
AATCTGTCGT TCGCTGGGCT GGAACAGGTG CCTAAAGGAC TGCCAGCCAA 750
GCTCA                                                   755
```

Figure 25

Figure 26. Quantification of rhCD14 proteins in seeds of T0 and T1 transgenic tobacco. Mature seeds (16-20 days after pollination) of transgenic plants transformed with different expression cassettes (WT1.8 or WT5.1) were subjected to protein extraction and analyzed by ELISA for their rhCD14 content. Seed extracts from non-transformed plants (NT) were assayed as a negative control. Results are expressed as means ± SD of triplicate cultures of one experiment representative of three.

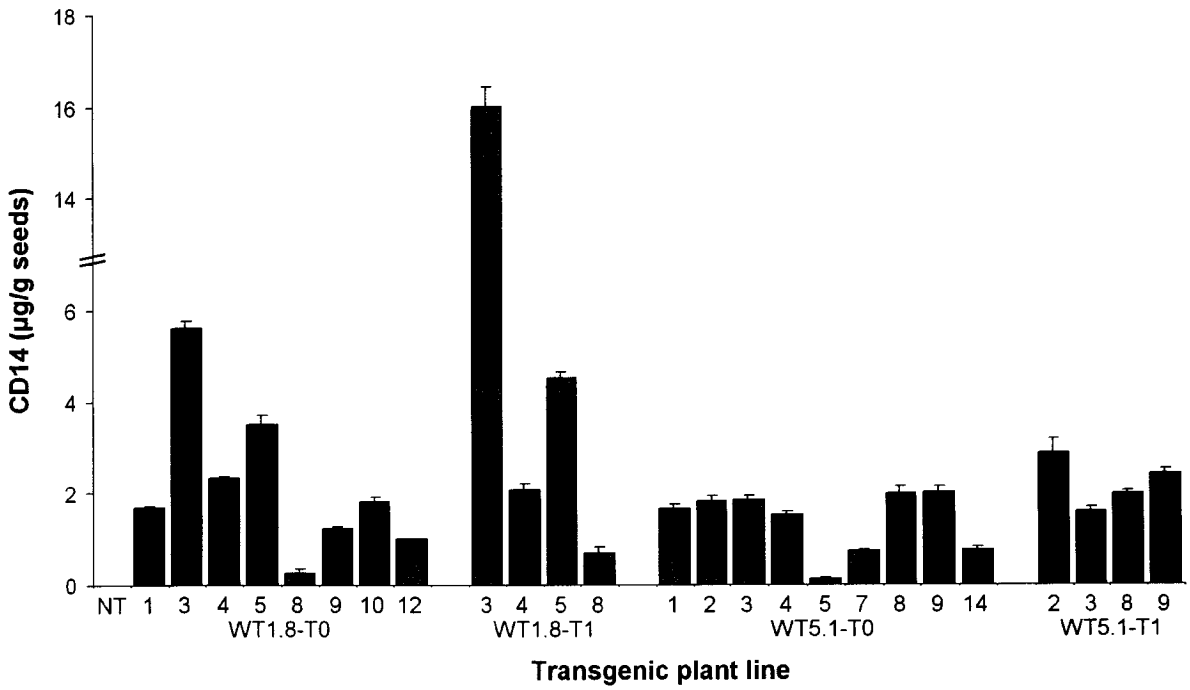
18
16
14
6
4
2
0
CD14 (µg/g seeds)
NT 1 3 4 5 8 9 10 12
WT1.8-T0
3 4 5 8
WT1.8-T1
1 2 3 4 5 7 8 9 14
WT5.1-T0
2 3 8 9
WT5.1-T1
Transgenic plant line

Figure 26

Plant produced rhCD14 has similar digestive resistance and biological activity to CHO produced rhCD14

To assess the half-life and the proteolytic resistance of rhCD14 synthesized in transgenic plants, plant rhCD14, CHO rhCD14 and human breast milk (a natural source of hCD14) were subjected to *in vitro* proteolysis with porcine pepsin and pancreatin enzymes. Plant produced rhCD14 showed a stronger resistance to pepsin digestion, compared to CHO rhCD14 (Figure 27a). Approximately one quarter of the original amount of plant rhCD14 was still remaining after the 10 mg/mL pepsin digestion (Figure 27a). Breast milk sCD14, however, had the highest resistance to the pepsin digestion, when compared to the two other sources of rhCD14 (Figure 27a). A similar trend in the digestive susceptibility of the three sources of CD14 was observed for the pancreatin digestion, where no plant rhCD14 could be detected after the 10 mg/mL digestion (Figure 27b). The third digestion, where pepsin and pancreatin digestions were added sequentially, both CHO produced and plant produced rhCD14 were proteolyzed at the shortest digestion period (30 min pepsin and 60 min pancreatin), while one quarter of the original amount of breast milk hCD14 was still remaining after the longest digestion period (60 min pepsin and 120 min pancreatin) (Figure 27c). In general, plant rhCD14 had a proteolytic susceptibility ranging between those of CHO rhCD14 and breast milk sCD14 (Figure 27).

To determine the ability of plant rhCD14 protein to initiate an endotoxin response, the production of proinflammatory molecules was analyzed in human primary corneal epithelial cells and HCEC line challenged with *Pseudomonas*-derived LPS in the presence of CHO rhCD14 or plant rhCD14. In comparison to the cell culture media, neither LPS nor the NT seed protein extract significantly induced IL-6 or IL-8 secretion by primary corneal epithelial cells (Figure 28 a,b) and HCEC line (Figure 28 c,d). The addition of CHO rhCD14 or plant rhCD14 with LPS to the cells increased both IL-6 secretion by three-fold, and increased IL-8 secretion by

Figure 27. Western analysis of pepsin and/or pancreatin digested rhCD14 from transgenic tobacco seeds, commercial control CHO rhCD14 and human breast milk. **(a)** The tobacco seed CD14 extract (plant rhCD14), as well as CHO produced rhCD14 and breast milk used as digestion susceptibility controls (data from Figures 16, 17, 18), were subjected to *in vitro* proteolysis with the indicated concentrations of pepsin for 30 min at 37°C, pH 4.5 and subjected to western blotting with the biotinylated anti-CD14 polyclonal antibody followed by the anti-biotin HRP-linked antibody. Lane P represents porcine pepsin (10 mg/mL) in PBS as a loading control. **(b)** The three CD14 samples were digested *in vitro* with the indicated concentrations of pancreatin for 60 min at 37°C, pH 7.0 and subjected to western blotting as described above. Lane P represents porcine pancreatin (10 mg/mL) in PBS as a loading control. **(c)** The three CD14 samples were digested *in vitro* at various incubation times with pepsin (1 mg/mL) at 37°C, pH 4.5 followed by a pancreatin digestion (1 mg/mL) at 37°C, pH 7.0 and subjected to western blotting as described above. Lane P represents porcine pepsin (1 mg/mL) and pancreatin (1 mg/mL) in PBS as a loading control.

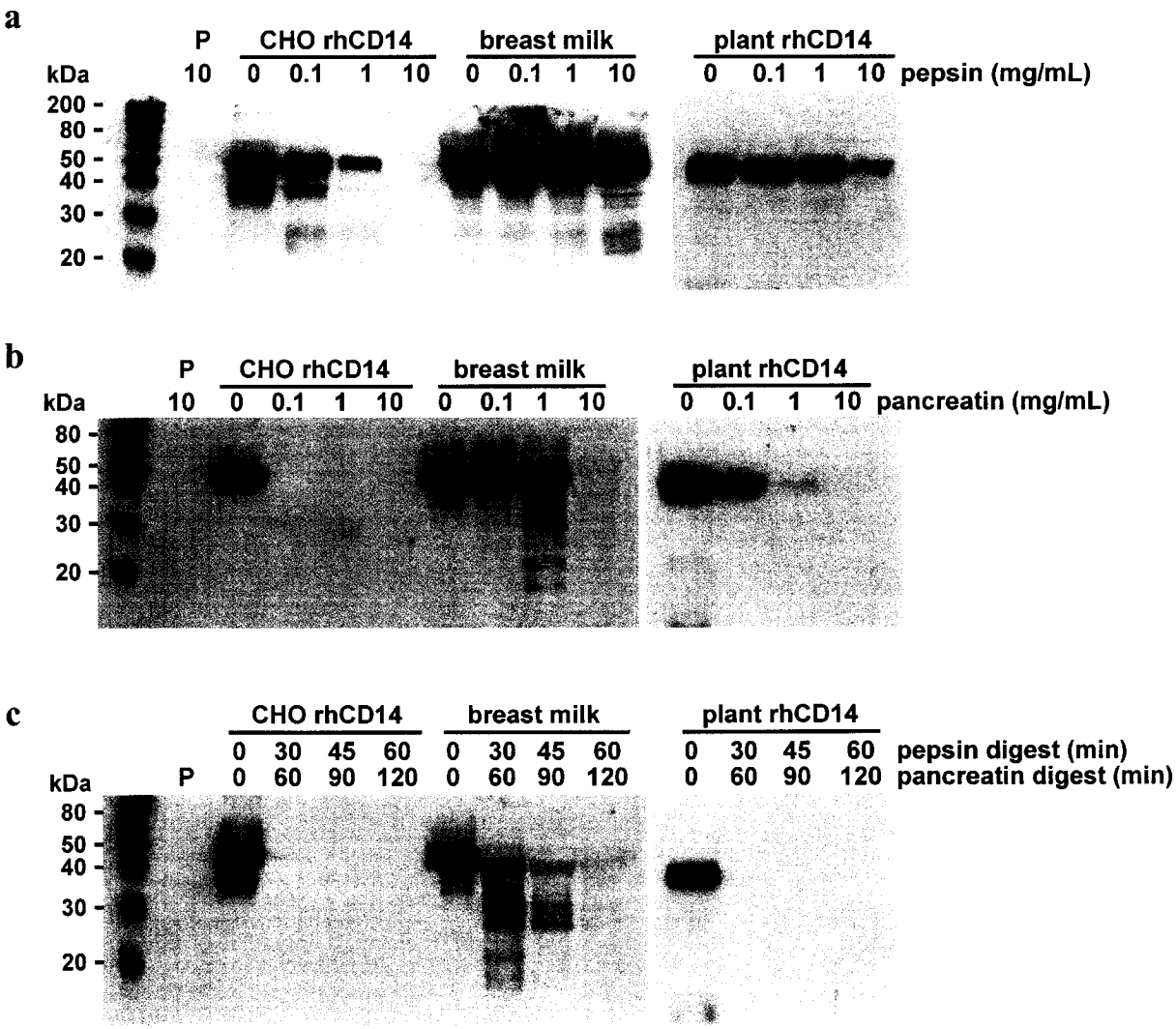
a
P
CHO rhCD14
breast milk
plant rhCD14
kDa
10
0 0.1 1 10
0 0.1 1 10
0 0.1 1 10
pepsin (mg/mL)
200
80
50
40
30
20
b
P
CHO rhCD14
breast milk
plant rhCD14
kDa
10
0 0.1 1 10
0 0.1 1 10
0 0.1 1 10
pancreatin (mg/mL)
80
50
40
30
20
c
CHO rhCD14
breast milk
plant rhCD14
0 30 45 60
0 30 45 60
0 30 45 60
pepsin digest (min)
kDa
P
0 60 90 120
0 60 90 120
0 60 90 120
pancreatin digest (min)
80
50
40
30
20

Figure 27

Figure 28. LPS response of primary corneal epithelial cells and HCEC line in presence of rhCD14 expressed in transgenic tobacco. Primary corneal epithelial cells **(a,b)** and HCEC line **(c,d)** were pretreated with control CHO rhCD14 (500 ng/mL) (data from figure 11), NT seed protein extract, rhCD14 expressed in WT1.8-3 T1 transgenic tobacco (500 ng/mL), anti-CD14 monoclonal antibody MY4 (10 μg/mL) and its isotype-matched control (IgG2b, 10 μg/mL) before addition of LPS from *P. aeruginosa* (100 ng/mL). Secretion of IL-6 and IL-8 proinflammatory cytokines in the cell culture media was assessed by ELISA. Results are expressed as means ± SD of triplicate cultures of one experiment representative of three. Statistically significant differences were determined using one-way ANOVA, with probabilities $*P < 0.05$ and $**P < 0.005$.

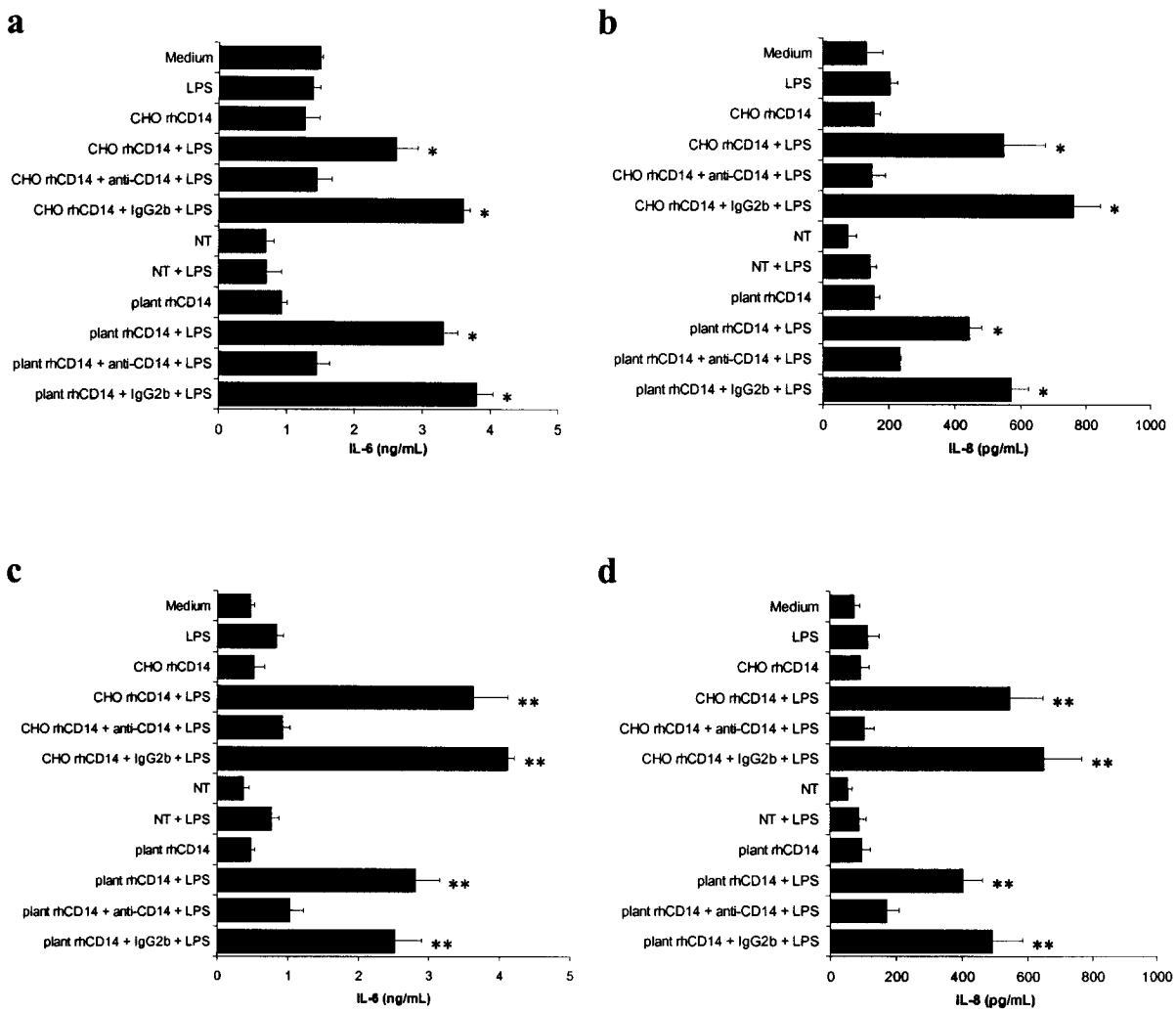
a
Medium
LPS
CHO rhCD14
CHO rhCD14 + LPS
CHO rhCD14 + anti-CD14 + LPS
CHO rhCD14 + IgG2b + LPS
NT
NT + LPS
plant rhCD14
plant rhCD14 + LPS
plant rhCD14 + anti-CD14 + LPS
plant rhCD14 + IgG2b + LPS
0 1 2 3 4 5
IL-6 (ng/mL)
b
Medium
LPS
CHO rhCD14
CHO rhCD14 + LPS
CHO rhCD14 + anti-CD14 + LPS
CHO rhCD14 + IgG2b + LPS
NT
NT + LPS
plant rhCD14
plant rhCD14 + LPS
plant rhCD14 + anti-CD14 + LPS
plant rhCD14 + IgG2b + LPS
0 200 400 600 800 1000
IL-8 (pg/mL)
c
Medium
LPS
CHO rhCD14
CHO rhCD14 + LPS
CHO rhCD14 + anti-CD14 + LPS
CHO rhCD14 + IgG2b + LPS
NT
NT + LPS
plant rhCD14
plant rhCD14 + LPS
plant rhCD14 + anti-CD14 + LPS
plant rhCD14 + IgG2b + LPS
0 1 2 3 4 5
IL-6 (ng/mL)
d
Medium
LPS
CHO rhCD14
CHO rhCD14 + LPS
CHO rhCD14 + anti-CD14 + LPS
CHO rhCD14 + IgG2b + LPS
NT
NT + LPS
plant rhCD14
plant rhCD14 + LPS
plant rhCD14 + anti-CD14 + LPS
plant rhCD14 + IgG2b + LPS
0 200 400 600 800 1000
IL-8 (pg/mL)

Figure 28

four- and three-fold respectively (Figure 28). The CD14-mediated activation was significantly abrogated by the neutralizing anti-CD14 MY4 antibody, but not by its isotype-antibody matched control. This indicates that plant rhCD14 and CHO rhCD14 in presence of LPS, signal the secretion of IL-6 and IL-8 cytokines (Figure 28).

Discussion

In this study, we analyzed the ability of genetically engineered tobacco plants to express biologically active rhCD14. To drive the expression of the rice glutelin Gt-1 signal sequence fused to the hCD14 coding sequence, two CD14 expression cassettes were generated, one containing the full-length (5.1 kb) rice glutelin Gt-1 promoter and the other containing a truncated (1.8 kb) version of the promoter. The detection of rhCD14 in transgenic tobacco using RT-PCR, ELISA and western blotting suggested that both rice Gt-1 promoters were active and capable to target the expression of rhCD14 exclusively in seeds. The levels of rhCD14 observed in tobacco seeds were similar to those of other human proteins (i.e. GM-CSF) under the control of the Gt-1 promoter (145). Similar protein levels obtained for rhCD14 and rhGM-CSF demonstrate the Gt-1 promoter constancy in controlling the expression of different human coding sequences in transgenic tobacco. Furthermore, the recombinant proteins were only detected in seeds, thus confirming the endosperm-specific expression of the Gt-1 promoter in tobacco (145, 169). Taken together, these results confirm that the Gt-1 monocot promoter is able to retain its activity and spatial expression in dicot plants.

Between the two groups of transgenic plants, one containing the full-length Gt-1 promoter and the other containing the truncated version, similar rhCD14 levels were observed in the seed extracts. The individual plant lines with the highest rhCD14 yields were those under the control of the truncated 1.8 kb Gt-1 promoter. A major positive *cis*-acting transcriptional regulatory element located in the far distal 5' region of the full-length (5.1 kb) Gt-1 promoter, and therefore absent from the truncated 1.8 Gt-1 promoter, was found responsible for a 20-fold increase of the promoter activity in rice endosperm (162, 170). The transcription factors in tobacco seeds did not seem to recognize this positive *cis*-regulatory element, because of the similar expression levels observed with the 5.1 kb and the 1.8 kb Gt-1 glutelin promoters. The

role of this regulatory element has never been studied in tobacco, since previous expression analyses of the rice Gt-1 promoter in tobacco were confined to the 1.3 kb proximal promoter, a smaller version of the 1.8 kb promoter (169). These results demonstrate that even if the Gt-1 monocot promoter retained its activity and specificity in dicot plants, different mechanisms of transcription regulation exist between the two *Angiospermae* subclasses.

Other factors, such as the number of transgene insertions, atypical codons, premature poly-A signals and mRNA destabilizing sequences, might influence the level of expression of the rhCD14 transgene. Southern blotting of independent transgene integration patterns indicated that the plants with a single or double transgene copy inserts generally had a higher rhCD14 expression compared to those with multiple transgene inserts. A similar trend has been observed with other transgenes (146) and is likely to be attributed to post-transcriptional gene silencing triggered by high transcription levels from the multiple transgene inserts (171). The detection of the entire and intact transgene by Southern blot suggests the absence of any rearrangements during its integration. The normal horticultural traits, development and fertility of the transformed plants indicated that the insertion sites of the transgene did not disrupt important endogenous genes. Following self-pollination, all the transgenic lines showed that the hCD14 transgene was stably inherited and expressed in the T1 progeny. Furthermore, the presence of rhCD14 protein in seeds did not show any toxicity towards the tobacco embryo, since germination occurred normally. These genetic and expression analyses demonstrated that the rhCD14 transgenes and the accumulation of rhCD14 in tobacco seeds were stably inherited in these transgenic tobacco lines.

The characterization of transgenically produced rhCD14 protein by western immunoblot suggests that the N-terminal rice Gt-1 signal peptide of 24 amino acids was cleaved from the

rhCD14 protein, since a smaller molecular weight (46 kDa) (Figure 24b, lanes 4-7) was observed for plant rhCD14 when compared to the molecular size (50 kDa) of its CHO produced counterpart (Figure 24b, lane 2). If rhCD14 had retained its Gt-1 signal peptide, its molecular mass would have been approximatively 2-3 kDa higher. The cleavage of the glutelin signal sequence would imply that the rhCD14 protein was correctly processed by the endoplasmic reticulum (ER) and subsequently deposited into the ER-derived protein bodies of the seed endosperm (172). It has been previously shown that the rice Gt-1 signal peptide is effective in targeting and accumulating human proteins in tobacco seed endosperm protein bodies (160, 173).

The difference in the molecular mass observed between rhCD14 synthesized in transgenic tobacco lines and CHO cells (Figure 24b, lanes 4 and 2) suggest that rhCD14 post-translation modifications, such as glycosylation, might vary between the two expression systems. The hCD14 protein has been shown to have N-linked and O-linked carbohydrates (Figure 3), accounting for an average of 20% of the total molecular weight of the mature glycoprotein (19). Previous studies demonstrated that the glycosylated state of hCD14 is neither likely to influence the protein's ability to bind LPS, nor its capacity to trigger an innate immune response (19).

However, it has been postulated that the degree of glycosylation of hCD14 might be involved in the stability and the half-life of the protein (19). To test this hypothesis, digestibility studies were performed and indicated that plant rhCD14 has a similar resistance to pepsin and pancreatin digestion to that of CHO rhCD14 and breast milk shCD14. The slightly enhanced proteolytic resistance observed for hCD14 naturally present in breast milk could be attributed to the abundance in breast milk of alternate substrates for the digestive enzymes and to the presence of protease inhibitors in breast milk (136). These results indicate that any tobacco-generated post-

translational modifications of rhCD14 did not seem to influence, either positively or negatively, rhCD14 stability and proteolytic susceptibility.

CD14 bioassays were performed to investigate if the tobacco endosperm post-translational modifications may have affected the protein activity. The rhCD14 fraction, purified from transgenic tobacco seeds, was able to induce the secretion of IL-6 and IL-8 pro-inflammatory cytokines in the presence of LPS, as in the case with commercial CHO rhCD14. The absence of any observable stimulation from primary corneal epithelial cells and HCEC with NT seed extract or neutralizing anti-CD14 antibody indicates that the activity observed from transgenic seed extracts originated from plant rhCD14. These biological assay results indicate that rhCD14 produced in seeds of transgenic tobacco is functionally active.

This third thesis project found that tobacco is a promising expression system for *in planta* production of stable and biologically active rhCD14. The accumulation of rhCD14 in tobacco seed endosperm from stably transformed plants offers an inexpensive and abundant supply of this immune protein. Such a low-cost preparation now facilitates the assessment of its role and impact on the innate immune system. The currently achieved levels of rhCD14 protein accumulation (16 μg/g seeds) in transgenic plants may be further increased by codon optimization of rhCD14 to match plant codon usage, selection of even stronger promoters and signal sequences, such as the KDEL retention signal. Ideally, one may want to generate transgenic cereals expressing rhCD14 for direct oral delivery and research of innate immune responses at mucosal surfaces.

Chapter 5

Conclusions and future directions

LPS is the major virulence factor of pathogenic and commensal Gram-negative bacteria. Due to high sensitivity of the LPS immune response, a Gram-negative infection can result in severe and occasionally deadly complications known as septic shock. The LPS response system must therefore be highly regulated, especially at mucosal surfaces where commensal and potential pathogenic Gram-negative bacteria are omnipresent.

The work presented in this thesis addresses ongoing efforts in understanding the innate immune role of the LPS receptor complex at mucosal surfaces. The mechanisms used by the LPS receptor complex to discriminate between commensal and pathogenic Gram-negative bacteria were investigated. The studies led to two different paths as the findings unfolded. The first project involved the presence and function of the LPS receptor complex at a directly exposed mucosal surface, the tear-corneal interface. The second project focused on a more confine mucosal surface, the digestive system and the gastrointestinal persistence of breast milk sCD14. Common to both, however, was exploring the controlled distribution of this LPS receptor complex in these mucosal environments to shed more light on the mechanisms by which the body can limit redundant inflammation against non-pathogenic bacteria. In addition, the production of rhCD14 in transgenic tobacco constitutes a promising source of abundant and cheap rhCD14 protein. This may eventually help facilitate further studies to elucidate the control mechanisms of the LPS response system.

In the first section of this thesis, the analysis of the LPS receptor complex at the tear-corneal interface suggested that the LPS receptor components are strategically and spatially expressed to restrain their LPS response to pathogenic Gram-negative bacteria. On the intact cornea, tear sCD14 and LBP would have very limited if no access to TLR4 and MD-2 expressed in the inner corneal epithelial layer, therefore minimizing LPS responsiveness and preventing detrimental inflammatory responses. However, in the presence of LPS from *P. aeruginosa*, tear sCD14 and LBP were found to induce pro-inflammatory IL-6 and IL-8 cytokine secretion from corneal epithelial cells, representative of the exposed inner epithelial layers of an injured cornea. To further investigate this wound regulated LPS response, *in vivo* studies using rats, with intact or mechanically injured corneas, could be challenged with LPS in presence or absence of human tears, transgenic tobacco-produced rhCD14, LBP and their respective neutralizing antibodies. The LPS-induced immune response in this *in vivo* model system could be monitored by analyzing the recruitment of immune cells (i.e. PMN) to the wound site.

In the second section, ingested breast milk sCD14 was found not to be present throughout the newborn gastrointestinal tract, as it was undetectable in stools. *In vitro* digestion analyses suggested that the gastrointestinal distribution of breast milk sCD14 was regulated by its susceptibility to enzymatic proteolysis. The protein is likely to survive in the low bacteria density lumen of the upper digestive system due to its resistance to pepsin digestion. However, its pancreatin susceptibility suggests that it is likely to be absent from the LPS-rich environment of the distal gastrointestinal tract. This non-ubiquitous gastrointestinal presence of breast milk sCD14 could be a way to limit potential overzealous immune responses against commensal bacteria flora in the distal bowel, while ensuring immune protection in the upper digestive system. This potential role of breast milk sCD14 could further be investigated by analyzing the proteolytic susceptibility of breast milk sCD14 with human newborn gastric and duodenal secretions obtained

from medically stable premature infants who need to be fed by gavage (174). In addition, *in vivo* studies conducted on suckling rat or pig animal models could be performed. CD14 synthesized by CHO and transgenic plant could be labeled with ^{125}I and fed by gavage to suckling animals. Sampling and biopsies could be performed at different time after ^{125}I-rhCD14 ingestion on different segments of the digestive track and other tissues from the anesthetized animals. Total count and western blot analysis performed on the various tissues and their contents could be use to detect the presence of intact or partially digested rhCD14 (175).

In the final chapter, transgenic tobacco plants were generated as an expression system for providing a low-cost and abundant source of rhCD14. Plant-made rhCD14 was found to be efficiently stored in a stable and biologically active form in tobacco seeds. Transgenic crops, such as rice, expressing the codon-optimized version of the hCD14 coding sequence, could one day further increase the yields of the recombinant protein. This expression system constitutes a promising source of rhCD14 for the aforementioned studies, helping to identify the roles of the LPS receptor. Furthermore, plant-made rhCD14 could one day be used for therapeutic medical applications, such as sepsis therapy. Other applications of plant-made rhCD14 could be targeted to the preventive side for contact lens users, nursing mothers and suckling neonates. Such applications could include the addition of rhCD14 to contact lens solutions or artificial tear drops to mimic the immune advantages of human tears, to creams for cracked nipples to prevent mammary infections during lactation, as well as to commercial milk formulas, to mimic the immune advantages of breast milk for the neonate.

Aug. 2001 - Jan. 2002	**Research Assistant** Nestlé Research Centre, Tours, France - Sequenced and analyzed the *Theobroma cacao oleosin* gene family and characterized *Coffea arabica* expressed sequence tag (EST) libraries - Discovered new cacao and coffee genes with potential commercial applications - Supervisor: Dr. James McCarthy
Summers of 1998 & 1999	**Research Assistant** Beauséjour Medical Research Institute, Georges-Dumont Hospital, Moncton, New Brunswick - Studied the roles of *Pax* genes in embryogenesis and cancer - Supervisor: Dr. Rodney Ouellette
Publication:	Guilloteau, M., M. Laloi, **D. Blais,** D. Crouzillat and J. McCarthy. 2003. Oil bodies in *Theobroma cacao* seeds: cloning and characterization of cDNA encoding the 15.8 and 16.9 kDa oleosins. *Plant Science* **164**: 597-606.
Scholarships:	- NSERC (PGS Doctoral Graduate Studies Scholarship) - NSERC (PGS Master's Graduate Studies Scholarship) - University of Ottawa National Excellence Scholarship - Nestlé Visitor Scientist Fellowship - Admission Scholarship in the Strategic Areas of Development - University of Ottawa Departmental and Faculty Scholarship - Alfred Bader Scholarship from the Canadian Society for Chemistry
Awards:	**2000 Excellence Merit Award**, Society of Chemical Industry, for the highest academic standing in the B.Sc. Biochemistry program

Conference presentations:

Mar. 2004	6th World Congress on Trauma, Shock, Inflammation and Sepsis, Munich, Germany
Nov. 2003	10th Annual BioNorth Life Sciences International Conference and Exhibition, Ottawa, Ontario

Extracurricular Activities:

March 2002 - present	**Member of scholarship interview panel** Interviewed high school graduates, from across the country, who demonstrated exceptional scientific research skills and curiosity. Recipients were awarded $8,000 Undergraduate Research Scholarships to perform fundamental scientific research at University of Ottawa laboratories through four years.

Scientific Conferences and Events:

June 2004	CBC National Radio "Quirks and Quarks" scientific interview on basal, reflex and emotional tears
Mar. 2004	6th World Congress on Trauma, Shock, Inflammation and Sepsis, Munich, Germany
Nov. 2003	10th Annual BioNorth Life Sciences International Conference and Exhibition, Ottawa, Ontario
Apr. 2002	First International Congress on Plant Metabolomics, Wageningen, The Netherlands
Nov. 2000	7th Pacific Rim Biotechnology Conference and BioExpo 2000, Vancouver, British Columbia
Aug. 2000	Cellular Basis of Adaptation to Salt and Water Stress in Plants Gordon Conference, Tilton, New Hampshire

Contribution of collaborators

The following people have contributed to the recruitment of patients, sample collections and experimental work in this thesis:

Chapter 2

Dr. George Mintsioulis, Associate Professor, University of Ottawa Eye Institute, The Ottawa Hospital, helped with the recruitment of tear donors.

Dr. Steven Gilbert, Associate Professor, University of Ottawa Eye Institute, The Ottawa Hospital, and Serge Bisson, Prosector, Anatomy Program, Department of Cellular and Molecular Medicine, University of Ottawa, performed the lacrimal gland biopsies.

Dr. Sandy Vascotto, Post-Doctoral Fellow, University of Ottawa Eye Institute, The Ottawa Hospital, provided the corneal specimens as well as the primary corneal epithelial cells and HCEC line.

Dr. Fraser Scott, Associate Professor, Department of Biochemistry, Immunology and Microbiology, University of Ottawa, allowed me to use his cell culture facilities.

Amber Graystone, Fourth year B.Sc. Biochemistry Honour student, University of Ottawa, helped with the tear collection and with the detection of sCD14 and LBP in tears by ELISA, western blot and immunofluorescence.

Chapter 3

Dr. JoAnn Harrold, Neonatologist, Department of Obstetrics, Gynecology and Newborn Care, The Ottawa Hospital, helped with the recruitment of nursing mothers and newborns.

References

1. Heumann, D. and T. Roger. 2002. Initial responses to endotoxins and Gram-negative bacteria. *Clin Chim Acta* **323**: 59-72.

2. Alexander, C. and E.T. Rietschel. 2001. Bacterial lipopolysaccharides and innate immunity. *J Endotoxin Res* **7**: 167-202.

3. Miller, S.I., R.K. Ernst and M.W. Bader. 2005. LPS, TLR4 and infectious disease diversity. *Nat Rev Microbiol* **3**: 36-46.

4. Annane, D., E. Bellissant and J.M. Cavaillon. 2005. Septic shock. *Lancet* **365**: 63-78.

5. Gioannini, T.L., A. Teghanemt, D. Zhang, N.P. Coussens, W. Dockstader, S. Ramaswamy and J.P. Weiss. 2004. Isolation of an endotoxin-MD-2 complex that produces Toll-like receptor 4-dependent cell activation at picomolar concentrations. *Proc Natl Acad Sci U S A* **101**: 4186-4191.

6. Fenton, M.J. and D.T. Golenbock. 1998. LPS-binding proteins and receptors. *J Leukoc Biol* **64**: 25-32.

7. Schumann, R.R., S.R. Leong, G.W. Flaggs, P.W. Gray, S.D. Wright, J.C. Mathison, P.S. Tobias and R.J. Ulevitch. 1990. Structure and function of lipopolysaccharide binding protein. *Science* **249**: 1429-1431.

8. Taylor, A.H., G. Heavner, M. Nedelman, D. Sherris, E. Brunt, D. Knight and J. Ghrayeb. 1995. Lipopolysaccharide (LPS) neutralizing peptides reveal a lipid A binding site of LPS binding protein. *J Biol Chem* **270**: 17934-17938.

9. Pugin, J., C.C. Schurer-Maly, D. Leturcq, A. Moriarty, R.J. Ulevitch and P.S. Tobias. 1993. Lipopolysaccharide activation of human endothelial and epithelial cells is mediated by lipopolysaccharide-binding protein and soluble CD14. *Proc Natl Acad Sci U S A* **90**: 2744-2748.

10. Tobias, P.S., K. Soldau, J.A. Gegner, D. Mintz and R.J. Ulevitch. 1995. Lipopolysaccharide binding protein-mediated complexation of lipopolysaccharide with soluble CD14. *J Biol Chem* **270**: 10482-10488.

11. Yu, B. and S.D. Wright. 1996. Catalytic properties of lipopolysaccharide (LPS) binding protein. Transfer of LPS to soluble CD14. *J Biol Chem* **271**: 4100-4105.

12. Wright, S.D., R.A. Ramos, P.S. Tobias, R.J. Ulevitch and J.C. Mathison. 1990. CD14, a receptor for complexes of lipopolysaccharide (LPS) and LPS binding protein. *Science* **249**: 1431-1433.

13. Frey, E.A., D.S. Miller, T.G. Jahr, A. Sundan, V. Bazil, T. Espevik, B.B. Finlay and S.D. Wright. 1992. Soluble CD14 participates in the response of cells to lipopolysaccharide. *J Exp Med* **176**: 1665-1671.

14. Ulevitch, R.J. and P.S. Tobias. 1995. Receptor-dependent mechanisms of cell stimulation by bacterial endotoxin. *Annu Rev Immunol* **13**: 437-457.

15. Palsson-McDermott, E.M. and L.A. O'Neill. 2004. Signal transduction by the lipopolysaccharide receptor, Toll-like receptor-4. *Immunology* **113**: 153-162.

16. Juan, T.S., M.J. Kelley, D.A. Johnson, L.A. Busse, E. Hailman, S.D. Wright and H.S. Lichenstein. 1995. Soluble CD14 truncated at amino acid 152 binds lipopolysaccharide (LPS) and enables cellular response to LPS. *J Biol Chem* **270**: 1382-1387.

17. Viriyakosol, S. and T.N. Kirkland. 1996. The N-terminal half of membrane CD14 is a functional cellular lipopolysaccharide receptor. *Infect Immun* **64**: 653-656.

18. McGinley, M.D., L.O. Narhi, M.J. Kelley, E. Davy, J. Robinson, M.F. Rohde, S.D. Wright and H.S. Lichenstein. 1995. CD14: physical properties and identification of an exposed site that is protected by lipopolysaccharide. *J Biol Chem* **270**: 5213-5218.

19. Stelter, F., M. Pfister, M. Bernheiden, R.S. Jack, P. Bufler, H. Engelmann and C. Schutt. 1996. The myeloid differentiation antigen CD14 is N- and O-glycosylated. Contribution of N-linked glycosylation to different soluble CD14 isoforms. *Eur J Biochem* **236**: 457-464.

20. Hailman, E., H.S. Lichenstein, M.M. Wurfel, D.S. Miller, D.A. Johnson, M. Kelley, L.A. Busse, M.M. Zukowski and S.D. Wright. 1994. Lipopolysaccharide (LPS)-binding protein accelerates the binding of LPS to CD14. *J Exp Med* **179**: 269-277.

21. Jungi, T.W., M. Brcic and S. Eperon. 1996. Human macrophages respond to LPS in a serum-independent, CD14-dependent manner. *Immunol Lett* **54**: 37-43.

22. Haziot, A., S. Chen, E. Ferrero, M.G. Low, R. Silber and S.M. Goyert. 1988. The monocyte differentiation antigen, CD14, is anchored to the cell membrane by a phosphatidylinositol linkage. *J Immunol* **141**: 547-552.

23. Simmons, D.L., S. Tan, D.G. Tenen, A. Nicholson-Weller and B. Seed. 1989. Monocyte antigen CD14 is a phospholipid anchored membrane protein. *Blood* **73**: 284-289.

24. Burgmann, H., S. Winkler, G.J. Locker, E. Presterl, K. Laczika, T. Staudinger, S. Knapp, F. Thalhammer, C. Wenisch, K. Zedwitz-Liebenstein, M. Frass and W. Graninger. 1996. Increased serum concentration of soluble CD14 is a prognostic marker in gram-positive sepsis. *Clin Immunol Immunopathol* **80**: 307-310.

25. Uehara, A., S. Sugawara, K. Watanabe, S. Echigo, M. Sato, T. Yamaguchi and H. Takada. 2003. Constitutive expression of a bacterial pattern recognition receptor, CD14, in human salivary glands and secretion as a soluble form in saliva. *Clin Diagn Lab Immunol* **10**: 286-292.

26. Labeta, M.O., K. Vidal, J.E. Nores, M. Arias, N. Vita, B.P. Morgan, J.C. Guillemot, D. Loyaux, P. Ferrara, D. Schmid, M. Affolter, L.K. Borysiewicz, A. Donnet-Hughes and E.J. Schiffrin. 2000. Innate recognition of bacteria in human milk is mediated by a milk-derived highly expressed pattern recognition receptor, soluble CD14. *J Exp Med* **191**: 1807-1812.

27. Hasday, J.D., W. Dubin, S. Mongovin, S.E. Goldblum, P. Swoveland, D.J. Leturcq, A.M. Moriarty, E.R. Bleecker and T.R. Martin. 1997. Bronchoalveolar macrophage CD14 expression: shift between membrane-associated and soluble pools. *Am J Physiol* **272**: L925-933.

28. Funda, D.P., L. Tuckova, M.A. Farre, T. Iwase, I. Moro and H. Tlaskalova-Hogenova. 2001. CD14 is expressed and released as soluble CD14 by human intestinal epithelial cells in vitro: lipopolysaccharide activation of epithelial cells revisited. *Infect Immun* **69**: 3772-3781.

29. Bussolati, B., S. David, V. Cambi, P.S. Tobias and G. Camussi. 2002. Urinary soluble CD14 mediates human proximal tubular epithelial cell injury induced by LPS. *Int J Mol Med* **10**: 441-449.

30. Harris, C.L., M.A. Vigar, J.E. Rey Nores, V. Horejsi, M.O. Labeta and B.P. Morgan. 2001. The lipopolysaccharide co-receptor CD14 is present and functional in seminal plasma and expressed on spermatozoa. *Immunology* **104**: 317-323.

31. Espinoza, J., T. Chaiworapongsa, R. Romero, R. Gomez, J.C. Kim, J. Yoshimatsu, S. Edwin, C. Rathnasabapathy and B.H. Yoon. 2002. Evidence of participation of soluble CD14 in the host response to microbial invasion of the amniotic cavity and intra-amniotic inflammation in term and preterm gestations. *J Matern Fetal Neonatal Med* **12**: 304-312.

32. Jones, C.A., J.A. Holloway, E.J. Popplewell, N.D. Diaper, J.W. Holloway, G.H. Vance, J.A. Warner and J.O. Warner. 2002. Reduced soluble CD14 levels in amniotic fluid and breast milk are associated with the subsequent development of atopy, eczema, or both. *J Allergy Clin Immunol* **109**: 858-866.

33. Bazil, V., V. Horejsi, M. Baudys, H. Kristofova, J.L. Strominger, W. Kostka and I. Hilgert. 1986. Biochemical characterization of a soluble form of the 53-kDa monocyte surface antigen. *Eur J Immunol* **16**: 1583-1589.

34. Bazil, V. and J.L. Strominger. 1991. Shedding as a mechanism of down-modulation of CD14 on stimulated human monocytes. *J Immunol* **147**: 1567-1574.

35. Bufler, P., G. Stiegler, M. Schuchmann, S. Hess, C. Kruger, F. Stelter, C. Eckerskorn, C. Schutt and H. Engelmann. 1995. Soluble lipopolysaccharide receptor (CD14) is released via two different mechanisms from human monocytes and CD14 transfectants. *Eur J Immunol* **25**: 604-610.

36. Metz, C.N., G. Brunner, N.H. Choi-Muira, H. Nguyen, J. Gabrilove, I.W. Caras, N. Altszuler, D.B. Rifkin, E.L. Wilson and M.A. Davitz. 1994. Release of GPI-anchored membrane proteins by a cell-associated GPI- specific phospholipase D. *Embo J* **13**: 1741-1751.

37. Hailman, E., T. Vasselon, M. Kelley, L.A. Busse, M.C. Hu, H.S. Lichenstein, P.A. Detmers and S.D. Wright. 1996. Stimulation of macrophages and neutrophils by complexes of lipopolysaccharide and soluble CD14. *J Immunol* **156**: 4384-4390.

38. Cario, E., I.M. Rosenberg, S.L. Brandwein, P.L. Beck, H.C. Reinecker and D.K. Podolsky. 2000. Lipopolysaccharide activates distinct signaling pathways in intestinal epithelial cell lines expressing Toll-like receptors. *J Immunol* **164**: 966-972.

39. Tabeta, K., K. Yamazaki, S. Akashi, K. Miyake, H. Kumada, T. Umemoto and H. Yoshie. 2000. Toll-like receptors confer responsiveness to lipopolysaccharide from *Porphyromonas gingivalis* in human gingival fibroblasts. *Infect Immun* **68**: 3731-3735.

40. Verhasselt, V., C. Buelens, F. Willems, D. De Groote, N. Haeffner-Cavaillon and M. Goldman. 1997. Bacterial lipopolysaccharide stimulates the production of cytokines and the expression of costimulatory molecules by human peripheral blood dendritic cells: evidence for a soluble CD14-dependent pathway. *J Immunol* **158**: 2919-2925.

41. Zhang, F.X., C.J. Kirschning, R. Mancinelli, X.P. Xu, Y. Jin, E. Faure, A. Mantovani, M. Rothe, M. Muzio and M. Arditi. 1999. Bacterial lipopolysaccharide activates nuclear factor-kappaB through interleukin-1 signaling mediators in cultured human dermal endothelial cells and mononuclear phagocytes. *J Biol Chem* **274**: 7611-7614.

42. Kitchens, R.L., P.A. Thompson, S. Viriyakosol, G.E. O'Keefe and R.S. Munford. 2001. Plasma CD14 decreases monocyte responses to LPS by transferring cell- bound LPS to plasma lipoproteins. *J Clin Invest* **108**: 485-493.

43. Wurfel, M.M., E. Hailman and S.D. Wright. 1995. Soluble CD14 acts as a shuttle in the neutralization of lipopolysaccharide (LPS) by LPS-binding protein and reconstituted high density lipoprotein. *J Exp Med* **181**: 1743-1754.

44. Troelstra, A., B.N. Giepmans, K.P. Van Kessel, H.S. Lichenstein, J. Verhoef and J.A. Van Strijp. 1997. Dual effects of soluble CD14 on LPS priming of neutrophils. *J Leukoc Biol* **61**: 173-178.

45. Haziot, A., G.W. Rong, V. Bazil, J. Silver and S.M. Goyert. 1994. Recombinant soluble CD14 inhibits LPS-induced tumor necrosis factor- alpha production by cells in whole blood. *J Immunol* **152**: 5868-5876.

46. Haziot, A., G.W. Rong, X.Y. Lin, J. Silver and S.M. Goyert. 1995. Recombinant soluble CD14 prevents mortality in mice treated with endotoxin (lipopolysaccharide). *J Immunol* **154**: 6529-6532.

47. Dziarski, R., A.J. Ulmer and D. Gupta. 2000. Interactions of CD14 with components of gram-positive bacteria. *Chem Immunol* **74**: 83-107.

48. Hamann, L., V. El-Samalouti, A.J. Ulmer, H.D. Flad and E.T. Rietschel. 1998. Components of gut bacteria as immunomodulators. *Int J Food Microbiol* **41**: 141-154.

49. Chow, J.C., D.W. Young, D.T. Golenbock, W.J. Christ and F. Gusovsky. 1999. Toll-like receptor-4 mediates lipopolysaccharide-induced signal transduction. *J Biol Chem* **274**: 10689-10692.

50. Nagai, Y., S. Akashi, M. Nagafuku, M. Ogata, Y. Iwakura, S. Akira, T. Kitamura, A. Kosugi, M. Kimoto and K. Miyake. 2002. Essential role of MD-2 in LPS responsiveness and TLR4 distribution. *Nat Immunol* **3**: 667-672.

51. Akashi, S., S. Saitoh, Y. Wakabayashi, T. Kikuchi, N. Takamura, Y. Nagai, Y. Kusumoto, K. Fukase, S. Kusumoto, Y. Adachi, A. Kosugi and K. Miyake. 2003. Lipopolysaccharide interaction with cell surface Toll-like receptor 4-MD-2: higher affinity than that with MD-2 or CD14. *J Exp Med* **198**: 1035-1042.

52. Visintin, A., E. Latz, B.G. Monks, T. Espevik and D.T. Golenbock. 2003. Lysines 128 and 132 enable lipopolysaccharide binding to MD-2, leading to Toll-like receptor-4 aggregation and signal transduction. *J Biol Chem* **278**: 48313-48320.

53. Espevik, T., M. Otterlei, G. Skjak-Braek, L. Ryan, S.D. Wright and A. Sundan. 1993. The involvement of CD14 in stimulation of cytokine production by uronic acid polymers. *Eur J Immunol* **23**: 255-261.

54. Dziarski, R., R.I. Tapping and P.S. Tobias. 1998. Binding of bacterial peptidoglycan to CD14. *J Biol Chem* **273**: 8680-8690.

55. Weidemann, B., J. Schletter, R. Dziarski, S. Kusumoto, F. Stelter, E.T. Rietschel, H.D. Flad and A.J. Ulmer. 1997. Specific binding of soluble peptidoglycan and muramyldipeptide to CD14 on human monocytes. *Infect Immun* **65**: 858-864.

56. Gupta, D., T.N. Kirkland, S. Viriyakosol and R. Dziarski. 1996. CD14 is a cell-activating receptor for bacterial peptidoglycan. *J Biol Chem* **271**: 23310-23316.

57. Cleveland, M.G., J.D. Gorham, T.L. Murphy, E. Tuomanen and K.M. Murphy. 1996. Lipoteichoic acid preparations of gram-positive bacteria induce interleukin-12 through a CD14-dependent pathway. *Infect Immun* **64**: 1906-1912.

58. Hattor, Y., K. Kasai, K. Akimoto and C. Thiemermann. 1997. Induction of NO synthesis by lipoteichoic acid from *Staphylococcus aureus* in J774 macrophages: involvement of a CD14-dependent pathway. *Biochem Biophys Res Commun* **233**: 375-379.

59. Cauwels, A., E. Wan, M. Leismann and E. Tuomanen. 1997. Coexistence of CD14-dependent and independent pathways for stimulation of human monocytes by gram-positive bacteria. *Infect Immun* **65**: 3255-3260.

60. Soell, M., E. Lett, F. Holveck, M. Scholler, D. Wachsmann and J.P. Klein. 1995. Activation of human monocytes by streptococcal rhamnose glucose polymers is mediated by CD14 antigen, and mannan binding protein inhibits TNF-alpha release. *J Immunol* **154**: 851-860.

61. Savedra, R., Jr., R.L. Delude, R.R. Ingalls, M.J. Fenton and D.T. Golenbock. 1996. Mycobacterial lipoarabinomannan recognition requires a receptor that shares components of the endotoxin signaling system. *J Immunol* **157**: 2549-2554.

62. Yu, W., E. Soprana, G. Cosentino, M. Volta, H.S. Lichenstein, G. Viale and D. Vercelli. 1998. Soluble CD14(1-152) confers responsiveness to both lipoarabinomannan and lipopolysaccharide in a novel HL-60 cell bioassay. *J Immunol* **161**: 4244-4251.

63. Sellati, T.J., D.A. Bouis, R.L. Kitchens, R.P. Darveau, J. Pugin, R.J. Ulevitch, S.C. Gangloff, S.M. Goyert, M.V. Norgard and J.D. Radolf. 1998. *Treponema pallidum* and *Borrelia burgdorferi* lipoproteins and synthetic lipopeptides activate monocytic cells via a CD14-dependent pathway distinct from that used by lipopolysaccharide. *J Immunol* **160**: 5455-5464.

64. Wooten, R.M., T.B. Morrison, J.H. Weis, S.D. Wright, R. Thieringer and J.J. Weis. 1998. The role of CD14 in signaling mediated by outer membrane lipoproteins of *Borrelia burgdorferi*. *J Immunol* **160**: 5485-5492.

65. Hmama, Z., A. Mey, G. Normier, H. Binz and J.P. Revillard. 1994. CD14 and CD11b mediate serum-independent binding to human monocytes of an acylpolygalactoside isolated from *Klebsiella pneumoniae*. *Infect Immun* **62**: 1520-1527.

66. Otterlei, M., K.M. Varum, L. Ryan and T. Espevik. 1994. Characterization of binding and TNF-alpha-inducing ability of chitosans on monocytes: the involvement of CD14. *Vaccine* **12**: 825-832.

67. Newman, S.L., S. Chaturvedi and B.S. Klein. 1995. The WI-1 antigen of *Blastomyces dermatitidis* yeasts mediates binding to human macrophage CD11b/CD18 (CR3) and CD14. *J Immunol* **154**: 753-761.

68. Cavaillon, J.M., C. Marie, M. Caroff, A. Ledur, I. Godard, D. Poulain, C. Fitting and N. Haeffner-Cavaillon. 1996. CD14/LPS receptor exhibits lectin-like properties. *J Endotoxin Res* **3**: 315-324.

69. Kurt-Jones, E.A., L. Popova, L. Kwinn, L.M. Haynes, L.P. Jones, R.A. Tripp, E.E. Walsh, M.W. Freeman, D.T. Golenbock, L.J. Anderson and R.W. Finberg. 2000. Pattern recognition receptors TLR4 and CD14 mediate response to respiratory syncytial virus. *Nat Immunol* **1**: 398-401.

70. Takeda, K. and S. Akira. 2005. Toll-like receptors in innate immunity. *Int Immunol* **17**: 1-14.

71. Schmitz, G. and E. Orso. 2002. CD14 signaling in lipid rafts: new ligands and co-receptors. *Curr Opin Lipidol* **13**: 513-521.

72. Triantafilou, M. and K. Triantafilou. 2004. Heat-shock protein 70 and heat-shock protein 90 associate with Toll-like receptor 4 in response to bacterial lipopolysaccharide. *Biochem Soc Trans* **32**: 636-639.

73. Jones, D.A. and D. Takemoto. 2004. Plant innate immunity - direct and indirect recognition of general and specific pathogen-associated molecules. *Curr Opin Immunol* **16**: 48-62.

74. Williams, R.C. and R.J. Gibbons. 1972. Inhibition of bacterial adherence by secretory immunoglobulin A: a mechanism of antigen disposal. *Science* **177**: 697-699.

75. Singh, P.K., M.R. Parsek, E.P. Greenberg and M.J. Welsh. 2002. A component of innate immunity prevents bacterial biofilm development. *Nature* **417**: 552-555.

76. Sack, R.A., I. Nunes, A. Beaton and C. Morris. 2001. Host-defense mechanism of the ocular surfaces. *Biosci Rep* **21**: 463-480.

77. Kurpakus-Wheater, M., K.A. Kernacki and L.D. Hazlett. 2001. Maintaining corneal integrity how the "window" stays clear. *Prog Histochem Cytochem* **36**: 185-259.

78. Zhang, J., K. Xu, B. Ambati and F.S. Yu. 2003. Toll-like receptor 5-mediated corneal epithelial inflammatory responses to *Pseudomonas aeruginosa* flagellin. *Invest Ophthalmol Vis Sci* **44**: 4247-4254.

79. Song, P.I., T.A. Abraham, Y. Park, A.S. Zivony, B. Harten, H.F. Edelhauser, S.L. Ward, C.A. Armstrong and J.C. Ansel. 2001. The expression of functional LPS receptor proteins CD14 and toll-like receptor 4 in human corneal cells. *Invest Ophthalmol Vis Sci* **42**: 2867-2877.

80. Ueta, M., T. Nochi, M.H. Jang, E.J. Park, O. Igarashi, A. Hino, S. Kawasaki, T. Shikina, T. Hiroi, S. Kinoshita and H. Kiyono. 2004. Intracellularly expressed TLR2s and TLR4s contribution to an immunosilent environment at the ocular mucosal epithelium. *J Immunol* **173**: 3337-3347.

81. WHO. 1979. Data on blindness throughout the world. *WHO Chronicle* **33**: 275-283.

82. Chang, M.A., S. Jain and D.T. Azar. 2004. Infections following laser in situ keratomileusis: an integration of the published literature. *Surv Ophthalmol* **49**: 269-280.

83. Hazlett, L.D. 2004. Corneal response to *Pseudomonas aeruginosa* infection. *Prog Retin Eye Res* **23**: 1-30.

84. Bonnapasart, S., N. Kasetsuwan, V. Puangsricharem, L. Pariyakanok and T. Jittpoonkusol. 2002. Infectious keratitis at King Chulalonghorn Memorial Hospital: a 12 year retrospective study of 391 cases. *J Med Assoc Thai* **85**: S217-S230.

85. McMonnies, C., A. Ho and D. Wakefield. 1998. Optimum dry eye classification using questionnaire responses. *Adv Exp Med Biol* **438**: 835-838.

86. Araki-Sasaki, K., Y. Ohashi, T. Sasabe, K. Hayashi, H. Watanabe, Y. Tano and H. Handa. 1995. An SV40-immortalized human corneal epithelial cell line and its characterization. *Invest Ophthalmol Vis Sci* **36**: 614-621.

87. Suuronen, E.J., M. Nakamura, M.A. Watsky, P.K. Stys, L.J. Muller, R. Munger, N. Shinozaki and M. Griffith. 2004. Innervated human corneal equivalents as in vitro models for nerve-target cell interactions. *Faseb J* **18**: 170-172.

88. Durieux, J.J., N. Vita, O. Popescu, F. Guette, J. Calzada-Wack, R. Munker, R.E. Schmidt, J. Lupker, P. Ferrara, H.W. Ziegler-Heitbrock and et al. 1994. The two soluble forms of the lipopolysaccharide receptor, CD14: characterization and release by normal human monocytes. *Eur J Immunol* **24**: 2006-2012.

89. Rehli, M., A. Poltorak, L. Schwarzfischer, S.W. Krause, R. Andreesen and B. Beutler. 2000. PU.1 and interferon consensus sequence-binding protein regulate the myeloid expression of the human Toll-like receptor 4 gene. *J Biol Chem* **275**: 9773-9781.

90. Fullard, R.J. and C. Snyder. 1990. Protein levels in nonstimulated and stimulated tears of normal human subjects. *Invest Ophthalmol Vis Sci* **31**: 1119-1126.

91. Kijlstra, A., S.H. Jeurissen and K.M. Koning. 1983. Lactoferrin levels in normal human tears. *Br J Ophthalmol* **67**: 199-202.

92. Seal, D.V. 1985. The effect of ageing and disease on tear constituents. *Trans Ophthalmol Soc U K* **104 (Pt 4)**: 355-362.

93. Labeta, M.O., J.J. Durieux, N. Fernandez, R. Herrmann and P. Ferrara. 1993. Release from a human monocyte-like cell line of two different soluble forms of the lipopolysaccharide receptor, CD14. *Eur J Immunol* **23**: 2144-2151.

94. Patel, N., H.M. Khalil, R. Amirfeyz and H.S. Kaddour. 2003. Lacrimal gland abscess complicating acute sinusitis. *Int J Pediatr Otorhinolaryngol* **67**: 917-919.

95. Gupta, S.K., R.S. Berk, S. Masinick and L.D. Hazlett. 1994. Pili and lipopolysaccharide of *Pseudomonas aeruginosa* bind to the glycolipid asialo GM1. *Infect Immun* **62**: 4572-4579.

96. Gupta, S.K., S. Masinick, M. Garrett and L.D. Hazlett. 1997. *Pseudomonas aeruginosa* lipopolysaccharide binds galectin-3 and other human corneal epithelial proteins. *Infect Immun* **65**: 2747-2753.

97. Zaidi, T.S., J. Lyczak, M. Preston and G.B. Pier. 1999. Cystic fibrosis transmembrane conductance regulator-mediated corneal epithelial cell ingestion of *Pseudomonas aeruginosa* is a key component in the pathogenesis of experimental murine keratitis. *Infect Immun* **67**: 1481-1492.

98. Lyczak, J.B., C.L. Cannon and G.B. Pier. 2000. Establishment of *Pseudomonas aeruginosa* infection: lessons from a versatile opportunist. *Microbes Infect* **2**: 1051-1060.

99. Streilein, J.W. 2003. Ocular immune privilege: therapeutic opportunities from an experiment of nature. *Nat Rev Immunol* **3**: 879-889.

100. Gegner, J.A., R.J. Ulevitch and P.S. Tobias. 1995. Lipopolysaccharide (LPS) signal transduction and clearance. Dual roles for LPS binding protein and membrane CD14. *J Biol Chem* **270**: 5320-5325.

101. Wright, S.D., P.S. Tobias, R.J. Ulevitch and R.A. Ramos. 1989. Lipopolysaccharide (LPS) binding protein opsonizes LPS-bearing particles for recognition by a novel receptor on macrophages. *J Exp Med* **170**: 1231-1241.

102. Baveye, S., E. Elass, D.G. Fernig, C. Blanquart, J. Mazurier and D. Legrand. 2000. Human lactoferrin interacts with soluble CD14 and inhibits expression of endothelial adhesion molecules, E-selectin and ICAM-1, induced by the CD14-lipopolysaccharide complex. *Infect Immun* **68**: 6519-6525.

103. Vreugdenhil, A.C., C.H. Rousseau, T. Hartung, J.W. Greve, C. van 't Veer and W.A. Buurman. 2003. Lipopolysaccharide (LPS)-binding protein mediates LPS detoxification by chylomicrons. *J Immunol* **170**: 1399-1405.

104. Holzfeind, P., P. Merschak, H. Dieplinger and B. Redl. 1995. The human lacrimal gland synthesizes apolipoprotein D mRNA in addition to tear prealbumin mRNA, both species encoding members of the lipocalin superfamily. *Exp Eye Res* **61**: 495-500.

105. Thompson, P.A., P.S. Tobias, S. Viriyakosol, T.N. Kirkland and R.L. Kitchens. 2003. Lipopolysaccharide (LPS)-binding protein inhibits responses to cell-bound LPS. *J Biol Chem* **278**: 28367-28371.

106. Akpek, E.K. and J.D. Gottsch. 2003. Immune defense at the ocular surface. *Eye* **17**: 949-956.

107. Adkins, B., C. Leclerc and S. Marshall-Clarke. 2004. Neonatal adaptive immunity comes of age. *Nat Rev Immunol* **4**: 553-564.

108. Hooper, L.V. 2004. Bacterial contributions to mammalian gut development. *Trends Microbiol* **12**: 129-134.

109. Marshall-Clarke, S., D. Reen, L. Tasker and J. Hassan. 2000. Neonatal immunity: how well has it grown up? *Immunol Today* **21**: 35-41.

110. Nanthakumar, N.N., R.D. Fusunyan, I. Sanderson and W.A. Walker. 2000. Inflammation in the developing human intestine: A possible pathophysiologic contribution to necrotizing enterocolitis. *Proc Natl Acad Sci U S A* **97**: 6043-6048.

111. Wenneras, C. and V. Erling. 2004. Prevalence of enterotoxigenic *Escherichia coli*-associated diarrhoea and carrier state in the developing World. *J Health Popul Nutr* **22**: 370-382.

112. WHO. 2003. State of the art of new vaccines: research and development. Initiative for Vaccine Research. World Health Organization. Geneva.

113. Lonnerdal, B. 2004. Protecting infants through human milk. *Adv. Exp. Med. Biol.* **554**: 11-25.

114. Hanson, L.A., L. Ceafalau, I. Mattsby-Baltzer, M. Lagerberg, A. Hjalmarsson, R. Ashraf, S. Zaman and F. Jalil. 2000. The mammary gland-infant intestine immunologic dyad. *Adv Exp Med Biol* **478**: 65-76.

115. Haneberg, B. 1974. Immunoglobulins in feces from infants fed human or bovine milk. *Scand J Immunol* **3**: 191-197.

116. Prentice, A., G. Ewing, S.B. Roberts, A. Lucas, A. MacCarthy, L.M. Jarjou and R.G. Whitehead. 1987. The nutritional role of breast-milk IgA and lactoferrin. *Acta Paediatr Scand* **76**: 592-598.

117. Davidson, L.A. and B. Lonnerdal. 1987. Persistence of human milk proteins in the breast-fed infant. *Acta Paediatr Scand* **76**: 733-740.

118. Goldman, A.S., C. Garza, R.J. Schanler and R.M. Goldblum. 1990. Molecular forms of lactoferrin in stool and urine from infants fed human milk. *Pediatr Res* **27**: 252-255.

119. Vidal, K., M.O. Labeta, E.J. Schiffrin and A. Donnet-Hughes. 2001. Soluble CD14 in human breast milk and its role in innate immune responses. *Acta Odontol Scand* **59**: 330-334.

120. Guerra, S., I. Carla Lohman, T.D. LeVan, A.L. Wright, F.D. Martinez and M. Halonen. 2004. The differential effect of genetic variation on soluble CD14 levels in human plasma and milk. *Am J Reprod Immunol* **52**: 204-211.

121. Ishihara, S., M.A. Rumi, Y. Kadowaki, C.F. Ortega-Cava, T. Yuki, N. Yoshino, Y. Miyaoka, H. Kazumori, N. Ishimura, Y. Amano and Y. Kinoshita. 2004. Essential role of MD-2 in TLR4-dependent signaling during *Helicobacter pylori*-associated gastritis. *J Immunol* **173**: 1406-1416.

122. Schmausser, B., M. Andrulis, S. Endrich, S.K. Lee, C. Josenhans, H.K. Muller-Hermelink and M. Eck. 2004. Expression and subcellular distribution of toll-like receptors TLR4, TLR5 and TLR9 on the gastric epithelium in *Helicobacter pylori* infection. *Clin Exp Immunol* **136**: 521-526.

123. Bocker, U., O. Yezerskyy, P. Feick, T. Manigold, A. Panja, U. Kalina, F. Herweck, S. Rossol and M.V. Singer. 2003. Responsiveness of intestinal epithelial cell lines to lipopolysaccharide is correlated with Toll-like receptor 4 but not Toll-like receptor 2 or CD14 expression. *Int J Colorectal Dis* **18**: 25-32.

124. Ortega-Cava, C.F., S. Ishihara, M.A. Rumi, K. Kawashima, N. Ishimura, H. Kazumori, J. Udagawa, Y. Kadowaki and Y. Kinoshita. 2003. Strategic compartmentalization of Toll-like receptor 4 in the mouse gut. *J Immunol* **170**: 3977-3985.

125. Vidal, K., A. Donnet-Hughes and D. Granato. 2002. Lipoteichoic acids from *Lactobacillus johnsonii* strain La1 and *Lactobacillus acidophilus* strain La10 antagonize the responsiveness of human intestinal epithelial HT29 cells to lipopolysaccharide and gram-negative bacteria. *Infect Immun* **70**: 2057-2064.

126. Filipp, D., K. Alizadeh-Khiavi, C. Richardson, A. Palma, N. Paredes, O. Takeuchi, S. Akira and M. Julius. 2001. Soluble CD14 enriched in colostrum and milk induces B cell growth and differentiation. *Proc Natl Acad Sci U S A* **98**: 603-608.

127. Arias, M.A., J.E. Rey Nores, N. Vita, F. Stelter, L.K. Borysiewicz, P. Ferrara and M.O. Labeta. 2000. Human B cell function is regulated by interaction with soluble CD14: opposite effects on IgG1 and IgE production. *J Immunol* **164**: 3480-3486.

128. Pao, E.M., J.M. Himes and A.F. Roche. 1980. Milk intakes and feeding patterns of breast-fed infants. *J Am Diet Assoc* 77: 540-545.

129. Rudloff, S. and B. Lonnerdal. 1992. Solubility and digestibility of milk proteins in infant formulas exposed to different heat treatments. *J Pediatr Gastroenterol Nutr* **15**: 25-33.

130. Lindh, E. 1975. Increased resistance of immunoglobulin A dimers to proteolytic degradation after binding of secretory component. *J Immunol* **114**: 284-286.

131. Goldblum, R.M., R.J. Schanler, C. Garza and A.S. Goldman. 1989. Human milk feeding enhances the urinary excretion of immunologic factors in low birth weight infants. *Pediatr Res* **25**: 184-188.

132. Hutchens, T.W., J.F. Henry and T.T. Yip. 1991. Structurally intact (78-kDa) forms of maternal lactoferrin purified from urine of preterm infants fed human milk: identification of a trypsin-like proteolytic cleavage event in vivo that does not result in fragment dissociation. *Proc Natl Acad Sci U S A* **88**: 2994-2998.

133. Hutchens, T.W., J.F. Henry, T.T. Yip, D.L. Hachey, R.J. Schanler, K.J. Motil and C. Garza. 1991. Origin of intact lactoferrin and its DNA-binding fragments found in the urine of human milk-fed preterm infants. Evaluation by stable isotopic enrichment. *Pediatr Res* **29**: 243-250.

134. Vukavic, T. 1983. Intestinal absorption of IgA in the newborn. *J Pediatr Gastroenterol Nutr* **2**: 248-251.

135. Piper, D.W. and B.H. Fenton. 1965. pH stability and activity curves of pepsin with special reference to their clinical importance. *Gut* **6**: 506-508.

136. Chowanadisai, W. and B. Lonnerdal. 2002. Alpha(1)-antitrypsin and antichymotrypsin in human milk: origin, concentrations, and stability. *Am J Clin Nutr* **76**: 828-833.

137. Lindberg, T., K. Ohlsson and B. Westrom. 1982. Protease inhibitors and their relation to protease activity in human milk. *Pediatr Res* **16**: 479-483.

138. Macpherson, A.J. and N.L. Harris. 2004. Interactions between commensal intestinal bacteria and the immune system. *Nat Rev Immunol* **4**: 478-485.

139. LeBouder, E., J.E. Rey-Nores, N.K. Rushmere, M. Grigorov, S.D. Lawn, M. Affolter, G.E. Griffin, P. Ferrara, E.J. Schiffrin, B.P. Morgan and M.O. Labeta. 2003. Soluble forms of toll-like receptor (TLR)2 capable of modulating TLR2 signaling are present in human plasma and breast milk. *J Immunol* **171**: 6680-6689.

140. Britton, J.R. and O. Koldovsky. 1989. Development of luminal protein digestion: implications for biologically active dietary polypeptides. *J Pediatr Gastroenterol Nutr* **9**: 144-162.

141. Brandtzaeg, P. 2003. Mucosal immunity: integration between mother and the breast-fed infant. *Vaccine* **21**: 3382-3388.

142. Ellison, R.T., 3rd and T.J. Giehl. 1991. Killing of gram-negative bacteria by lactoferrin and lysozyme. *J Clin Invest* **88**: 1080-1091.

143. Wakabayashi, H., M. Takase and M. Tomita. 2003. Lactoferricin derived from milk protein lactoferrin. *Curr Pharm Des* **9**: 1277-1287.

144. WHO. 2002. Traditional and alternative medicine. *WHO Fact Sheet* **271**: 1-3.

145. Sardana, R.K., Z. Alli, A. Dudani, E. Tackaberry, M. Panahi, M. Narayanan, P. Ganz and I. Altosaar. 2002. Biological activity of human granulocyte-macrophage colony stimulating factor is maintained in a fusion with seed glutelin peptide. *Transgenic Res* **11**: 521-531.

146. Panahi, M., Z. Alli, X. Cheng, L. Belbaraka, J. Belgoudi, R. Sardana, J. Phipps and I. Altosaar. 2004. Recombinant protein expression plasmids optimized for industrial *E. coli* fermentation and plant systems produce biologically active human insulin-like growth factor-1 in transgenic rice and tobacco plants. *Transgenic Res* **13**: 245-259.

147. Thanavala, Y., M. Mahoney, S. Pal, A. Scott, L. Richter, N. Natarajan, P. Goodwin, C.J. Arntzen and H.S. Mason. 2005. Immunogenicity in humans of an edible vaccine for hepatitis B. *Proc Natl Acad Sci U S A* **102**: 3378-3382.

148. Horn, M.E., S.L. Woodard and J.A. Howard. 2004. Plant molecular farming: systems and products. *Plant Cell Rep* **22**: 711-720.

149. Arcalis, E., S. Marcel, F. Altmann, D. Kolarich, G. Drakakaki, R. Fischer, P. Christou and E. Stoger. 2004. Unexpected deposition patterns of recombinant proteins in post-endoplasmic reticulum compartments of wheat endosperm. *Plant Physiol* **136**: 3457-3466.

150. Giddings, G., G. Allison, D. Brooks and A. Carter. 2000. Transgenic plants as factories for biopharmaceuticals. *Nat Biotechnol* **18**: 1151-1155.

151. Stelter, F., M. Bernheiden, R. Menzel, S. Witt, R.S. Jack, U. Grunwald, X. Fan and C. Schutt. 1998. The molecular basis for therapeutic concepts utilizing CD14. *Prog Clin Biol Res* **397**: 301-313.

152. Lee, J.W., M.J. Paape, T.H. Elsasser and X. Zhao. 2003. Recombinant soluble CD14 reduces severity of intramammary infection by *Escherichia coli*. *Infect Immun* **71**: 4034-4039.

153. Schutt, C., B. Furll, F. Stelter, R.S. Jack and S. Witt. 1997. CHO transfectants produce large amounts of recombinant protein in suspension culture. *J Immunol Methods* **204**: 99-102.

154. Yin, J., J. Bai, W. Wang, W. Song and Z. Wang. 2002. Gene cloning of human soluble CD14 and its expression in eucaryotic cells. *Chin J Traumatol* **5**: 156-160.

155. Majerle, A., J. Kidric and R. Jerala. 2000. Bacterial expression and refolding of different fragments of human CD14. *Pflugers Arch* **439**: R109-110.

156. Nomura, S., K. Inamori, T. Muta, S. Yamazaki, Y. Sunakawa, S. Iwanaga and K. Takeshige. 2003. Purification and characterization of human soluble CD14 expressed in *Pichia pastoris*. *Protein Expr Purif* **28**: 310-320.

157. Girard, L.S., M. Bastin and D. Courtois. 2004. Expression of the human milk protein sCD14 in tobacco plant cell culture. *Plant Cell, Tissue and Organ Culture* **78**: 253-260.

158. Michaux, G. and D.F. Cutler. 2004. How to roll an endothelial cigar: the biogenesis of Weibel-Palade bodies. *Traffic* **5**: 69-78.

159. Adeli, K. and I. Altosaar. 1984. Compartmentalization of seed reserve proteins : Proposed discriminatory factors. *FEBS. Lett.* **178**: 193-198.

160. Wright, K.E., F. Prior, R. Sardana, I. Altosaar, A.K. Dudani, P.R. Ganz and E.S. Tackaberry. 2001. Sorting of glycoprotein B from human cytomegalovirus to protein storage vesicles in seeds of transgenic tobacco. *Transgenic Res* **10**: 177-181.

161. Ferrero, E. and S.M. Goyert. 1988. Nucleotide sequence of the gene encoding the monocyte differentiation antigen, CD14. *Nucleic Acids Res* **16**: 4173.

162. Zheng, Z., Y. Kawagoe, S. Xiao, Z. Li, T. Okita, T.L. Hau, A. Lin and N. Murai. 1993. 5' distal and proximal cis-acting regulator elements are required for developmental control of a rice seed storage protein glutelin gene. *Plant J* **4**: 357-366.

163. Datla, R.S., J.K. Hammerlindl, B. Panchuk, L.E. Pelcher and W. Keller. 1992. Modified binary plant transformation vectors with the wild-type gene encoding NPTII. *Gene* **122**: 383-384.

164. An, G. 1987. Binary Ti vectors for plant transformation and promoter analysis. *Methods Enzymol* **153**: 292-305.

165. Horsch, R.B., J.E. Fry, N.L. Hoffmann, D. Eichholtz, S.G. Rogers and R.T. Fraley. 1985. A simple and general method for transferring genes into plants. *Science* **227**: 1229-1231.

166. Chaudhry, B., A. Yasmeen, T. Husnain and S. Riazuddin. 1999. Mini-scale genomic DNA extraction from cotton. *Plant Molecular Biology Reporter* **17**: 1-7.

167. Sambrook, J., P. MacCallum and D. Russell. 2000. Molecular Cloning. A Laboratory Manual (3rd edition). Cold Spring Harbor Laboratory Press, Cold Spring Harbor, New York.

168. Okita, T.W., Y.S. Hwang, J. Hnilo, W.T. Kim, A.P. Aryan, R. Larson and H.B. Krishnan. 1989. Structure and expression of the rice glutelin multigene family. *J Biol Chem* **264**: 12573-12581.

169. Takaiwa, F., K. Oono and A. Kato. 1991. Analysis of the 5' flanking region responsible for the endosperm- specific expression of a rice glutelin chimeric gene in transgenic tobacco. *Plant Mol Biol* **16**: 49-58.

170. Zheng, Z., K. Sumi, K. Tanaka and N. Murai. 1995. The bean seed storage protein B-phaseolin is synthesized, processed, and accumulated in the vacuolar type-II protein bodies of transgenic rice endosperm. *Plant Physiol* **109**: 777-786.

171. Bahramian, M.B. and H. Zarbl. 2005. GENE impedance: a natural process for control of gene expression and the origin of RNA interference. *J Theor Biol* **233**: 301-314.

172. Bagga, S., H.P. Adams, F.D. Rodriguez, J.D. Kemp and C. Sengupta-Gopalan. 1997. Coexpression of the maize delta-zein and beta-zein genes results in stable accumulation of delta-zein in endoplasmic reticulum-derived protein bodies formed by beta-zein. *Plant Cell* **9**: 1683-1696.

173. Tackaberry, E.S., A.K. Dudani, F. Prior, M. Tocchi, R. Sardana, I. Altosaar and P.R. Ganz. 1999. Development of biopharmaceuticals in plant expression systems: cloning, expression and immunological reactivity of human cytomegalovirus glycoprotein B (UL55) in seeds of transgenic tobacco. *Vaccine* **17**: 3020-3029.

174. Britton, J.R. and O. Koldovsky. 1989. Gastric luminal digestion of lactoferrin and transferrin by preterm infants. *Early Hum Dev* **19**: 127-135.

175. Miller-Gilbert, A.L., S.H. Dubuque, B. Dvorak, C.S. Williams, J.G. Grille, S.S. Woodward, O. Koldovsky and P.J. Kling. 2001. Enteral absorption of erythropoietin in the suckling rat. *Pediatr Res* **50**: 261-267.